# DOSIMETRIC COMPARISON OF THREE-DIMENSIONAL CONFORMAL RADIATION THERAPY (3D-CRT), INTENSITY MODULATED RADIATION THERAPY (IMRT) AND VOLUMETRIC MODULATED ARC THERAPY (VMAT) FOR DISTAL ESOPHAGEAL CANCER TREATED WITH EXTERNAL RADIATION

# DOSIMETRIC COMPARISON OF THREE-DIMENSIONAL CONFORMAL RADIATION THERAPY (3D-CRT), INTENSITY MODULATED RADIATION THERAPY (IMRT) AND VOLUMETRIC MODULATED ARC THERAPY (VMAT) FOR DISTAL ESOPHAGEAL CANCER TREATED WITH EXTERNAL RADIATION

By

WAQAAS AHMED ZIA, BMRSc

A Thesis

Submitted to the School of Graduate Studies

in Partial Fulfillment of the Requirements for the Degree of

Master of Science

McMaster University

McMaster University MASTER OF SCIENCE (2022) Hamilton, Ontario (RADIATION SCIENCE – RADIATION BIOLOGY)

TITLE: Dosimetric Comparison of Three-Dimensional Conformal Radiation Therapy (3D-CRT), Intensity Modulated Radiation Therapy (IMRT) and Volumetric Modulated Arc Therapy (VMAT) for Distal Esophageal Cancer treated with External Radiation

AUTHOR: Waqaas Ahmed Zia, BMRSc (McMaster University)

SUPERVISOR: Dr. Thomas Farrell

NUMBER OF PAGES: x, 95.

# ABSTRACT

**Purpose/Objectives:**

Intensity Modulated Radiation Therapy (IMRT) and Volumetric Modulated Arc Therapy (VMAT) provide advantages in delivery of radiation allowing conformality of delivered dose to the planning target and reducing dose to organs at risk (OAR), however, at the potential cost of low dose spread. Due to the central location of the esophagus and GE junction, dose to lungs, heart, spinal cord, liver, and kidneys must be considered. Low dose spread is of particular concern with respect to healthy lung tissue. This study comprehensively compares volumetric dose statistics of the standard three-dimensional conformal radiation therapy (3D-CRT) compared with VMAT and IMRT for distal esophageal cancer treatment.

**Materials/Methods:**

Forty patients who underwent pre-operative radiation therapy for esophageal cancer between 2012-2014 were retrieved from our database. Pinnacle planning software was used to create 3D-CRT, VMAT and IMRT radiation plans for all patients. Forty-five (45) Gy was prescribed for each patient with $D_{95\%}$ > 42.75Gy for the planning target volume (PTV). All plans were optimized to maintain PTV coverage while reducing dose to OAR with specific emphasis on lung and heart dose. Volumetric dose statistics were obtained, and Wilcoxon signed rank test was used to compare 3D-CRT vs IMRT and VMAT for Conformity Index, Integral Dose, Monitor Units, lung ($V_{5Gy}$, $V_{20Gy}$, mean, max), heart ($V_{30Gy}$, mean, max), spinal cord max, bilateral kidneys ($V_{20Gy}$, mean) and liver mean dose. Comparison was also made for IMRT vs VMAT.

**Results:**

For both IMRT and VMAT compared with 3D-CRT, statistically significant pairwise differences were noted for Conformity Index (-28.51%, -30.70%, *P*<.001), Integral Dose (-14.0%, -14.8%, *P*<.001), Monitor Units (107.2%, 80.4%, *P*<.001), lung ($V_{20Gy}$: -49.7%,-57.4%, mean: -20.3%,-24.9%, *P* <.001), heart ($V_{30Gy}$ : -10.1%,-14.3%, mean -10.4%,-13.4%, *P* <.001), spinal cord (max 13.3%,9.5%, *P* <.001) and liver (mean -29.9%,-24.3%, *P* <.001). No significant differences were noted for VMAT and IMRT compared with 3D-CRT for lung ($V_{5Gy}$, max dose), heart (max dose) and bilateral kidneys (mean). VMAT did offer statistically significant improvement in Conformity Index, Monitor Units, lung $V_{20Gy}$ and mean dose as well as heart $V_{30Gy}$ and mean dose compared to IMRT.

**Conclusion:**

VMAT and IMRT offer excellent sparing of key organs (lung, heart) with respect to volumetric constraints. Max point doses as well as lung $V_{5Gy}$, which can be an indication of low dose spread for esophageal treatment, were not conclusively different. While 3D-CRT offers acceptable treatment, VMAT should be the standard modality of radiation treatment where facilities exist.

## ACKNOWLEDGEMENTS

I am extremely grateful for the opportunity to work on this thesis and would not have completed it without the guidance of my supervisor, help from friends and support from family.

I would like to express my deepest appreciation to my supervisor, Dr. Thomas Farrell. The door to Dr. Farrell's office was always open when I needed advice, guidance, and a little motivation. I knew I could always rely on Dr. Farrell to point me in the right direction and his knowledge and insight was the steady force needed as I progressed through the program. I am grateful for his patience as I navigated working, being a father and a student.

I would also like to sincerely thank my advisors Dr. Ranjan K. Sur and Dr. Crystal Hann. Their commitment to patient care and serving the community was the inspiration to push forward with this project. I greatly valued their expertise and advice to craft a project that could be of benefit to patient care.

I am thankful to Dr. Martin Shim for his help in verifying radiation plans for accuracy and completeness. Many thanks to Jack Skoczny and Clarence Yu for providing benchmark plans and their expertise and advice in advanced radiation planning.

Many thanks to Dr. Gregory R. Pond for his help in data analysis.

I am also grateful for many colleagues and friends at work, especially Emilia Timotin who believed in me to pursue further education. I would not have made it to this point if it were not for her guidance and advice.

Finally, I would not be in this position without the love and support of my family. They always encouraged me with well wishes and sound advice. They have made countless sacrifices to ensure I would have the best chance at success and for that I am eternally grateful. I am especially thankful to my wife, Maha, who supported our lives in all aspects as I pursued further education. Her love and support were a source of comfort throughout this process. I am also

thankful to my daughter, Ilyana, who came along for the ride towards the end. Her unbridled joy brightens up any room.

# TABLE OF CONTENTS

# LIST OF FIGURES AND TABLES

# LIST OF ABBREVIATIONS

| | |
|---|---|
| OAR | Organs at Risk |
| 3D-CRT | Three-dimensional Conformal Radiation Therapy |
| IMRT | Intensity Modulated Radiation Therapy |
| VMAT | Volumetric Modulated Arc Therapy |
| AC | Adenocarcinoma |
| SCC | Squamous Cell Carcinoma |
| GERD | Gastroesophageal reflux disease |
| OR | Odds Ratio |
| BMI | Body Mass Index |
| CBC | Complete Blood Count |
| EUS | Endoscopic Ultrasound |
| EMR | Endoscopic Mucosal Resection |
| PET | Positron Emission Tomography |
| 4D-CT | Four-dimensional Computed Tomography |
| Gy | Gray (unit of energy absorbed from ionizing radiation) |
| cGy | Centigray ($1/100^{th}$ of a Gray) |
| GE | Gastroesophageal |
| GU | Genitourinary |
| GTV | Gross Tumour Volume |
| CTV | Clinical Target Volume |
| PTV | Planning Target Volume |
| MRI | Magnetic Resonance Imaging |

# 1.0 Introduction

## 1.1 Esophageal Cancer

### 1.1.1 Anatomy and Incidence

*Anatomy*

The esophagus is a tubular shaped organ that connects the pharynx to the stomach as part of the digestive tract [1]. It follows a path behind the trachea and heart, in front of the spinal column and through the diaphragm where it enters the stomach. The central location of the esophagus and the multitude of critical structures surrounding it make treatment of the esophagus with radiation and surgery a difficult endeavour.

The esophagus travels over 3 anatomic regions. The cervical esophagus is approximately 5cm long and starts at the level of the $6^{th}$ cervical spine to interspace of $1^{st}$ and $2^{nd}$ thoracic vertebrae. The thoracic esophagus is approximately 20cm long extending from the thoracic inlet to diaphragm and the abdominal esophagus starts at the diaphragm to where it joins the cardia of the stomach with an approximate length of 2-6cm [2]. Multiple layers make up the esophageal wall including the mucosa, which contains squamous epithelium, the submucosa which is the strongest layer and includes elastic and fibrous tissues and lastly the esophageal muscle. The upper third consists of skeletal muscle while the lower two thirds contain smooth muscles [3].

Lymphatic drainage for the esophagus is complex and as a result, the rate of lymph node metastasis is very high [4]. Lymphatic involvement will guide the treatment options and prognosis for the patient. The lymphatic flow of thoracic esophagus can run both up towards the neck and down towards the celiac area. Because of complex lymphatic drainage, skip lesions may be present along the length of esophagus [5]. Lymphatic spread within the esophagus primarily has 2 modes of spread, traversing through esophageal wall and shifting longitudinally (superiorly or inferiorly). Figure 1 demonstrates lymphatic drainage among different tissues that comprise of the esophagus. Controversy remains with respect to lymphatic drainage and target areas for radiation treatment and surgery.

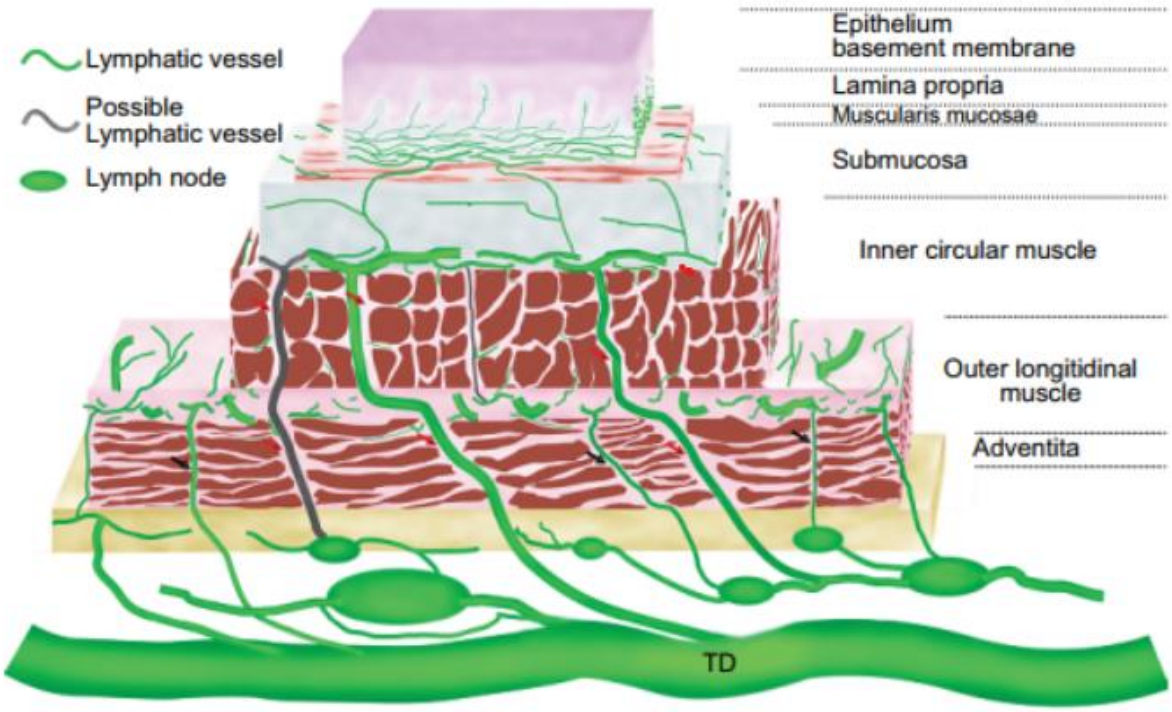


**Figure 2.1.1.1** – Layers of esophagus tissue [132].

*Incidence and Mortality*

Incidence of esophageal cancer differs slightly between males and females in Canada. In males, incidence was increasing slowly from 1984 to 2006 (0.3%) [2]. There was no significant change from 2006 to 2010, however since 2010 incidence has decreased immensely (-2.4%). For females, incidence has been decreasing slowly since 1984 (-0.4%). The projected new cases for males in 2019 was 1800 and 540 for females for a total of 2340 in Canada [6]. A similar trend is also noted in the United States of America. In the past 10 years, incidence of esophageal cancer has been decreasing by an average of 1.0% each year [7]. It is estimated that in 2020 there will be 18,440 new cases in the United States alone, which represents approximately 1.0% of all new cancer cases. This trend changes on a more global scope. The incidence rate of esophageal cancer is 20 to 30 times higher in China than in the United States. An "esophageal cancer belt" can be described as the area from northeast China to the Middle East [8]. In a 2017 review of the

epidemiology for esophageal cancer, Liang *et al* noted that 80% of new cases occur in less developed regions of the world and 60% of those occur in China [9]. It was estimated that there would have been 286,700 new cases and it was noted that age specific incidence increases rapidly after age 40. Overall, incidence rates have decreased from 15.93/100,000 to 10.01/100,000 in the timeframe of 2000 to 2011 with respect to China.

In a review completed by Otterstatter *et al* in 2012, there were findings in Canada related to incidence with respect to tumour pathology and anatomical location. Incidence of esophageal adenocarcinoma rose by 3.9% (males) and 3.6% (females) from 1986 to 2006. On the other hand, squamous cell carcinoma incidence declined by 3.3% and 3.2% in the early 1990s for males and females respectively [10]. Projected incidence shows a potential increase in adenocarcinoma of 40%-50% and decrease of 30% for squamous cell carcinoma by 2026. Of note, data from 2004 to 2006 suggests that 69% of all new esophageal cancer cases in Canada occurred in the lower third of the esophagus.

In Canada, cancer mortality for all cancer types combined has been decreasing since a peak reached in 1988. Although the rate has been decreasing, the total number of cancer deaths continue to rise due to an increase in general population, more specifically the growing and aging population. The five leading cancer types that results in death are lung, colorectal, pancreas, breast and prostate [6]. These account for over 50% of cancer death with lung cancer representing approximately 26% of all cancer related death. With respect to esophageal cancer, a similar trend is noted in both males and females. For males, the average annual percentage change in mortality rate for esophagus increased by 0.6% from 1984-1999 but decreased from 1999-2015 by -1.0%. For females, that rate has been decreasing from 1984-2015 by -0.5%. Advancements in treatment as well as earlier detection might be an explanation for the decrease in mortality rate.

While mortality rate of esophageal cancer in relation to all other cancers may seem low, the five-year net survival remains one of the poorest of all cancer subtypes. In Canada, all cancers combined net survival is 63% at 5 years and 57% at 10 years. Five-year survival was lowest for pancreas (8%), esophageal (15%), lung (19%) and liver (19%). In relation to esophageal cancer,

this has increased from a rate of 10% in 1992-1994. Multi modality treatments as well as increased detection rates have certainly improved survival as well as palliation and pain reduced living. Effective treatment begins with early detection, which is difficult with esophageal cancer. As the organ is hollow and expandable, patients do not immediately recognize any mass or obstruction. Unfortunately, spread is easy with a rich lymphatic system supplying the organ so by time there are symptoms or cancer is detected, it is often later stage.

Mortality on the world stage carries a similar outlook. In America, overall 5-year survival from 2002-2008 was 16.9% [8]. It was interesting to note that for the same time period, there was a large discrepancy with respect to race. 5-year survival for white men was 18.1% compared to just 10.4% for black men. A similar trend was noted for females, 17.0% survival for white women and 12.6% for black women. Worldwide, approximately 70% of esophageal cases occur in men with a 2-3x difference in incidence and mortality rate between sexes [11]. Esophageal cancer is also the leading cause of mortality in Kenyan men. Malawi also has the highest incidence rate in men and women globally. Of note, adenocarcinoma incidence is rapidly rising in highly developed countries whereas squamous cell carcinoma dominates the rest of the world. An analysis of worldwide cancer trends from 2010-2014 revealed that that 5-year age standardised net survival was in the range of approximately 10-30%. Survival was highest in developed Asian countries with Japan, China and Korea at 36%, 34% and 31% respectively. Contrasted by the report of Canada having a net survival of 16.1% and the USA at 20.0% during the same time, discrepancy among developed nations across the world is alarming. One of the main reasons for the discrepancy is the screening programs instituted in areas of high risk. Japan has instituted a screening program since 1960 with results indicating risk of death is significantly lower in the screened group compared to the unscreened group [12]. Similar results are noted in Korea where a national screening program was instituted in 1999 with biennial contrast radiology or endoscopy in adults aged 40 or over [13]. Early detection can prove critical as esophageal resection may be curative with small tumours and clear resection margins. Screening programs need to be considered for populations where the tumours are common or the subset of patients which may be at higher risk.

### 1.1.2 Risk Factors and Presentation

*Risk Factors*

The major risk factors for esophageal cancer are generally smoking and alcohol consumption. Table 1.1.2.1 represent major categories of risk factors and their prevalence on the 2 major histological type of esophageal cancer.

**Table 2.1.2.1** - Risk factors for esophageal cancer [8].

| Risk Factor | Squamous-Cell Carcinoma | Adenocarcinoma |
|---|---|---|
| First or second-hand smoke | +++ | ++ |
| Alcohol Consumption | +++ | - |
| Consumption of red meat | + | + |
| Barrett's esophagus | - | ++++ |
| Reflux symptoms | - | +++ |
| Obesity | - | ++ |
| Poverty | ++ | - |
| Caustic injury to esophagus | ++++ | - |
| History of head and neck cancer | ++++ | - |
| History with radiation therapy | +++ | +++ |
| Frequent consumption of extremely hot drinks | + | - |

-: No effect; +: Suspicious effect; ++: Positive effect; +++, ++++: Strong positive effect

Smoking is one of the main etiological factors associated with both adenocarcinoma and squamous cell carcinoma of the esophagus [14]. It has been noted that the risk of incidence correlates directly with the duration of smoking as well as the number of cigarettes smoked per day. Large-scale studies with the relationship of marijuana use is limited. In a population-based

case-control study conducted by Hashibe *et al*, it was noted that the association of esophageal cancer with marijuana use was not strong and almost below detectable limits [15]. A review of epidemiological studies conducted by Huang *et al* confirms the lack of study done with respect to esophageal cancer incidence and prolonged marijuana use [16]. More well-designed studies are warranted with increased legalization of marijuana in the western hemisphere and across the world.

Alcohol consumption also presents as a consistent risk factor specifically for squamous cell carcinoma [17]. This risk also increases with amount of alcohol consumed. Heavy drinkers (≥12 drink a week) had a relative risk increase range from 2.9-7.4 [18]. Many studies have also shown a synergistic effect of alcohol and smoking. A case-controlled study in Italy and Switzerland conducted by Garavello *et al* demonstrated that compared to patients without family history, noncurrent smokers and drinking <49 drinks a week, the odds ratio was 2.9 for family history alone. If adding in current smokers drinking ≥ 49 drinks a week and no family history, the odds ratio increased to 15.5 and it was increased to 107.0 for patients who were current smokers, drinking ≥ 49 drinks a week and had family history [19]. 5 studies that examined the relationship of alcohol consumption and risk of adenocarcinoma found no positive association (20). The conclusion drawn by Lagergren [20] is that there is no increased risk of adenocarcinoma based on alcohol consumption. Lindblad *et al* further corroborate this [21].

Risk factors differ between squamous cell carcinoma and adenocarcinoma. Globally, SCC remains the most diagnosed histology representing 87% of all cases of esophageal cancer in 2012 [22]. However, in the western world there has been an increase in AC with incidence an incidence rate of 0.4/100,000 in 1973 to 2.8/100,000 in 2012 in USA. Similar increases have been noted in the United Kingdom, Australia, and Northern Europe. The change in incidence is thought to be related to an increase in prevalence of known risk factors for AC, namely obesity and gastroesophageal reflux.

GERD is a risk factor for both Barrett's esophagus and esophageal AC. Chronic reflux causes Barrett's esophagus which is a columnar-cell metaplasia that replaces the native epithelium of

the esophageal mucosa [23]. This new epithelium has been linked to a significantly increased risk of esophageal AC. Lagergren *et al* found that there is a strong association between GERD and AC regardless of Barrett's esophagus. It was found that the frequency of symptoms were strongly related to risk as the more frequent symptoms of GERD, the higher the risk. Interestingly, there was no association with GERD and the incidence of SCC. A factor that relates to a possible increase in GERD would be diet. Consumption of fruit, vegetables and non-fried fish can be a protective measure against Barrett's esophagus compared to a more Western style diet which can consist of more fast food and meat [24]. A meta-analysis of studies conducted by Sun *et al* found that a 10 gram/day increase in dietary fibre was associated with a 31 % decrease in Barrett's esophagus and therefore esophageal cancer [25].

Obesity is also a risk factor for developing AC. The incidence of AC increases directly with increasing BMI. A BMI of greater than 25 was associated with an increased risk of AC in both males and females (OR of 2.2 and 1.9 respectively). In a review by Hoyo *et al*, it was found that compared to individuals with BMI <25, a BMI of ≥ 40 was associated with an increase in odds ratio of 4.76 (26). These results were similar even when stratified by gender and GERD symptoms. Interestingly, there is an inverse relationship between BMI and risk of SCC. In data analyzed by Smith *et al* from a large population-based study, it was demonstrated that there was a strong inverse relation between BMI and esophageal cancer death in SCC [27]. High blood pressure was also found to be correlated with higher risk of SCC (relative risk increase of 2.60 comparing top and bottom quintile of mid blood pressure) [28]. However, alcohol is also a confounding variable as it increases risk of SCC and could cause hypertension.

Socioeconomic factors do play a role in incidence. In a Swedish study conducted by Jansson *et al* it was found that AC and SCC were both linked to lower socioeconomic status [29]. The odd-ratio for unskilled or semi-skilled manual workers was 3.7 compared to professionals for risk of AC. Interestingly, odd-ratio was greater than 2 for those living with a partner for less than a year. This suggests an increased risk of AC and SCC for patients without a long-term partner. Another potential risk factor is the infection of Helicobacter pylori. H pylori causes chronic inflammation leading to gastritis which could in turn lead to reduction in acid production. One theory is that

this change could then reduce risk of AC by changing the nature of refluxate [17]. However, a review of data by Ye *et al* suggests that reduction in AC risk by H pylori may occur but not by acidity changes. It was also suggested that infection with CagA-postiive strains of H pylori may increase risk for SCC [30]. In the aforementioned Swedish study, no risk estimates changed adjusting for H pylori status.

*Presentation*

Clinical presentation is similar for both SCC and ACC. The most common symptom is dysphagia (difficulty swallowing) or odynophagia (painful swallowing) [31]. Another frequently assessed symptom related to difficulty swallowing is weight loss. In a retrospective review completed by Gibbs *et al*, 5 years of clinical data was analyzed with respect to clinical presentation of both SCC and ACC. It was found that dysphagia occurred in 83% of patients and weight loss occurred in 58% of patients. Other symptoms included abdominal pain, chest pain and GI bleeding [32]. The observations of the study are presented (Table 1.1.2.1).

**Table 1.1.2 2 -** Presenting symptoms of patients with esophageal carcinoma [32].

| Symptoms | % of Patients |
|---|---|
| Dysphagia | 83 |
| Weight Loss | 58 |
| Abdominal pain | 9 |
| Chest pain | 7 |
| GI Bleed | 6.5 |
| GERD | 5.5 |
| Nausea/vomiting | 5 |
| Hoarseness | 2 |
| Fatigue | 1 |
| Back pain | 1 |
| Neck pain or mass | 1 |
| Early satiety | <1 |
| Hiccups | <1 |
| Hemoptysis | <1 |
| Barrett's surveillance | 1 |

Due to the pliable nature of the esophagus, it is often estimated that at least 75% of the circumference of the esophagus needs to be blocked to experience the sensation of food sticking or dysphagia. This presents a challenge of early detection and as a result about one-half of esophageal cancers present with unresectable disease or distant metastasis [33]. Because of the often advanced stage at detection, importance is placed on treatment options that restore ability to eat and swallow food to gain weight and possibly allow for further intervention. As discussed earlier, a rich lymphatic supply surrounds the entire length of the esophagus. As a result, there is a possibility of "skip lesions". This phenomenon refers to lesions appearing in the esophagus with some gap between them that complicates management and in many cases forces treatment to the whole organ rather than spot treatment.

### 1.1.3 Diagnostics

As with many diseases, accurate and efficient diagnostics are required to diagnose and stage esophageal cancer for proper treatment. Table 1.1.3.1 summarizes common testing used to diagnose and stage this subset of patients.

**Table 1.1.3.2 -** Possible diagnostic and staging testing [34].

| **Diagnostic tests** | **Staging and other tests** |
|---|---|
| Health history and physical exam | CBC |
| Complete blood count (CBC) | Blood chemistry tests |
| Blood chemistry tests | Upper GI endoscopy |
| Upper GI series | EUS |
| Upper GI endoscopy | CT scan |
| EUS | PET scan |
| Biopsy | MRI |
| | Pulmonary function tests |

| | |
|---|---|
| | Heart function tests |
| | Nutritional assessment |
| | Thoracoscopy |
| | Laparoscopy |
| | Bronchoscopy |

Diagnosis relies heavily on a thorough and complete patient history. As mentioned earlier, most patients present with a history of dysphagia and weight loss. Along with blood work, initial barium-swallow allow studies are a cost-effective way to determine if there are any masses that are obstructing or occluding the esophagus (Figure 1.1.3.1) [14].

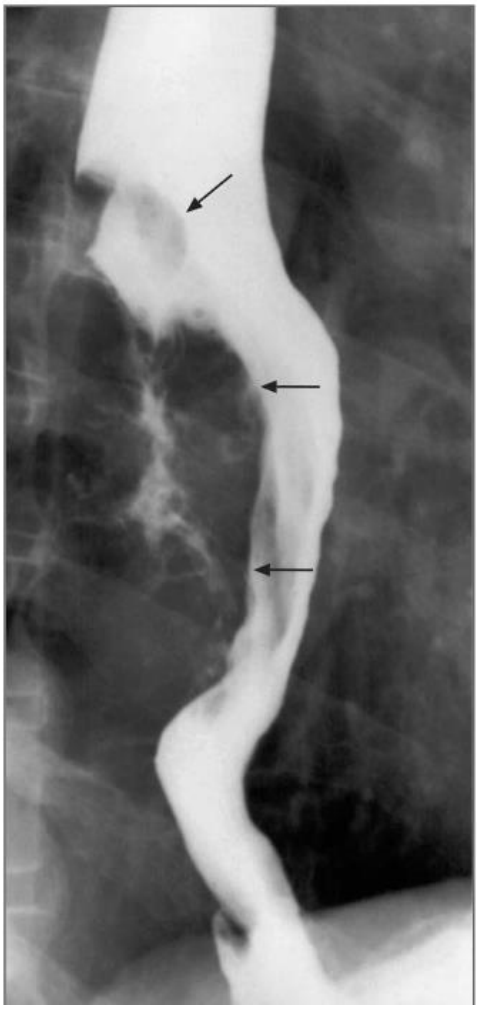

**Figure 1.1.3.2** - Barium swallow showing esophageal strictures [14].

Diagnosis can be confirmed with further imaging and biopsy to determine histology. A combination of radiological imaging studies has proven to be effective enough to negate the often invasive thoracoscopy or laparoscopic staging. EUS has proven to display excellent sensitivity and specificity in diagnosing T4 lesions with 92.4% and 97.4% respectively [35]. When fine-needle aspiration is added, sensitivity to diagnose N-stage is 96.7%. In addition to EUS, PET is now routinely offered for these patients where facilities exist. PET is particularly effective in diagnosing distant nodal and metastatic disease. In a study by Heeren *et al*, PET was able to upstage 20% of patients and downstage 5% of patients which can dramatically alter the most effective treatment course [36].

### 1.1.4 Pathology and Staging

*Pathology*

There are 2 dominant types of primary esophageal cancers: squamous cell carcinoma and adenocarcinoma. Squamous cell carcinoma is the most common pathological type of esophageal cancer in the world with highest rates seen in Asian/Eastern countries [37]. In the western world, rates of squamous cell carcinoma have decreased, and adenocarcinoma has increased. Squamous cell carcinoma can be found anywhere in the esophagus but is most prevalent in the middle third. Invasive squamous cell carcinoma involves neoplastic squamous cells invading into the lamina propria and deeper layers of the esophagus. Adenocarcinoma is predominantly found in the lower esophagus and GE junction from gland cells. Barrett's esophagus is often considered a precursor to adenocarcinoma. Other types of esophageal cancer such as sarcomas and lymphomas are also prevalent, although less frequent with no signs of increasing incidence.

*Staging*

Esophageal cancer is currently staged using the 8$^{th}$ edition of the American Joint Committee on Cancer (AJCC) manual as well as the 8$^{th}$ edition publication by the Union for International Cancer Control (UICC). Tumour, node and metastasis (TNM) classification system is used to specify

tumour size, nodal involvement, and metastatic spread. Based on the TNM staging, a stage of cancer can be quantified [38]. Both esophagus and esophagogastric junction tumours are classified with the same system (Table 1.1.4.1 and 1.1.4.2).

**Table 1.1.4.2**- Cancer staging categories esophageal and esophagogastric cancer [38].

| **Category** | Criteria |
|---|---|
| **T Category** | |
| TX | Tumor cannot be assessed |
| T0 | No evidence of primary tumor |
| Tis | High-grade dysplasia, defined as malignant cells confined by the basement membrane |
| T1 | Tumor invades the lamina propria, muscularis mucosae, or submucosa |
| T1a | Tumor invades the lamina propria or muscularis mucosae |
| T1b | Tumor invades the submucosa |
| T2 | Tumor invades the muscularis propria |
| T3 | Tumor invades adventitia |
| T4 | Tumor invades adjacent structures |
| T4a | Tumor invades the pleura, pericardium, azygos vein, diaphragm, or peritoneum |
| T4b | Tumor invades other adjacent structures, such as aorta, vertebral body, or trachea |
| **N Category** | |
| NX | Regional lymph nodes cannot be assessed |
| N0 | No regional lymph node metastasis |
| N1 | Metastasis in 1–2 regional lymph nodes |
| N2 | Metastasis in 3–6 regional lymph nodes |
| N3 | Metastasis in 7 or more regional lymph nodes |
| **M Category** | |
| M0 | No distant metastasis |
| M1 | Distant metastasis |
| **Adenocarcinoma G Category** | |
| Gx | Differentiation cannot be assessed |
| G1 | Well differentiated. >95% of tumor is composed of well-formed glands |
| G2 | Moderately differentiated. 50% to 95% of tumor shows gland formation |

| | |
|---|---|
| G3 | Poorly differentiated. Tumors composed of nest and sheets of cells with <50% of tumor demonstrating glandular formation |
| **Squamous cell carcinoma G category** | |
| Gx | Differentiation cannot be assessed |
| G1 | Well-differentiated. Prominent keratinization with pearl formation and a minor component of nonkeratinizing basal-like cells. Tumor cells are arranged in sheets, and mitotic counts are low |
| G2 | Moderately differentiated. Variable histologic features, ranging from parakeratotic to poorly keratinizing lesions. Generally, pearl formation is absent |
| G3 | Poorly differentiated. Consists predominantly of basal-like cells forming large and small nests with frequent central necrosis. The nests consist of sheets or pavement-like arrangements of tumor cells, and occasionally are punctuated by small numbers of parakeratotic or keratinizing cells |
| **Squamous cell carcinoma L category** | |
| LX | Location unknown |
| Upper | Cervical esophagus to lower border of azygos vein |
| Middle | Lower border of azygos vein to lower border of inferior pulmonary vein |
| Lower | Lower border of inferior pulmonary vein to stomach, including esophagogastric junction |

**Table 1.1.4.2** – Clinical (cTNM) stage groups [38].

| cStage group | cT | cN | cM |
|---|---|---|---|
| **Squamous cell carcinoma** | | | |
| 0 | Tis | N0 | M0 |
| I | T1 | N0-1 | M0 |
| II | T2 | N0-1 | M0 |
| | T3 | N0 | M0 |
| III | T3 | N1 | M0 |
| | T1-3 | N2 | M0 |
| IVA | T4 | N0-2 | M0 |
| | T1-4 | N3 | M0 |
| | T1-4 | N0-3 | M1 |
| **Adenocarcinoma** | | | |
| 0 | Tis | N0 | M0 |
| I | T1 | N0 | M0 |
| IIA | T1 | N1 | M0 |

| | | | |
|---|---|---|---|
| IIB | T2 | N0 | M0 |
| III | T2 | N1 | M0 |
| | T3-4a | N-1 | M0 |
| | T1-4a | N2 | M0 |
| | T4b | N0-2 | M0 |
| | T1-4 | N3 | M0 |
| | T1-4 | N0-3 | M1 |

### 1.1.5 Treatment options

With the advancement of modern medicine, many treatments options have become available with varying levels of success. Treatment options vary depending on resources, patient's functional status and most importantly stage of disease. Commonly, a multi modality treatment regimen is required with support from multiple disciplines for best patient care. Figure 1.1.5.1 shows an example treatment algorithm used in Japan [39].

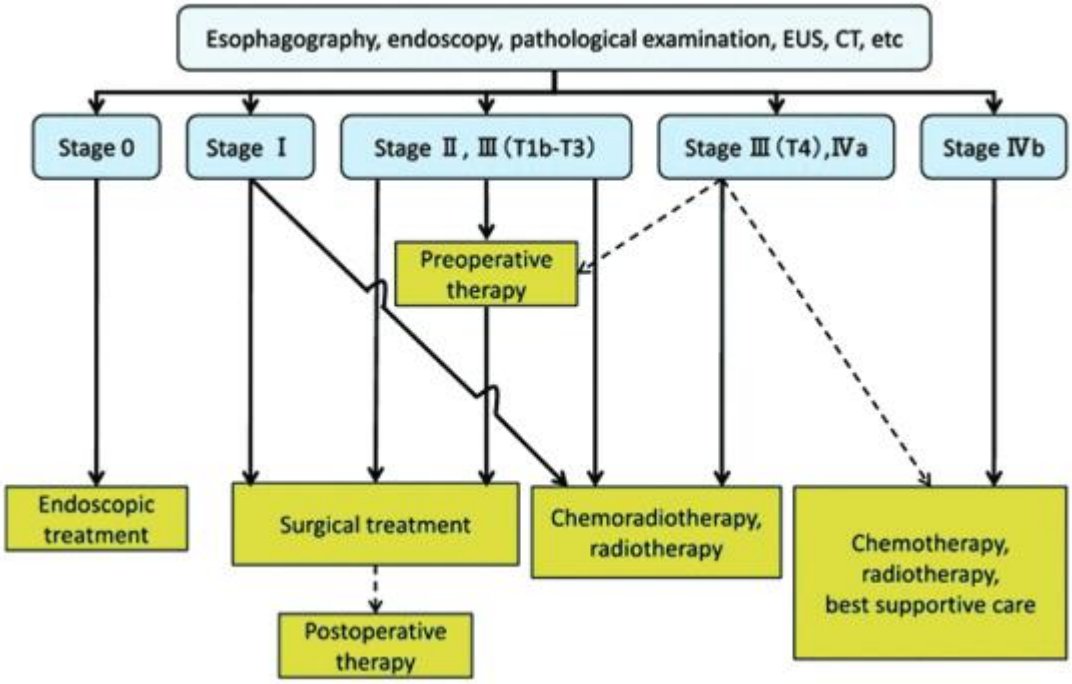


**Figure 1.1.3.1** – Therapeutic algorithm developed for use in Japan [39].

Early stage, localized disease allows for many options with endoscopic techniques often preferred. EMR can be used for carcinoma in situ [40]. Other endoscopic techniques include laser treatment, photodynamic therapy, stent placement and dilation to relieve dysphagia.

Generally speaking, chemotherapy regimens can be the same for both squamous cell carcinoma and adenocarcinoma. A combination of cisplatin and 5-flurouracil is the most common and most used regimen [40]. Ilson demonstrates that the combination of cisplatin (60-100 mg/m2) and 5-FU (750-1000 mg/m2) given in continuous infusion for 4 to 5 days has considerable academic backing [41]. Evidence has shown the importance of chemotherapy in a pre or post operative setting as well as primary modality treatment in combination with radiation therapy for squamous cell carcinoma.

Surgery plays an important role in cancer control and is often considered for best chance of cure in localized and locoregional disease. Many different surgical techniques exist with each containing specific risks and benefits. Common approaches include minimally invasive Ivor Lewis (transthoracic) technique as well as McKeown (three-hole) method. These methods use a combination of laparoscopic and thoracoscopic approaches with Ivor Lewis technique having two incisions and an esophagogastric anastomosis in the chest. The Mckeown approach refers to a three-incision technique in the chest, abdomen, and neck to create anastomosis in the neck [42]. Sabra *et al* did a retrospective analysis of the American College of Surgeons National Surgical Quality Improvement Project database (2005-2017) and compared Ivor Lewis to McKeown technique and concluded that the McKeown technique is associated with more post operative complications and longer hospital length of stay. Overall, the authors noted a trend towards using Ivor Lewis technique for minimally invasive esophageal cancer surgery.

Radiation therapy is involved as a standard of care for a large subset of patients. Definitive radiation alone is not advised based on multiple studies. The control arm of RTOG 8501 which consisted of radiation alone had a 5-year survival of 0% compared to chemoradiation which demonstrated 26% survival [43]. Preoperative radiation alone provided some increase in survival. Shridhar *et al* conducted a meta-analysis of 5 randomized trials and concluded that

there was an 11% reduction in mortality with absolute survival benefit of 3% at 2 years and 4% at 5 years [44]. The authors also mentioned postoperative radiation alone provided no survival benefits despite loco regional control. Radiation combined with chemotherapy is highly recommended if patients can undergo such a regimen. In the Intergroup Study 0116, analysis was done to compare chemoradiation after surgery vs surgery alone. Macdonald *et al* found that there was significant increase in relapse-free and overall survival among the chemoradiation group [45]. Median duration of survival was 36 months in the chemoradiation group vs 27 months in surgery alone. Three-year survival rates were also significantly different with 50% vs 41% respectively. Of the chemoradiation group, 54% experienced major hematologic side effects while 33% experienced gastrointestinal effects grade 3 or higher. In this study, patients were treated between 1991 and 1998 where radiation planning and treatment is vastly different from today's technology. With increased precision and study of radiation planning, there is opportunity for improvement on associated toxicity. The role of neoadjuvant chemoradiation was not well established until the CROSS group study published in 2012 with long term results published in 2015 [46, 47]. Median overall survival improved from 24 months in the surgery alone group to 49.4 months in the chemoradiation plus surgery cohort. In the chemoradiation group, 7% of patients had grade 3 hematologic toxic effects with 13% reporting other nonhematological effects of grade 3 or higher. While the adverse effects of chemoradiation is improved from pervious older studies, there remains areas of improvement should patients undergo this regimen. Post-op chemoradiation has proven to be an effective treatment options for patients who qualify.

## 1.2 Radiation Therapy and Treatment Planning

### 1.2.1 Radiation Therapy Background

Radiation therapy has developed immensely over a century of advancements and studies. Slater offers a concise review of the history of radiation therapy, which can be divided into the discovery era, orthovoltage era, megavoltage era and finally the modern era [48]. The early discovery X-rays by Rontgen in 1885 followed by further study by Bequerel and Curie lead the

way to radiation use in treating disease long before fully understanding the physiological effects. As time went on, radiobiologists better understood cell effects and physicists researched new isotopes which could be harnessed for therapy. Henri Coutard demonstrated that delivering external radiation in fractionated therapy could control head and neck cancer without severe reactions that a single large dose causes [49]. Simultaneously, understanding and development of the delivery of radiation was increasing. Scientists were starting to discover more about the properties of radiation delivery and effects. In the early times of radiation treatment, skin cancers were the most treated because of the low penetration of x-rays and radium. Intracavitary and interstitial methods of delivery were more widely used than externally delivered radiation. William Coolidge was able to develop an improvement on the x-ray tube, which converted electrical current into x-rays [50]. This allowed higher energy to be applied to a target (typically tungsten) which produced higher energy x-rays that could be used in improved imaging and deeper treatment. This is the basis of the linear accelerator which ushered in the "orthovoltage era" from 1920's to 1950's.

E.O Lawrence recognized the need to accelerate charged particles and to harness this capability. It was recognized that there needed to be a production of high voltage as well as tubes that can handle such voltage. Rolf Wideröe published an article from Germany describing a technique of multiple acceleration of positive ions by oscillating voltages to a series of cylindrical electrodes in a line [51]. Lawrence used this idea to develop the cyclotron which was able to accelerate charged particles in a spiral path to produce high energy protons. Proton therapy is used in treatment today for various types of cancer. Electrons became a treatment option when Kerst developed the betatron. Similar to the cyclotron in the spiral path used to accelerate the particle, the betatron was able to accelerate electrons to high energy and the first machine produced 2MeV electrons [52].

Radiation safety was also being developed in lock step with radiation generation. The International Congress of Radiology was first formed in 1925 with the congress being held in London [53]. The International Commission on Radiological Protection was formed, and suggestions made to standardize radiation unit measurements as well as techniques to limit

radiation exposure to operators. As time went on, understanding also increased across the world. Measurement tools such as the Geiger counter were also used to detect not only alpha and beta radiation, but also gamma radiation.

The megavoltage era followed and was a precursor to the modern age of radiation therapy planning and delivery. From the 1950's and onwards, development has occurred quickly with the advent of higher and higher energy machines as well as improved diagnostic abilities. The need for deeper penetrating x-rays while sparing healthy tissue along the way was apparent. While the x-ray tube is useful in superficial treatments, producing higher energies required extremely high voltage which meant large and costly machines. Harold Johns is credited with pioneering the use of Cobalt-60 as a gamma ray source for therapeutic purposes. Radium was noted to have too low of a radiation intensity to be effective at any distance for the required depth. Cobalt-60 was developed at Chalk River facilities in Canada, and it was noted that 1 gram of Cobalt-60 produced the same output as 36-96 grams of Radium [54]. These gamma rays were able to be controlled with constructed apparatus that can be rotated to expose the source in a controlled manner. Field sizes were also controlled to allow for fields from 4 cm x 4 cm to 20 cm x 20 cm at 100cm distance. Figure 1.3.1.1 shows a comparison table of Cobalt-60 to 2MeV and 3MeV energies with respect to depth-dose data at 100cm distance and 70cm distance. Radiation therapy was now becoming more accessible and cost effective for use around the world.

**Table 1.2.1.1** – Depth-dose comparison for Cobalt-60 to 2MeV and 3MeV energies at 100cm and 70cm source to skin distances [54].

| Depth (cm) | Field: 100cm2<br>Distance: 100cm | | Field: 100cm2<br>Distance: 70cm | |
|---|---|---|---|---|
| | Cobalt-60 (%) | 2MeV (%) | Cobalt-60 (%) | 3MeV (%) |
| 0.5 | 100 | 100 | 100 | 100 |
| 1.0 | 99 | 98 | 98 | 98 |
| 5.0 | 80 | 79 | 77 | 76 |
| 10.0 | 58 | 54 | 54 | 53 |
| 15.0 | 41 | 37 | 37 | 36 |
| 20.0 | 29 | 25 | 26 | 25 |

The first clinical linear accelerator was developed at Stanford Medical Center in California. Linear accelerators function by accelerating electrons at a high energy using electromagnetic waves. These electrons can then be used directly for superficial therapy or can be used to strike materials in high atomic number to produce bremsstrahlung radiation, photons emitted as electrons slow down in the material [55]. This accelerator, which was designed to operate at 6MeV, was installed in 1955 with the first clinical use beginning in early 1956. It was recognized early that accuracy of treatment would always be in question. With that thought in mind, the linear accelerator was developed with a diagnostic quality x-ray tube that could be used prior to delivery of high energy photons. Figure 1.2.1.1 provides a diagram of the unit used in Stanford.

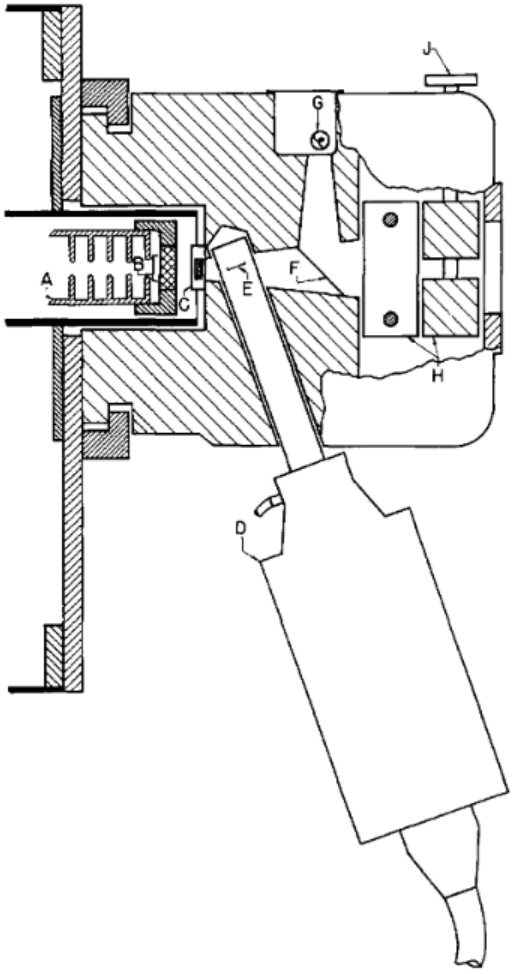


**Figure 1.2.1.1**- Diagram of the first linear accelerator head used in Stanford. End of accelerator (A), output window and target assembly (B), monitor chamber (C), housing of retractable radiographic x-ray tube (D), target of radiographic x-ray tube (E), inclined mirror (F), light source (G) localizer, adjustable lead jaws (H) and field size adjustment knob (J) [55].

High energy x-rays do not produce high quality radiographs so the diagnostic quality x-ray tube can be used to first localize and confirm the patient position. Once this film is developed while the patient and source are not moved, localization can be confirmed, and treatment is then delivered. With the ability to rotate the machine around the patient and capability to control the field size, this represented a significant jump forward towards conformal treatment and minimizing dose to healthy tissues.

Radiation planning was initially only achieved manually with radiographic cross-sectional images. Calculations were crude with many assumptions made to density and overall depth to develop an exposure or delivery time. Radiation planning took a large step forward with the rapid development of computer software and specifically the introduction of the CT scanner. CT scanners became widely used in the early 1970's and soon after were used in radiation planning [56]. Three-dimensional planning did not develop until the 1980's when personal computers and minicomputers became powerful enough to calculate treatment plans in essentially real time [57]. As theoretical ideas were developed, machine capabilities were also advanced. IMRT was suggested in 1982 but not clinically a reality until the early 1990's with the advent of the NMOS MIMiC. A multi-leaf collimator, placed after the primary jaws of the x-ray beam, allowed for a more conformal shaping of the radiation beam to suit individual patient needs. This also allowed modulation of the beam, which could compensate for patients missing tissue as well as vary the intensity of the radiation beam. This technology combined with the ability to have multiple angles around the patient allowed for more conformal treatment that minimized dose to healthy structures nearby. Radiation dose could now safely increase to the tumour while maintaining acceptable dose to the tissues nearby.

### 1.2.2 Importance of dose to organs at risk

Much has been discussed about the need to deliver high radiation doses to tumours while keeping minimal dose to healthy tissues that surround it. While the human body is very complex with many studies conducted on many organs, for the purposes of this study focus will be made on major areas of interest in the thoracic and upper abdominal regions.

*General Radiation Effects*

The field of radiobiology can be associated with the invention of the x-ray in the early 1900's. Skin effects were noticed almost immediately and from there great interest has been developed into the biological effects of radiation on cancerous cells as well as healthy tissues. Cell DNA contains the most vital information with regards to cell growth and lifespan. Ionizing radiation works by damaging cell DNA and therefore effectively killing the cell. Radiation delivered to a cell can work as direct or indirect action. Direct action refers to particles that can disrupt the cell biology by which they pass through. Indirect action does not cause damage by themselves, however the medium which they pass though can absorb the radiation energy and produce a by product of a charged particle which can cause the cell damage. Approximately two-thirds of the damage caused by x-rays and gamma-rays is a result of indirect action [58].

In 1975, a paper titled "The 4 R's of Radiotherapy" was published by HR Withers that summarized a short list of mechanisms that outlined response of biological tissues after doses of radiation [59]. These 4 R's are commonly referred to Repair, Reoxygentation, Redistribution and Regeneration. Another mechanism was suggested in 1989 by Steel *et al* which described radio sensitivity as being an important factor in the mechanism of radiation therapy effectiveness [60]. This is the basis of fractionated radiation therapy.

*Repair*

Radiation damage can be divided into 3 categories: lethal damage, potentially lethal damage and sublethal damage. Lethal damage is fatal to the cell and is damage which is irreversible or irreparable. Potentially lethal damage refers to damage that can be repaired under certain circumstances. Sub lethal damage is damage which can be repaired. It has been shown that there is increase in cell survival if a given radiation dose is split into 2 intervals with sufficient time in between. Normal cells are most likely able to repair themselves before another fraction of radiation is delivered while tumour cells are not. It is commonly accepted that the minimal time interval between radiation fractions should be 6 hours.

*Reoxygentation*

Oxygen is an important radio sensitizer discovered to influence cell death. Oxygen participates in the reactions that lead to cell death after absorption of ionizing radiation [61]. Anoxic cells during irradiation are three times more resistant than cells that are well oxygenated. After radiation, the proportion of hypoxic cells increase. Fractionation allows for enough time to reoxygenate cells and cells that were hypoxic become more susceptible to radiation doses. This process repeats with each fraction and allows for the tumour cells to deplete. This has clinical value as well; it is advisable for patients to minimize substances that reduce oxygenation (smoking).

*Redistribution*

Redistribution or reassortment refers to the progression of cells through the cell cycle (Figure 1.2.2.1) between split radiation doses. Different cell cycles have varying levels of radio sensitivity with the M and G2 phases the most sensitive. After a dose of radiation, the cells that survived would typically be in S-phase which is least sensitive. These cells move into the more sensitive M and G2 phases before the next fraction of delivery. Fractionation increases the chance of a cell being in the radiosensitive phase during treatment.

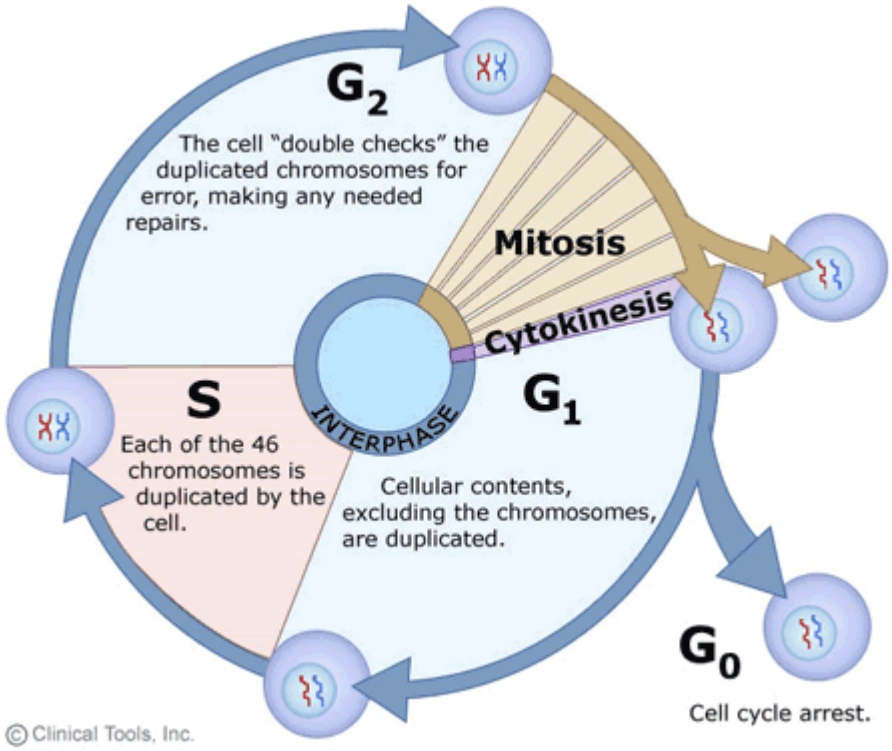


**Figure 1.2.2.1** – Cell cycle [62].

*Regeneration*

A reduction in cells in either tumour or normal tissues results in a response to increase the number of cells to compensate. Regeneration or repopulation refers to cells entering the cell cycle to repopulate cells that were killed during irradiation. This effect occurs in tumour cells as well and it is important to complete treatment as quick as reasonably possible to not encourage faster tumour cell repopulation.

*Radiosensitivity*

Cells from different types of tumours differ in their radiosensitivity based on factors introduced by Bergonie and Tribendau [63]. They noted that if cells are less differentiated, have a greater proliferative capacity and divide more rapidly, they would in turn be more susceptible to the

effects of ionizing radiation. This is an intrinsic effect and helps explain differing doses required for adequate tumour control depending on histology.

*Dose Escalation for Esophageal Cancer*

Determining radiation dosage for the treatment of esophageal cancer has developed along with advancements in planning technologies. A major trial completed by Herskovic *et al* in 1992 demonstrated the new standard approach of combined chemoradiation therapy for patients as a primary form of treatment [64]. Combined chemoradiation with a radiation total dose of 50.4 Gy was superior in local control and overall survival compared to radiation delivered alone to a dose of 64 Gy. With a standard approach of 50.4 Gy established, questions arose regarding dose escalation with respect to improved survival and control. In a 2002 study conducted by Minsky *et al*, concurrent chemo radiation was compared for 2 different dose regimens. Keeping the chemotherapy the same, doses of the standard 50.4 Gy was compared to an escalated 64.8 Gy. This trial was stopped after an interim analysis. There was no significant improvement in local control or overall survival. There were 11 treatment related deaths in the high dose arm compared to 2 in the low dose arm. It was the conclusion of this study that 50.4Gy remained optimal for this subset of patients [65]. In the pre-operative setting, the study conducted by Van Hagen *et al* demonstrates that 41.4 Gy combined with chemotherapy followed by surgery is a valid and tolerated treatment regimen [46]. Safe dose escalation efforts are limited by tolerance dose of organs at risk, treatment conformality and faith in accurate and reproducible treatment setup. In a review published in 2010 by Werner-Wasik *et al*, it was recognized that acute esophagitis was correlated more significantly with doses > 40-50 Gy. In addition, it did appear safe to deliver dose as high as 74 Gy to a segment of esophagus [66].

An article published in 1991 by Emami *et al* has become one of the most widely cited articles with respect to dose tolerance of normal tissues. A taskforce was set up which reviewed current literature and drew on their own experiences to develop a list of tolerance doses based on conventional fractionation of 180 to 200 cGy [67]. Figure 1.2.2.2 represents the results of the endeavour. Doses were tabulated based on 3 volume categories (one-third, two-third, whole

organ) at two dose levels of TD 5/5, which is the probability of 5% complication within 5 years of treatment and TD 50/5 which refers to the probability of 50% complication within 5 years.

| Organ | TD 5/5 Volume | | | TD 50/5 Volume | | | Selected endpoint |
|---|---|---|---|---|---|---|---|
| | $\frac{1}{3}$ | $\frac{2}{3}$ | $\frac{3}{3}$ | $\frac{1}{3}$ | $\frac{2}{3}$ | $\frac{3}{3}$ | |
| Kidney I | 5000 | 3000* | 2300 | | 4000* | 2800 | Clinical nephritis |
| Kidney II | | | | | | | |
| Bladder | N/A | 8000 | 6500 | N/A | 8500 | 8000 | Symptomatic bladder contracture and volume loss |
| Bone: | | | | | | | |
| Femoral Head I and II | — | — | 5200 | — | — | 6500 | Necrosis |
| T-M joint mandible | 6500 | 6000 | 6000 | 7700 | 7200 | 7200 | Marked limitation of joint function |
| Rib cage | 5000 | — | — | 6500 | — | — | Pathologic fracture |
| Skin | $\frac{10\ cm^2}{-}$ | $\frac{30\ cm^2}{-}$ | $\frac{100\ cm^2}{5000}$ | $\frac{10\ cm^2}{-}$ | $\frac{30\ cm^2}{-}$ | $\frac{100\ cm^2}{6500}$ | Telangiectasia |
| | 7000 | 6000 | 5500 | — | — | 7000 | Necrosis Ulceration |
| Brain | 6000 | 5000 | 4500 | 7500 | 6500 | 6000 | Necrosis Infarction |
| Brain stem | 6000 | 5300 | 5000 | — | — | 6500 | Necrosis Infarction |
| Optic nerve I & II | No partial volume | | 5000 | — | — | 6500 | Blindness |
| Chiasma | No partial volume | | 5000 | No partial volume | | 6500 | Blindness |
| Spinal cord | $\frac{5\ cm}{5000}$ | $\frac{10\ cm}{5000}$ | $\frac{20\ cm}{4700}$ | $\frac{5\ cm}{7000}$ | $\frac{10\ cm}{7000}$ | $\frac{20\ cm}{-}$ | Myelitis necrosis |
| Cauda equina | No volume effect | | 6000 | No volume effect | | 7500 | Clinically apparent nerve damage |
| Brachial plexus | 6200 | 6100 | 6000 | 7700 | 7600 | 7500 | Clinically apparent nerve damage |
| Eye lens I and II | No partial volume | | 1000 | — | — | 1800 | Cataract requiring intervention |
| Eye retina I and II | No partial volume | | 4500 | — | — | 6500 | Blindness |
| Ear mid/external | 3000 | 3000 | 3000* | 4000 | 4000 | 4000* | Acute serous otitis |
| Ear mid/external | 5500 | 5500 | 5500* | 6500 | 6500 | 6500* | Chronic serous otitis |
| Parotid* I and II | — | 3200* | 3200* | — (TD 100/5 is 5000) | 4600* | 4600* | Xerostomia |
| Larynx | 7900* | 7000* | 7000* | 9000* | 8000* | 8000* | Cartilage necrosis |
| Larynx | — | 4500 | 4500* | — | — | 8000* | Laryngeal edema |
| Lung I | 4500 | 3000 | 1750 | 6500 | 4000 | 2450 | Pneumonitis |
| Lung II | | | | | | | |
| Heart | 6000 | 4500 | 4000 | 7000 | 5500 | 5000 | Pericarditis |
| Esophagus | 6000 | 5800 | 5500 | 7200 | 7000 | 6800 | Clinical stricture/ perforation |
| Stomach | 6000 | 5500 | 5000 | 7000 | 6700 | 6500 | Ulceration, perforation |
| Small intestine | 5000 | | 4000* | 6000 | | 5500 | Obstruction perforation/fistula |
| Colon | 5500 | | 4500 | 6500 | | 5500 | Obstruction perforation/ ulceration/fistula |
| Rectum | Volume 100 $cm^3$ No volume effect | | 6000 | Volume 100 $cm^3$ No volume effect | | 8000 | Severe proctitis/ necrosis/fistula, stenosis |
| Liver | 5000 | 3500 | 3000 | 5500 | 4500 | 4000 | Liver failure |

*<50% of volume doesn't make a significant change.

**Figure 1.2.2.2** – Normal tissue tolerance published in 1991 [67].

As radiation planning has advanced, so has the need for updated information that could be trusted. QUANTEC (Quantitative Analyses of Normal Tissue Effects in the Clinic) was an initiative that began in 2009 to help modernize dose constraints based on a review of literature since 1991 [68]. Many studies have been conducted both in clinical trails on humans as well as animals to help standardize acceptable risk for normal tissues. The article published in 2010 by Marks *et al* summarizes the methods and findings for an updated clinical reference of tolerance doses [69]. Figure 1.2.2.3 displays tolerance doses to organs of interest in this study.

| Organ | Volume segmented | Irradiation type (partial organ unless otherwise stated)† | Endpoint | Dose (Gy), or dose/volume parameters† | Rate (%) | Notes on dose/volume parameters |
|---|---|---|---|---|---|---|
| Spinal cord | Partial organ | 3D-CRT | Myelopathy | Dmax = 50 | 0.2 | Including full cord cross-section |
| | Partial organ | 3D-CRT | Myelopathy | Dmax = 60 | 6 | |
| | Partial organ | 3D-CRT | Myelopathy | Dmax = 69 | 50 | |
| | Partial organ | SRS (single fraction) | Myelopathy | Dmax = 13 | 1 | Partial cord cross-section irradiated |
| | Partial organ | SRS (hypofraction) | Myelopathy | Dmax = 20 | 1 | 3 fractions, partial cord cross-section irradiated |
| Lung | Whole organ | 3D-CRT | Symptomatic pneumonitis | V20 ≤ 30% | <20 | For combined lung. Gradual dose response |
| | Whole organ | 3D-CRT | Symptomatic pneumonitis | Mean dose = 7 | 5 | Excludes purposeful whole lung irradiation |
| | Whole organ | 3D-CRT | Symptomatic pneumonitis | Mean dose = 13 | 10 | |
| | Whole organ | 3D-CRT | Symptomatic pneumonitis | Mean dose = 20 | 20 | |
| | Whole organ | 3D-CRT | Symptomatic pneumonitis | Mean dose = 24 | 30 | |
| | Whole organ | 3D-CRT | Symptomatic pneumonitis | Mean dose = 27 | 40 | |
| Heart | Pericardium | 3D-CRT | Pericarditis | Mean dose <26 | <15 | Based on single study |
| | Pericardium | 3D-CRT | Pericarditis | V30 <46% | <15 | |
| | Whole organ | 3D-CRT | Long-term cardiac mortality | V25 <10% | <1 | Overly safe risk estimate based on model predictions |
| Liver | Whole liver – GTV | 3D-CRT or Whole organ | Classic RILD†† | Mean dose <30-32 | <5 | Excluding patients with pre-existing liver disease or hepatocellular carcinoma, as tolerance doses are lower in these patients |
| | Whole liver – GTV | 3D-CRT | Classic RILD | Mean dose <42 | <50 | |
| | Whole liver – GTV | 3D-CRT or Whole organ | Classic RILD | Mean dose <28 | <5 | In patients with Child-Pugh A preexisting liver disease or hepatocellular carcinoma, excluding hepatitis B reactivation |
| | Whole liver – GTV | 3D-CRT | Classic RILD | Mean dose <36 | <50 | as an endpoint |
| | Whole liver –GTV | SBRT (hypofraction) | Classic RILD | Mean dose <13 | <5 | 3 fractions, for primary liver cancer |
| | | | | <18 | <5 | 6 fractions, for primary liver cancer |
| | Whole liver – GTV | SBRT (hypofraction) | Classic RILD | Mean dose <15 | <5 | 3 fractions, for liver metastases |
| | | | | <20 | <5 | 6 fractions, for liver metastases |
| | >700 cc of normal liver | SBRT (hypofraction) | Classic RILD | $D_{max}$ <15 | <5 | Critical volume based, in 3–5 fractions |
| Kidney | Bilateral whole kidney‡ | Bilateral whole organ or 3D-CRT | Clinically relevant renal dysfunction | Mean dose <15–18 | <5 | |
| | Bilateral whole kidney‡ | Bilateral whole organ | Clinically relevant renal dysfunction | Mean dose <28 | <50 | |
| | Bilateral whole kidney‡ | 3D-CRT | Clinically relevant renal dysfuntction | V12 <55%<br>V20 <32%<br>V23 <30%<br>V28 <20% | <5 | For combined kidney |

**Figure 1.2.2.3** – QUANTEC Normal tissue tolerance published in 2010 [69].

*Heart*

Acute radiation injury to the heart is rare with much of the radiation induced effects not prevalent for months to decades. However, care must be taken to limit heart dose due to reported increase in cardiovascular disease [70-72]. Much literature for heart tolerance comes from radiation delivered for lymphoma treatment, breast cancer treatment and atomic bomb survivors [73]. The study by Gagliardi *et al* recommended that conservative NTCP model estimates predict $V_{25Gy}$ <10% will be associated with <1% probability of cardiac mortality in ~15 years [74]. Whole heart radiation of 30Gy appeared to be tolerated however a recommendation of limiting to 15 Gy is made. Pericarditis risk increases as demonstrated by a study conducted by Wei *et al* [75]. $V_{30Gy}$ was the only parameter that was significantly associated with pericardial effusion with rates increasing if greater than 46% received 30Gy.

*Kidneys*

The kidneys are an extremely important organ in the human body responsible for filtering blood, modulating blood pressure, and stimulating red blood cell production. Complications from kidney toxicity could include elevated blood pressure, increased weight, edema, coma and even death. In a review conducted by Lawson *et al*, suggestions were made to tolerance doses for kidneys based on studies previously conducted. For less than 5% complication, suggested mean dose ranges from 15Gy (TBI pts) to 18Gy (partial kidney irradiation). In addition, $V_{12Gy}$<55%, $V_{20Gy}$ <32%, $V_{23Gy}$<30%, $V_{28Gy}$<20% were also suggested [76]. With low dose tolerances reported, care must be taken for conformal planning and localization if the treatment area extends into the upper abdomen.

*Lungs*

80% of clinically significant radiation pneumonitis can clinically manifest within 10 months of radiation treatment. In a review by Marks *et al*, over 70 published articles were identified with respect to dose-volume parameters and pneumonitis. While difficult to recommend dose and

volume limits, it was thought to be important to limit $V_{20Gy}$ < 30% and mean lung dose limited to 20Gy. This is in reference to limiting the risk of radiation pneumonitis to <20%. Central dose should be limited to <80Gy to minimize risk of bronchial stricture [77].

*Liver*

Radiation-induced liver disease is a complication of radiation treatment to the liver with clinical presentation of ascites, elevated liver enzymes and hepatomegaly. Tolerance for whole liver radiation is low and a review by Lawson *et al* found that radiation liver disease was seen in 5%-10% of patients with 30-35Gy delivered to the whole liver. Partial liver irradiation could be viable to higher doses provided enough normal liver is spared from high doses [78]. It was found that liver had a large relation to volume effects and therefore mean dose may be useful to set limits. In patients without pre-existing liver disease, a mean dose < 30Gy is suggested to minimize risk of complication.

*Spinal Cord*

Radiation injury to spinal cord is rare but can be severe leading to pain, sensory deficits and even paralysis. Taking a closer look at the whole spinal cord cross section, maximum dose limits of 50Gy, 60Gy and ~69 Gy were recommended by Kirkpatrick *et al*. These doses represented a 0.2%, 6% and 50% rate of myelopathy respectively [79].

*Integral Dose*

Radiation therapy is associated with a small but significant risk of secondary malignancy. With advanced planning techniques able to deliver radiation from multiple angles to achieve a high dose conformality, there is a concern for low dose spread due to the increase in angles. Furthermore, there can be a monitor unit increase in beams delivering more conformal treatments which increases leakage and potential for further low dose spread. Integral dose can be defined as the volume integral of the dose deposited and is equal to mean dose times the

volume of irradiated tissue at any dose [80]. In a study by Aoyama *et al*, it was concluded that in their study of 25 patients the difference in non tumour integral dose was small between 3DCT and IMRT. Further, higher energy beams reduced integral dose. In another study be D'Souza *et al*, variation in NTID with 4 or more beams was minimal. A further study by Patel *et al* in the pediatric treatment of whole CNS found that mean NTID was lower with VMAT treatment compared to 3D-CRT and helical TomoTherapy. There was an increase in the mean of low doses (1Gy, 2Gy and 5Gy) but larger reductions in high doses of 20Gy-30Gy [82].

### 1.2.3 Current radiation planning

Accurate delivery of radiation therapy is a complex procedure with many disciplines involved in ensuring theory meets reality. After the patient and physician make the determination that radiation therapy would be in the best interest of the patient, processes are in place to accurately immobilize the patient for treatment, identify the area of treatment and plan for radiation doses to be delivered to tumour cells.

*Immobilization*

The success of radiation therapy relies on delivering a therapeutic dose to tumour cells while minimizing dose to healthy surrounding tissues to allow for healing. One of the first steps to achieve this is to immobilize the patient in a reproducible manner that is achievable for the patient while satisfying requirements for the most efficient planning and treatment. A review by Saw *et al* outlines some of the technologies in use for immobilization including thermoplastic casts as well as Vac-Lok bags [83]. Thoracic radiation immobilization studies are limited and even more so for esophageal treatment. Li *et al* evaluated 2 different methods of immobilization used at their facilities and found that combined with image guidance there was no statistical difference with respect to setup accuracy [84]. The use of CBCT allows for selection of an immobilization device that is cost effective and efficient for the department to use. At the Juravinski Cancer Centre, non-SBRT patients are typically immobilized with a chest board which allows for a consistent head rest and chin position. Arms are then up and out of the way of the

radiation beam while holding a handlebar set at a comfortable position for the patient. Figure 1.2.3.1 shows an immobilization device used for thoracic radiation. A cushion is also placed under the patient's knees for added comfort and to take pressure off the lower back.

**Figure 1.2.3.1** – Vac-Lok immobilization bag for thoracic or upper abdomen localization [84].

*Localization*

*4D-CT*

After the patient has been immobilized, care must be taken to select the most effective tools available to evaluate the extent of the tumour. Where uncertainties exist, general practice has been to cover extra tissue to ensure that cancerous cells are not missed. Radiation planning conducted with CT scanners initially used a free breathing approach where the patient would breathe normally while being scanned. The result was what appeared to be a blurring of certain organs with motion artifact. Balter *et al* published a paper in 1996 that recognized uncertainties associated with free breathing in treatment planning of the esophagus or upper abdomen. Patients were scanned with a free breathing scan then once while holding their breath at normal inhalation and again at exhalation. Liver and kidney movement was noted to be 2cm and PTV path length differences of >1cm were noted [85]. It was not until 2003 that a method to efficiently obtain a 4D-CT was formalized [86]. The underlying objective in the approach of 4D-CT scans is to acquire helical CT images while recording the patients breathing pattern. The data is

then reorganized, and CT data sets are available in multiple phases of breathing. Most interest in radiation planning lies in the maximal inhalation and exhalation phases to properly assess tumour and normal tissue motion. One of the first studies to evaluate respiratory motion for distal esophagus patients was conducted by Yaremko *et al* in 2008. The intra-abdominal esophagus was found to be one of the most mobile sections of esophagus with movement of 1.06 +- 0.04cm along the central axis. It was concluded that esophageal GTV stayed within a radial margin of 0.8cm and an axial margin of 1.8cm [87]. This also provides guidance to centers without the use of 4D-CT to account for tumour motion. A study conducted by Brandner *et al* for abdominal organs demonstrated an average displacement in the superior to inferior direction of 1.3cm for liver, 1.3cm for spleen, 1.1cm for left kidney and 1.3cm for right kidney [88]. These results have implications with respect to planned dose and delivered dose to organs at risk. While there are numerous benefits of using 4D-CT there are also other factors to consider. Some centres are not equipped with the technology and computing power to process thousands of images in relation to breathing phases. Also, there is an increase in exposure during a 4D-CT compared to that of a normal scan. In a study by Mori *et al*, it was demonstrated that 4D-CT led to approximately 4 times higher exposure compared to conventional CT scanning [89]. Protocols have been developed to minimize excessive dose during 4D-CT and care must be taken to minimize repeat scans. During the period of retrospective analysis of this study, 4D-CT was not routinely used for esophageal patients. Care was taken to appropriately contour primary disease with adequate margins to account for intrafractional motion.

*Clinical Imaging*

In addition to CT images used in planning, other modalities such as PET and MRI can be used to aid in target delineation. While imaging in the treatment position is ideal, diagnostic images can be brought in the planning software and automatic fusion can be completed. PET utilizes biological based information to provide clinicians with information on cancer location and grading. PET scanning uses a radioactive material attached to a sugar to identity tissues that are using high amount of energy such as cancer cells. The radioactive material gives off positrons which is recorded and overlaid with a corresponding CT scan to identify the exact location of

uptake [91]. PET is often able to provide superior sensitivity, specificity and accuracy compared to conventional staging modalities [92]. PET is an excellent candidate to be used in conjunction with standard CT scanning for esophageal cancer planning due to accurate nodal delineation as well as displaying longitudinal extent of disease. In a study by Duong *et al*, the findings of PET scans impacted the management of 40% of the studied patients [93]. In another study conducted by Zabotto *et al*, GTV alterations took place in 56% of patients with the use of PET scanning [94]. PET scans have proven to be of beneficial use in the population of esophagus patients undergoing radiation treatment. The limitations lie with cost and timely availability in a socialized health care setting.

MRI can also be used in treatment delineation in much the same way as PET imaging. MRI is non-invasive and provides excellent soft tissue contrast. In a review conducted by van Rossum *et al*, it was noted that earlier iterations of MRI were inferior in accuracy due to limited technology and image sequencing [95]. Studies comparing the effectiveness of MRI to PET in target delineation is limited and therefore routine use of MRI in radiation planning for esophageal patients is minimal. However, in a study conducted by Vollenbrock *et al*, promising results were demonstrated with the use of MRI. GTV delineation was smaller overall on MRI when compared to PET. Variability was also similar to that of PET among physicians. Further work is required to develop proper protocols for esophagus imaging as well as a consensus guideline for contouring based on MR imaging [96].

*Treatment Planning Software*

With the computerization of the world advancing life in many aspects, so too was radiation treatment planning. The use of CT offered 3D perspective on patient anatomy and tumour volumes. However, methods to accurately calculate dose that would be delivered to the patient were still required and not developed until the late 1980's into the early 1990's. Mohan *et al* described a method of 3D radiation planning that could be carried out with the aid of a computer system [97]. Major advancements introduced were the use of beams eye view, accurate dose calculation, beam compensation, rotational beams, and tools for plan evaluation. Dose volume histograms summarize dose information by plotting percentages of volume at

various dose levels. At the time of this development, there was enormous amounts of spatial data generated so comparison of plans for the same patient was limited. Dose calculation in heterogeneous tissues of a patient have also developed. The Monte Carlo simulation is one method of calculating the energy departed on tissues that also considers secondary methods of transport [98]. Ander Ahnesjo described the collapsed cone convolution method which is an efficient way to calculate dose in the presence of inhomogeneity. Other methods have also been developed such as the anisotropic analytical algorithm and multigrid superposition/convolution [99]. These calculation methods serve as the base of major clinical radiation treatment planning software. In the case of this study, Philips Pinnacle treatment planning software was used to generate all plans.

*3D-CRT*

Conformal treatment with use of multiple angles was theorized early in the megavoltage era of radiation therapy [100]. As mentioned earlier, the routine use of the CT allowed for accurate delineation as well as dose calculation due to electron density information obtained directly from the scan. Along with software development, hardware was also being developed and the first computer controlled multi-leaf collimator was developed in Sweden [101]. A multileaf collimator consists of 2 sets of thin tungsten leaves that could be modulated to shape around a target in the head of the machine. Physical lead shielding would not be necessary making this an effective way to modulate a radiation beam. Another function of the multileaf collimator is the compensation effect that is possible. In areas of the patient where less radiation is required for a certain beam angle, the multileaf collimator can close a portion of the field to ensure that no overdose to that region occurs while still delivering radiation to the required area. Much of the early benefits of 3D-CRT came in the form of safe dose escalation. In a study by Zelefsky *et al* that began accruing in 1988 and was published in 1998, there was a significant advantage of dose escalation in prostate treatment with the use of 3D-CRT. Highly conformal plans were able to confidently be developed while minimizing high doses in bladder and rectum [102]. Fiveash *et al* confirmed these findings in a multi-institutional review for high grade prostate treatment [103]. Similar results were noted with conformal treatment to lung. Dose escalation was now a

possibility with the improvement in doses to organs at risk [104-105]. Due to radical treatment for esophagus patients being in lower frequency compared to other sites, studies determining effectiveness of 3D-CRT were limited. With studies of other sites demonstrating the value of 3D-CRT, esophagus treatment followed suit. However, a study by Guzel *et al* attempted to evaluate conventional planning with 3D-CRT. It was determined there was benefit in a two-phase approach to reducing lung dose [106]. Around the same time, a study of clinical practice across Canada was done which indicated that widespread adoption of conformal treatment had not yet taken place for cervical esophagus treatment [107]. In the major study published by the CROSS group to evaluate effectiveness of concurrent chemoradiation to chemotherapy alone in pre-operative patients, 3D-CRT was used as the radiation technique. Radiation was planned using a multifield technique with a combination of anterior/posterior, oblique or lateral fields. Fields were customized with blocks or multi-leaf collimator. This validated the effectiveness of this treatment technique for confident use in distal esophagus and GE junction patients [108].

*IMRT*

Intensity modulated radiation therapy was the next major breakthrough in radiation planning and delivery. The first suggestion of modern day IMRT came from the work of Brahme *et al* in 1982 [109]. In a basic sense, the goal of IMRT is to modulate the intensity of incoming radiation beams to allow for high conformality of treatment. Radiation beams are then able to reduce intensity through sensitive critical structures while increasing intensity into tumour tissues [110]. With modulation of one beam, this would result in areas of hot and cold within the target. Therefore, there is a reliance on multiple beams to compensate for this and provide multiple avenues of delivery. While theoretical algorithms were being developed in the 1980s and early 1990s, it wasn't until the widespread use of MLC that accurate delivery became convenient and achievable. With 3D-CRT, radiation planning was done in a trial-and-error approach. The field parameters are setup, and the planner alters the intensity and angle of beams until an acceptable dose distribution is achieved. This is also known as forward planning. IMRT utilizes what is referred to as inverse planning. When dose objectives and target prescription are known, field parameters are found using a computerized algorithm which in turn eliminates the trial-

and-error approach. This however does come at a cost of computing power and time as these are mathematically very intense calculations [111]. One of the first clinical applications of IMRT based planning came in the treatment of prostate cancer. Ling *et al* demonstrated an acceptable method of inverse planning with modulation done using dynamic multileaf collimators. There was reduction in high dose to rectum while also recognizing that radiation planning could become less labour intensive [112]. The clinical benefits were published by Zelefsky *et al* in 2000 with IMRT proving to provide lower dose to rectal and bladder walls and patients having reduced rates of grade 1 and 2 rectal toxicities [113]. Similar results were noted in various tumour sites [114-117]. Esophagus cancer treatment was not a focus of study until a few years later when IMRT was well established at multiple treatment sites. In an early study by Nutting *et al*, 4 field conformal treatment was dosimetrically compared to 9 field IMRT as well as 4 field IMRT. The 9 field IMRT did not provide much benefit due to increase in low dose setting. 4 field IMRT was able to provide improvement in lung sparing while providing acceptable dose homogeneity [118]. This sheds some light on the importance of beam placement for specific target volumes. Wu *et al* sought to compare conformal treatment with inversely planned conformal treatment as well as IMRT. With the use of a 5 beam IMRT plan, it was found that lung volume that received less than 25 Gy was significantly reduced. There was also significant reduction in heart mean dose as well as spinal cord maximum [119]. These reductions allow the possibility of dose escalation and potential decrease in longer term toxicity. A further study by Chandra *et al* demonstrated that multiple beam IMRT such as 7 or 9 beams resulted in lower lung irradiation and improved conformity. This contrasted with the study by Nutting and could be attributed to different planning algorithms or planning philosophy. The authors recognized the need to limit low dose to lung and therefore entry of multiple beams and suggested that 5-6 beam IMRT to be sufficient [120]. Median improvement for Lung $V_{10Gy}$ was 10% and mean lung dose reduced 2.5Gy when comparing IMRT to 3D-CRT. Fenkell *et al* also demonstrated improvement in cervical esophagus planning with reduced dose to spinal cord, brainstem, and parotids [121]. These studies demonstrate that implementing IMRT for esophageal treatment is a viable option. While 3D-CRT is still an appropriate treatment technique with excellent target coverage, IMRT can provide increased dose sparing to critical structures such as the heart and lungs. A meta-analysis by Xu *et al* found limited but positive studies with respect to benefits of IMRT over 3DCT. There

was improved dosimetric values in organs at risk and a noted increase in overall survival based on 3 studies. More studies are required to draw conclusions with respect to potential benefit in overall survival for esophagus cancer patients [122].

*VMAT*

The theory of volumetric modulated arc therapy can be traced back to a paper published by Yu in 1995. IMAT was presented as an idea to deliver continuous radiation in an arc around the patient while adjusting the field shape with MLC as the gantry rotates [123]. This technique was limited at the time with MLC limitations as well as length of time for delivery. Multiple arcs were required for different radiation intensities with total delivery time reaching 15 minutes. This technique was not investigated with much interest at the time, and it was not until 2008 when Karl Otto published an article on VMAT that this technique gained interest in the wider community. In his paper, Otto describes VMAT as a technique that can be delivered efficiently with a single arc, high conformality with a full 360 degrees of gantry direction as well as accurate beam sampling during planning [124]. VMAT can modulate gantry speed and dose rate to maximize an IMRT like treatment with the maximum possible beam orientations. This modulation of a multitude of factors allows for efficient delivery of radiation in terms of time as well as minimizing monitor units or radiation output. Reduction in monitor units allows for a reduction in scatter and minimizing low dose to the patient. Multiple full arcs or even partial arcs can be planned depending on the clinical situation.

One of the earliest studies comparing VMAT to IMRT and 3D-CRT was conducting in the prostate disease site. Palma *et al* utilized 10 datasets to create a 3D-CRT, five-field IMRT, constant dose rate VMAT and variable dose rate VMAT plans. Variable dose rate VMAT achieved the most desirable plans with significant sparing of rectum and femoral heads as well as a 42% reduction in monitor units when compared to IMRT [125]. Figure 1.3.3.2 demonstrates beam arrangements for 3D-CRT, IMRT and VMAT respectively. In another study conducted by Zhang *et al*, 11 prostate cancer patients were planned with VMAT and IMRT. A similar conclusion was made in the reduction of rectal wall dose, which decreases normal tissue complication

probability. However, the major benefit noted was a 55% reduction in beam on time which reduces intrafractional motion and increases efficiency of delivery [126].

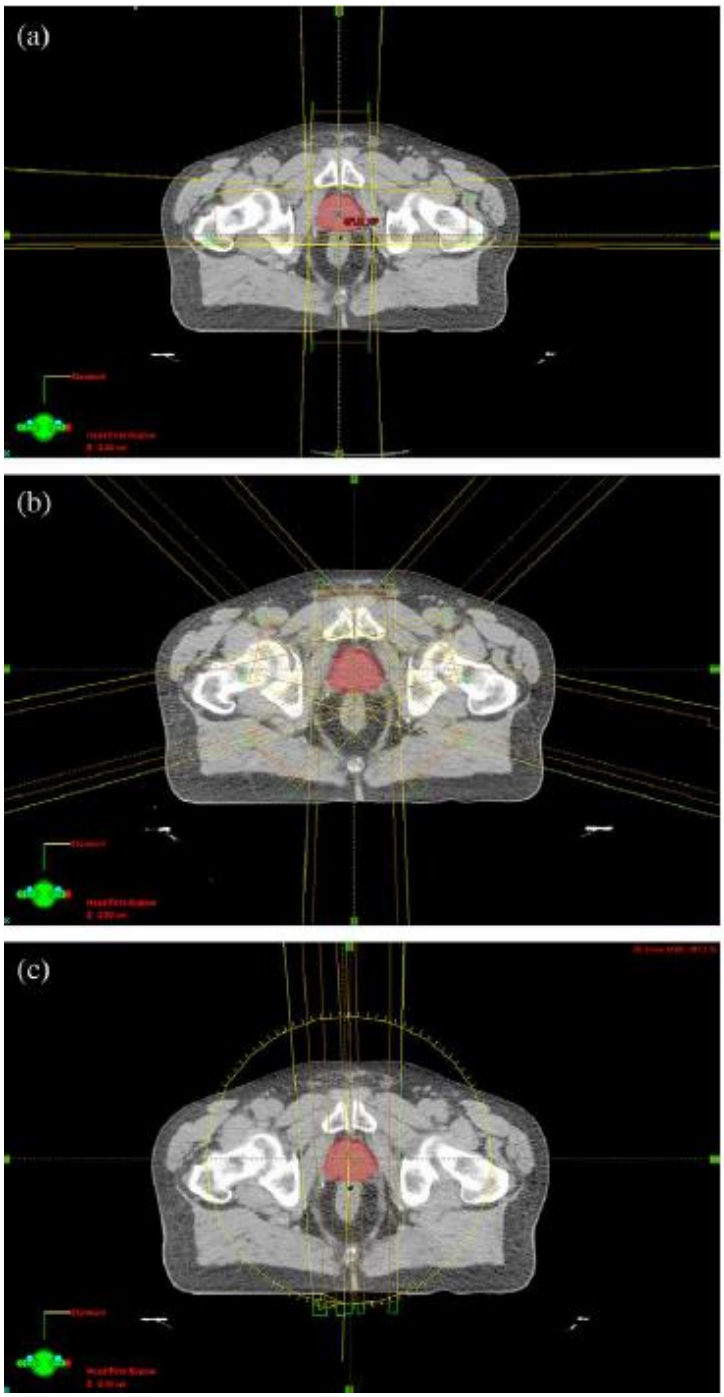


**Figure 1.2.3.2** – Axial CT image in the plane of the prostate displaying beam arrangements for (a) 3D-CRT, (b) IMRT and (c) VMAT [125].

Other disease sites also report positive results with the implementation of VMAT planning and delivery. Head and neck cancer is a complex disease with a challenging radiation treatment plan involving sparing of several critical structures. Verbakel *et al* demonstrated that VMAT plans allowed for a similar sparing of organs at risk while reducing monitor units by 60% [127]. In a larger study conducted by Vanetti *et al*, 29 patients were planned with IMRT, single arc VMAT and double arc VMAT. 2 arc plans yielded the best target coverage and homogeneity while both arc plans reduced dose to organs at risk when compared to IMRT [128].

In most dosimetry studies that evaluated VMAT with 3D-CRT, it is clear that VMAT offers superior dose conformity and sparing of OAR. Some disease sites, such as GU or Gynae, have significant advantages which warrant the implementation of VMAT treatment. Compared with IMRT, the differences are decreased as IMRT can provide highly conformal treatment. There are still advantages in OAR sparing but the major advantage between VMAT and IMRT lies in a reduction of monitor units and delivery time. More efficient delivery and less treatment time is advantageous in a clinical setting under constant financial duress.

Although VMAT can deliver highly conformal treatment, it does so while delivering radiation 360 degrees around a patient. There are conflicting reports on integral dose when comparing VMAT and IMRT. For IMRT plans, beams are delivered in several fixed, static beams. Zhang *et al* report that normal tissue dose in intermediate or high dose range (28-48 Gy) is lower in VMAT but higher in the low dose range below 22 Gy [126]. This does correspond to expectations as low dose spread is expected to be increased with a radiation beam being modulated as it moves around the patient. In a study by Slosarek *et al*, integral dose was analyzed between CyberKnife, TomoTherapy, VMAT and IMRT plans. Integral dose to the whole body was calculated as ID [Gy · L] = $D^{-}$ [Gy] · V [L], where $D^{-}$ [Gy] is the mean dose delivered to volume V [L] (where L – liter) [129]. The results differed significantly with CyberKnife and TomoTherapy having the highest integral dose to body and IMRT and VMAT having the lowest respectively. In a study of treatment techniques for cervical cancer, Cozzi *et al* found a similar reduction in the medium to high dose (20 Gy to 30 Gy) in VMAT plans compared with IMRT. Also noted was a reduction in low dose volume [130]. Part of the potential for lower integral dose in VMAT plans is the

consistent discovery of less monitor unit delivery and less beam on time. As a result, there would be less MLC leakage as well as less scatter dose. Low dose spread becomes a significant concern in certain treatment pathways such as pediatric cancers. There is an increased risk of radiation-induced secondary malignancy in patients treated with external beam radiation at a young age. In a study by Lee *et al*, VMAT was compared to 3D-CRT for craniospinal treatment of pediatric patients. With respect to integral dose, there was a significant reduction in the volume of 10Gy and 15Gy irradiated with VMAT compared to 3D-CRT. There was an increase in the 2Gy and 5Gy volumes [131]. Benefits and risks need to be assessed on an individual case basis before determining the most effective treatment technique.

While VMAT and IMRT can provide higher conformality of treatment, there is concern with increased low dose delivery and spread within the patient. Ruben *et al* sought to quantify the effect of IMRT on radiation induced secondary malignancy [133]. Existing 3D-CRT plans were restored and equivalent IMRT plans were developed. Plans were then delivered to a phantom with TLD's evenly distributed through the normal tissue. Much of the data of radiation induced malignancy comes from atomic bomb survivors. Since conditions of therapeutic treatment and atomic bomb data differ significantly, data must be interpreted appropriately with respect to dose and fractionation. In this study, the carcinogenic risk is comparable with IMRT compared to 3D-CRT. Despite low dose spread out to more tissue in the body, the effect of this was found to be minimal. One concern with IMRT is the increased monitor units which in turn leads to increased leakage from the head of the machine. This leakage could also increase dose to the total body however again the increased risk was found to be negligible. In a study of breast cancer patients conducted by Abo-Madyan *et al*, the group assumed that cancer incidence is directly related to organ equivalent dose. Doses to the contralateral breast and lungs were used to determine if there was an increase in secondary malignancy [134]. It was found that tangential IMRT had a similar risk as 3D-CRT but multi-beam IMRT and VMAT represented a 34% increase using a linear model and 50% increase with a linear-exponential model. It should be noted that the authors concluded that although the relative risk between methods may be significant, the absolute risk remains low. Clinically, the results may be relevant if VMAT or multi-beam IMRT were adopted as routine for younger patients. When deciding on treatment

techniques, a multitude of factors needs to be considered. Not all patients are candidates for more advanced treatment techniques due to possible draw backs of these technologies. With respect to this study, concern with integral dose and secondary malignancy always remains. However, with difficult outcomes expected with this subset of patients and the relative older age of the population, secondary malignancy becomes less of a concern compared to acute toxicity and disease control.

*Esophagus radiation treatment advances*

As mentioned earlier, radiation treatment has evolved across all disease sites. What was once treated based on orthogonal x-rays has developed into 3D planning with accurate target delineation. 3D-CRT remained the standard of care for many years for radiation treatment of esophagus cancer. In the major study comparing neoadjuvant chemoradiation plus surgery with surgery alone, 3D-CRT was used as the standard with positive results that has guided the standard of care for distal esophagus patients [47]. 3D-CRT does provide excellent tumour coverage with a relatively simple treatment planning and delivery technique. This allows for efficient planning and treatment without compromising the intent of treatment. Doses to organs at risk would be adhered thereby allowing confidence in this technique. IMRT studies have been conducted and as mentioned previously, reductions in lung, heart and spinal cord dose are evident. With highly conformal treatment, there is excellent control of medium to high dose. There is a potential for increase in low dose to peripheral tissue such as lung however that can be mitigated with careful beam selection and planning parameters. Long term studies on the benefits of IMRT compared to 3D-CRT are limited. While the theoretical benefit of dose reduction to organs at risk is evident, real-world results for this subset of patients are lacking. This is a difficult disease to treat and long-term survival for this subset of patients is underwhelming. Nonetheless, a study conducted by Lin *et al* sought to compare overall survival and locoregional recurrence between IMRT and 3D-CRT. It was found that at this institution there was a significant improvement in overall survival and locoregional control in IMRT treated patients compared to 3D-CRT [135]. There was no difference noted in cancer-specific mortality or distant metastasis. There was an excess in non-cancer related deaths in the 3D-CRT group

which the authors partially attribute to potential toxicity to OAR. There was a weak link identified with potentially increased cardiac dose and non-cancer related death. The authors do note that many of the 3D-CRT non-cancer related deaths had causes unknown as patients were not followed by this group specifically. In another study conducted by Haefner *et al*, comparison was made between 3D-CRT and IMRT with respect to outcomes and acute toxicity. This study contrasted the study presented by Lin *et al* as no survival benefits were noted [136]. IMRT was used in dose escalation for this subset of patients which the authors do suggest was an influence on the improved local relapse rate of IMRT compared to 3D-CRT. This study does support possible safe dose escalation but again the data is conflicting on overall benefit. Regardless, because of the organ sparing of IMRT dose escalation is a feasible endeavour. Interestingly, there was a notable increase in dysphagia (70.5% for IMRT vs 42.9% in 3D-CRT). This could be in relation to the higher dose delivered with IMRT techniques.

VMAT has demonstrated an improvement over IMRT with respect to plan quality or reduction in monitor units in several studies for various disease sites such as prostate, cervical cancer and head and neck disease. Large scale studies for esophageal cancer are limited. Earliest studies date back to 2011 when VMAT was well established for other disease sites. In a study conducted by Van Benthuysen *et al* 14 patients were retrospectively analyzed to compare IMRT to VMAT. From a dosimetric perspective, results were similar for IMRT vs VMAT with respect to doses to OAR. Interestingly, the authors found that IMRT had a slightly more homogenous dose distribution as VMAT had cold spots within the GTV [137]. Figure 1.2.3.3 displays an axial slice of a dose distribution comparing IMRT and VMAT which demonstrates the increased homogeneity of the IMRT plan.

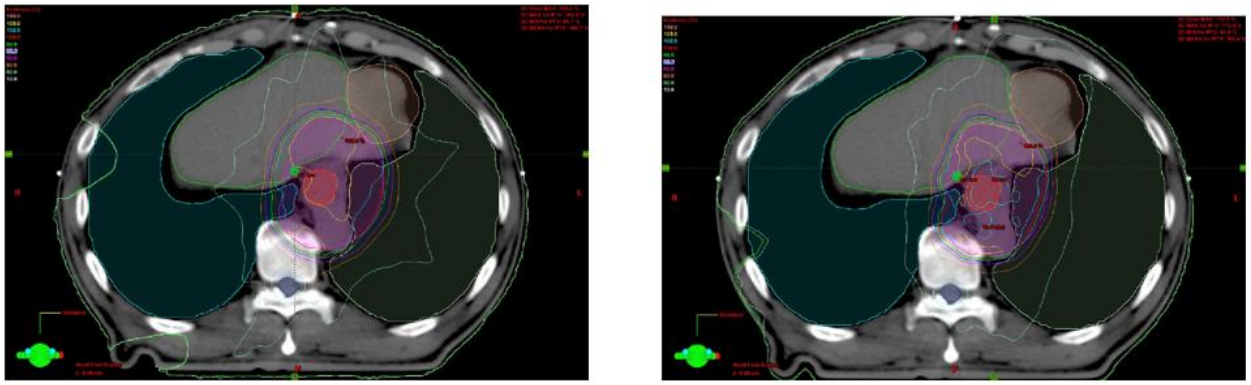

**Figure 1.2.3.3** – Axial image demonstrating dose distribution of IMRT (left) compared to VMAT (right) [137].

While VMAT was not superior in terms of plan quality, there was a noticeable improvement in the reduction of monitor units required for treatment. Reduction in monitor units could lead to decreased treatment and as discussed earlier a reduction in scatter dose. To measure low dose spread the authors investigated body $V_{5Gy}$ which was the volume of the body receiving 5 Gy. There was an increase in body $V_{5Gy}$ for VMAT plans with an average additional 15% of body volume receiving 5 Gy. This study is limited in the sample size which makes it difficult to draw any significant conclusions. There was also limited information in the decision to plan most patients with a single arc vs 2 arcs in the VMAT plans. It appears the decision may have been arbitrary. The method of introducing the 2$^{nd}$ arc for the limited patients is also interesting as it was not optimized that way from the beginning. Rather, the second arc was added after a plan with one arc was optimized. This could limit the efficiency of the optimizer as in our experience the treatment planning software is better able to optimize with 2 arcs from the beginning when most degrees of freedom are available to the computer planning software. In another study conducted by Yin *et al*, IMRT was compared to VMAT for cervical, upper, middle, and lower thorax esophagus patients. 20 patients were included in this study, and it was noted that in middle and lower thoracic treatment areas, homogeneity was similar. Lung $V_{20Gy}$ and $V_{30Gy}$ were lower in VMAT however $V_{5Gy}$ and $V_{10Gy}$ were increased [138]. VMAT was concluded to have similar OAR sparing with better PTV coverage and a reduction of monitor units. While this study does include a slightly higher sample size than the previous study, it is again limited as there were multiple sites of focus. The esophagus is a long organ that spans over multiple areas of the

body with each area presenting a unique challenge in treatment. By limiting each site to only 5 cases there is difficulty in making significant conclusions about treatment technique. In another study conducted by Wu *et al*, 3D-CRT was compared to both IMRT and VMAT for 8 middle esophagus patients. 3D-CRT was conducted with an antero-posterior and postero-anterior beam arrangement for 18 fractions followed by 12 fractions of off-cord beams. IMRT was limited to 5 beams and VMAT to 1 arc. The authors concluded that all treatment techniques were able to meet PTV coverage requirements sufficiently. IMRT and VMAT only decreased high dose delivered to the heart or lungs but increased low dose delivered. Monitor unit delivery was lowest in 3D-CRT followed by VMAT then IMRT. The authors also document optimization time of VMAT was significantly longer than that of IMRT. 3D-CRT also had the lowest time to calculate final dose and shortest delivery time [139]. This study was one of the few that included 3D-CRT in the comparison to IMRT and VMAT. The authors conclude that 3D-CRT is still a feasible option especially from a cost-effective perspective. Again, this study was limited to a sample size of only 8 patients. 3D-CRT planning was completed in a two-phase approach with the majority of treatment coming from two beams. This can influence the results as one would expect a slightly high heart dose and decreased lung dose at the expense of target conformality and dose homogeneity. Also, this can decrease the amount of low dose delivered to lungs but again at the cost of those parameters as well as increased spinal cord dose. A study conducted by Munch *et al* investigated not only dosimetric parameters but also acute toxicity and overall survival. Dose-volume histograms were used to compare the 17 patients treated with VMAT and the 20 patients treated with 3D-CRT. As has been consistent with the previous studies discussed, lung $V_{5Gy}$ and $V_{10Gy}$ as well as heart $V_{5Gy}$ and $V_{10Gy}$ were higher in the VMAT group compared to 3D-CRT. VMAT provided better lung and heart $V_{30Gy}$ as well as lower heart median dose [140]. Despite these dosimetric differences, there was no clear clinical benefit. This could be in part due to the small number of patients included in study as well not having enough time to follow up possible complications to organs such as the heart. In addition, the same patient cohort was not compared in planning. There are multiple factors that could influence dosimetric results such as target volume size and organ size and location. It would be difficult to make dosimetric conclusions based on different base data sets. There is no mention of possible monitor unit reduction or efficiency of treatment.

While studies of treatment techniques for this disease site is limited, there are some studies comparing VMAT with IMRT and 3D-CRT. Study samples are generally small to draw any significant conclusions however certain trends can start to be identified. This study hopes to address this gap in research and provide clear guidance on the selection of treatment technique for distal esophagus patients.

### 1.3 Objectives, Aims and Hypothesis

The objectives and aims of this study are to compare the radiation dose delivered to OAR and target volumes for 3D-CRT, IMRT and VMAT external beam radiation techniques for preoperative esophageal radiation treatment. In particular, investigation will be made on a large dataset with dose to heart, lungs, kidney, spinal cord, liver, general body tissues and target volumes analyzed and compared. In addition, evaluation will be done to determine which technique would be most beneficial with respect to tumour location and size. This data will provide insight into which treatment technique would be advisable to institutions with the capabilities.

It is expected that doses to critical structures will be reduced with the more conformal radiation planning techniques of VMAT and IMRT. Similar studies in other disease sites have shown improvements with more advanced planning techniques to quantitatively reduce the dose to OAR around a target volume. This study will address both the volumetric doses received by the OAR of interest as well as the total mean doses received to these organs using both techniques. It is hypothesized that there will be a decreased lung $V_{20Gy}$ as well as mean dose with concomitant $V_{5Gy}$. It is also expected to see decreased heart $V_{30Gy}$ and mean dose. If there is a statistically significant difference in doses to OAR, these results will be used to influence the radiation planning approach in the treatment of these patients. There is a potential for future studies to address the quantitative benefits of reduced long-term toxicities to the heart and lungs in this patient population.

## 2.0 Patients and Methods

*Patient Information and set-up*

Forty patients who underwent pre-operative chemoradiation between 2012-2014 to the distal esophagus were selected for this study. Approval was obtained from Hamilton Health Sciences Research Ethics Board for retrospective analysis of patient charts. The patient list was retrieved from MOSAIQ Radiation Oncology Information System (Elekta, Sweden). The sample size of forty patients was determined to be a statistically significant number of patients based on the variance of the first few patients who were planned. Patients were simulated head-first supine with arms above their heads. No contrast was used for target delineation. Standard 3mm slice CT images were used for planning. The physician contoured the GTV in thirty-five cases, the CTV in four cases and the PTV directly in one case. PTV margins were determined by the treating physician with a standard margin of 1 cm uniform, except 2cm superiorly and inferiorly from the target volume. PTV was modified by the treating physician as desired to accurately encompass the treatment area. The PTV volume ranged from 219.3 $cm^3$-1883.7 $cm^3$. Thirty-three males and seven females were included in this study. For the purpose of this study the heart along with lungs, spinal cord, kidneys, and liver were delineated as OAR.

*Planning*

All patients treated during this time period were planned and treated with 3D-CRT. At the time of initial planning and treatment, heart contouring was not standardized. Therefore, the original 3D-CRT plan was re-optimized with the heart now included. Other OAR such as lungs, heart, liver, spinal cord, and kidneys were checked and contoured if not already done so. All contours done for the purpose of this study were corroborated by a staff Radiation Oncologist. One patient had a single kidney. Optimization structures were created for IMRT and VMAT plans, and all plans were optimized to maintain target coverage while reducing dose to OAR with specific focus on lung and heart dose. All patients were planned in Pinnacle planning system version 9.10 (Phillips, USA). Dose computation was completed using Adaptive Convolution

method. Plans were calculated with a dose resolution of 0.25cm x 0.25cm x 0.25cm. All plans were optimized to ensure that at least 95% of the PTV received 95% of the prescribed (45 Gy) dose. The maximum dose was limited to 107% of the prescribed dose. Figure 2.1 represents the axial image at isocenter for 1 case of all treatment techniques. All plans were completed by the study investigator with experience in the treatment planning department of the Juravinski Cancer Centre. Plans were checked and evaluated by a staff Medical Physicist at the Juravinski Cancer Centre to evaluate treatment plan efficiency, feasibility, and deliverability.

Inter-rater reliability with an experienced dosimetrist in the Radiation Therapy department was assessed. Fifteen patients were re-planned by the dosimetrist for each treatment technique and results were evaluated compared with the study investigator. Krippendorff's alpha was calculated to evaluate agreement between plans. Calculations were completed with MATLAB software (Massachusetts, USA).

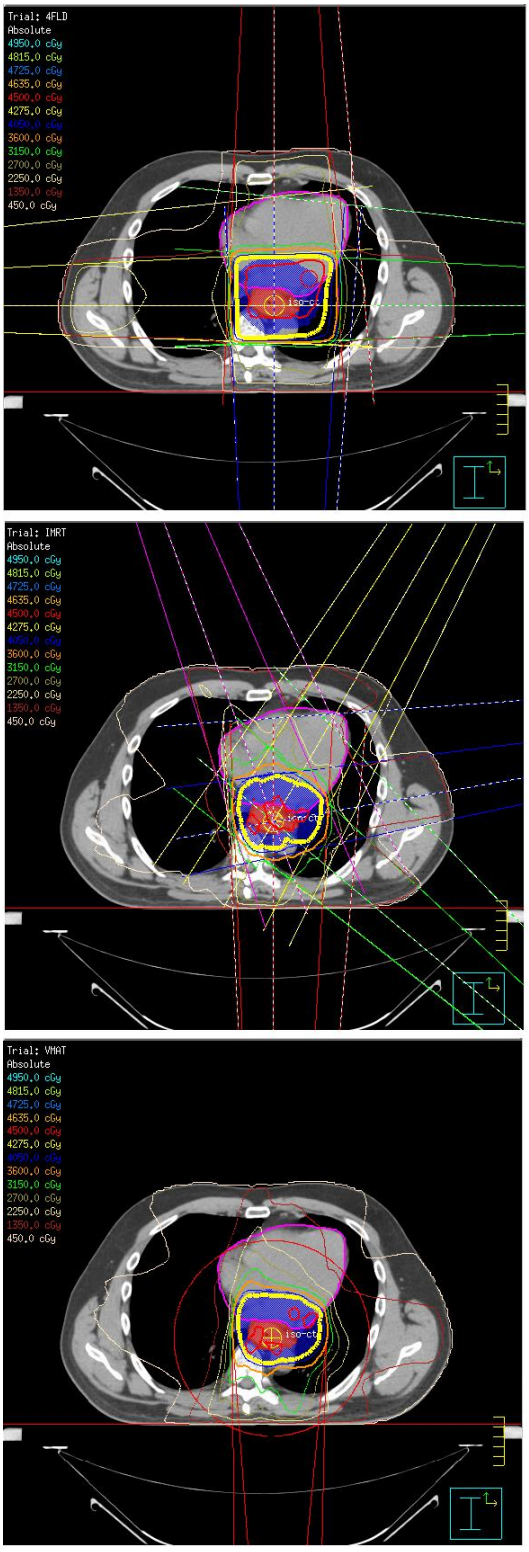


**Figure 2.1** – Axial CT image in the plane of the isocenter displaying beam arrangements for 3D-CRT, IMRT and VMAT of a sample case.

The 3D-CRT plans were all planned with a 4-field arrangement with the majority of plans using the cardinal angles of $0^0$, $90^o$, $180^o$ and $270^o$. In select cases, the lateral beam angles were adjusted to better spare kidneys from entry and exit dose. Four fields were used as a standard beam arrangement to balance dose to heart, lungs and spinal cord and achieve the most uniform plan possible. All plans had the option of in field segmentation and was used as necessary to limit hot spots and maximum dose if required. Field shielding was outlined by the planner around the PTV and MLC were used for shielding. Margin was left around the target volume to ensure adequate coverage. All fields were planned with energy 18 MV due to depth of the target and minimizing dose to normal body tissues. All fields were weighted to achieve a balanced plan with respect to coverage and entry/exit dosing of normal tissues.

IMRT planning was customized to the patient target volume and treatment beam angles were varied accordingly to achieve the best possible plan. The number of coplanar beam angles ranged from 5-9 with the number of beams ranging from 5-12. Depending on the target size, some beam angles were split to maintain a maximum field size width of 14.5cm. This width corresponds to the maximum travel distance of an MLC leaf and therefore allows the optimizer to plan with deliverable beams. Direct machine parameter optimization was used which allows for MLC settings to be implemented within the optimization process removing the need for conversions [141]. Automatic jaw motion was allowed (with a maximum width of 14.5cm). The maximum number of segments for a plan was chosen at 10 per beam if required. Other IMRT settings included minimum segment area of $6cm^2$ and minimum segment MU of 7. These parameters were kept for plan efficiency and accurate deliverability to replicate a clinical scenario. All beams were planned with 6 MV and a step and shoot MLC delivery system. Optimization structures were created as required.

VMAT plans utilized full coplanar arc(s) around the patient. 1 or 2 arcs were used depending on target shape complexity. Arcs were planned with start and stop angles $178^o$-$182^o$ or vice versa and in the cases of 2 arcs both directions were used. Collimator angle of $10^o$ or $350^o$ was used to spread interleaf leakage. If 2 arcs were utilized, complimentary collimator angles were used to allow for more optimization options and minimizing overlapping tongue and groove effects of

each arc. The final gantry control spacing used was 2 degrees meaning a control point was used every other degree of rotation. Leaf motion was constrained to 0.46cm/degree. Optimization structures were created as required to achieve a clinically acceptable and desirable plan.

*Evaluation*

Dose analysis was completed using DVH statistics. PTV analysis included the assessment of conformity index which is defined as the volume receiving 95% of prescribed dose as a ratio of target volume: Conformity indexRTOG =V RI/TV whereas $V_{RI}$ is volume of reference isodose and TV refers to target volume [142]. Conformity index is a quality measure of radiation plans referring to conformation of a specific dose level. In this study, conformation of the 95% dose around PTV was assessed. A conformity index equal to 1 would indicate ideal conformation. Values less than one would imply that the irradiated volume is less than the target volume. Values greater than one indicate that the irradiated volume is greater than the target volume. There is a limitation to this analysis as the amount of overlapping of these volumes can not be assessed. For example, a conformity index of 1 could be achieved with the volume of irradiated tissue and target volume situated away from each other [142]. Analysis of the CT slices and DVH should be used in conjunction with this parameter to judge plan quality.

Integral dose is the volume of dose deposited in the patient and is accepted as the mean dose times the volume of irradiated to any dose. Integral dose can be calculated for any volume such as OAR or normal tissues. Integral dose was calculated as ID(Gy * L) = D(Gy) * V(L) whereas D(Gy) is the mean dose delivered and V(L) is the volume [80]. Normal tissue for this calculation was the volume outside the PTV at all slices of PTV. The volume was limited to the extent of the PTV to better study the normal tissue around the high dose delivered. It could be argued that a portion of the PTV outside the GTV or CTV contains normal tissue however as the dose prescription involves coverage of the PTV target this volume was excluded in calculation.

Dose statistics included in analysis include bilateral lung ($V_{5Gy}$, $V_{20Gy}$, mean, max), heart ($V_{30Gy}$, mean, max), spinal cord (max), bilateral kidneys ($V_{20Gy}$, mean) and liver (mean). $V_{xGy}$ refers to the

volume of tissue studied receiving *x* dose. In the example of $V_{5Gy}$, this parameter represents the volume (percentage) receiving 5Gy of dose. The Wilcoxon signed rank test was used to compare 3D-CRT vs IMRT and VMAT for the organ parameters studied. Statistical analysis was performed with RStudio: Integrated Development Environment for R (Massachusetts, USA). Initial sampling of data was conducted and it was determined that the data did not follow normal probability. Thus, the decision was made to utilize the Wilcoxon signed rank test for all statistical analysis.

## 3.0 Results

Figures 3.1, 3.2 and 3.3 display each of 3D-CRT, IMRT and VMAT plans respectively in the axial, sagittal and coronal plans for an example case. Images are taken at calculation point with isodose lines displayed. Colourwash display of GTV (red) and PTV (blue) is represented.

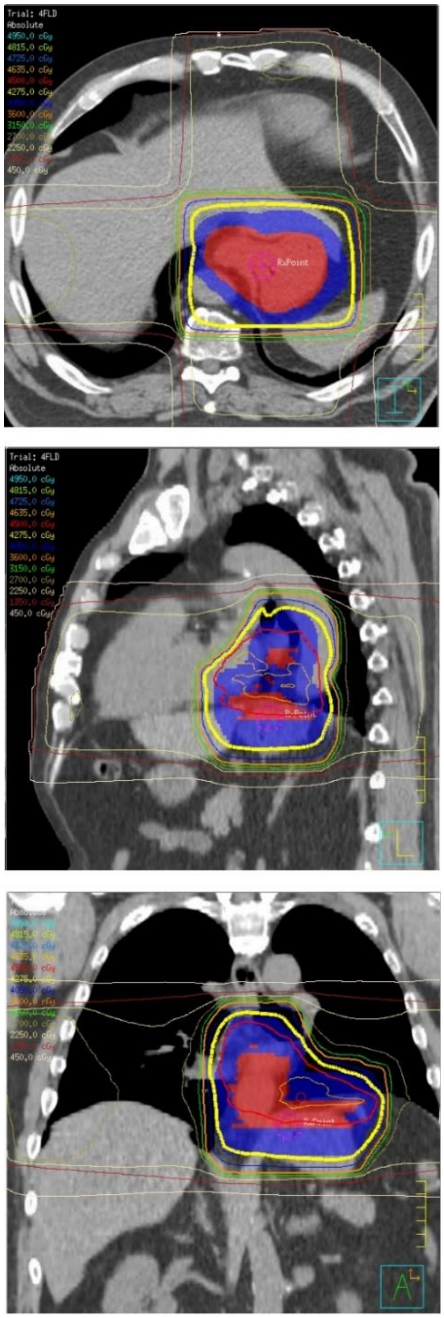

**Figure 3.1** – Axial, sagittal and coronal view of 3D-CRT plan for an example case.

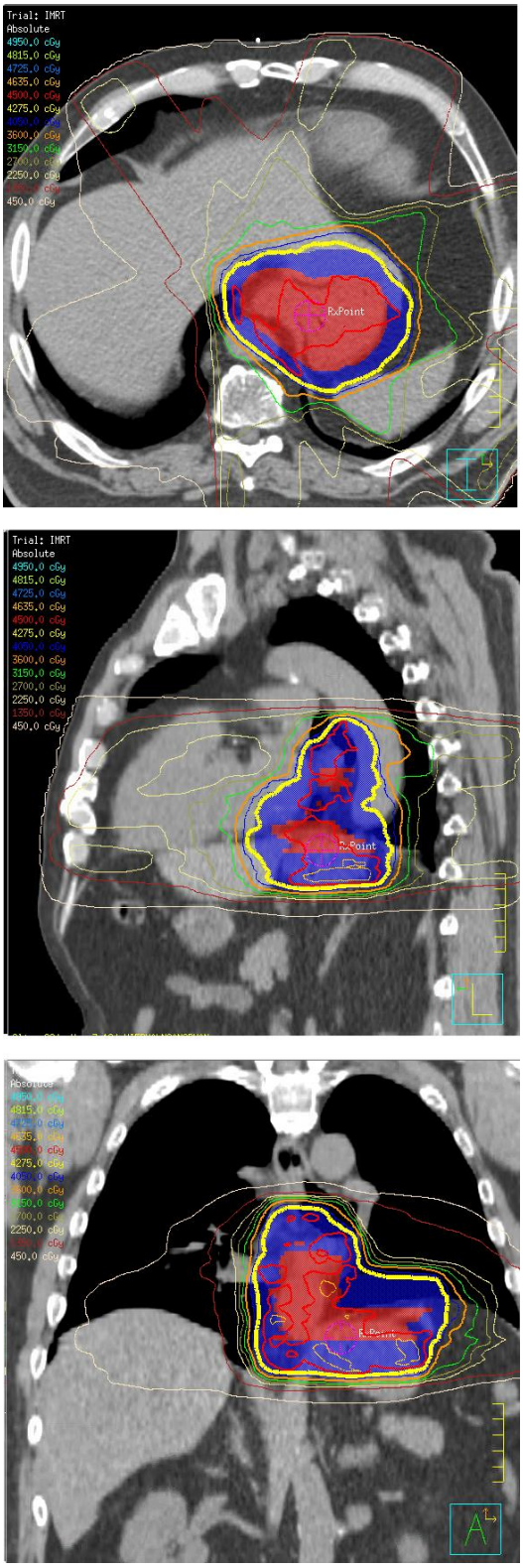


**Figure 3.2** – Axial, sagittal and coronal view of IMRT plan for an example case.


**Figure 3.3** – Axial, sagittal and coronal view of VMAT plan for an example case.

Dose being deposited in the patient can be visualized among the three treatment techniques. Conformality of the 95% isodose line (yellow) is improved in IMRT and VMAT when compared to 3D-CRT as there is less normal tissue irradiated to a high dose with these techniques respectively.

Figure 3.4 displays the DVH (dose-volume histogram) of the 3 planning techniques for this example case overlaid on the same graph. Each of the studied OAR as well as the target PTV are displayed. The thin solid line represents the 3D-CRT plan, the thick solid line represents the IMRT plan, and the dashed line represents the VMAT plan. Each corresponding colour refers to the target PTV or OAR as displayed.

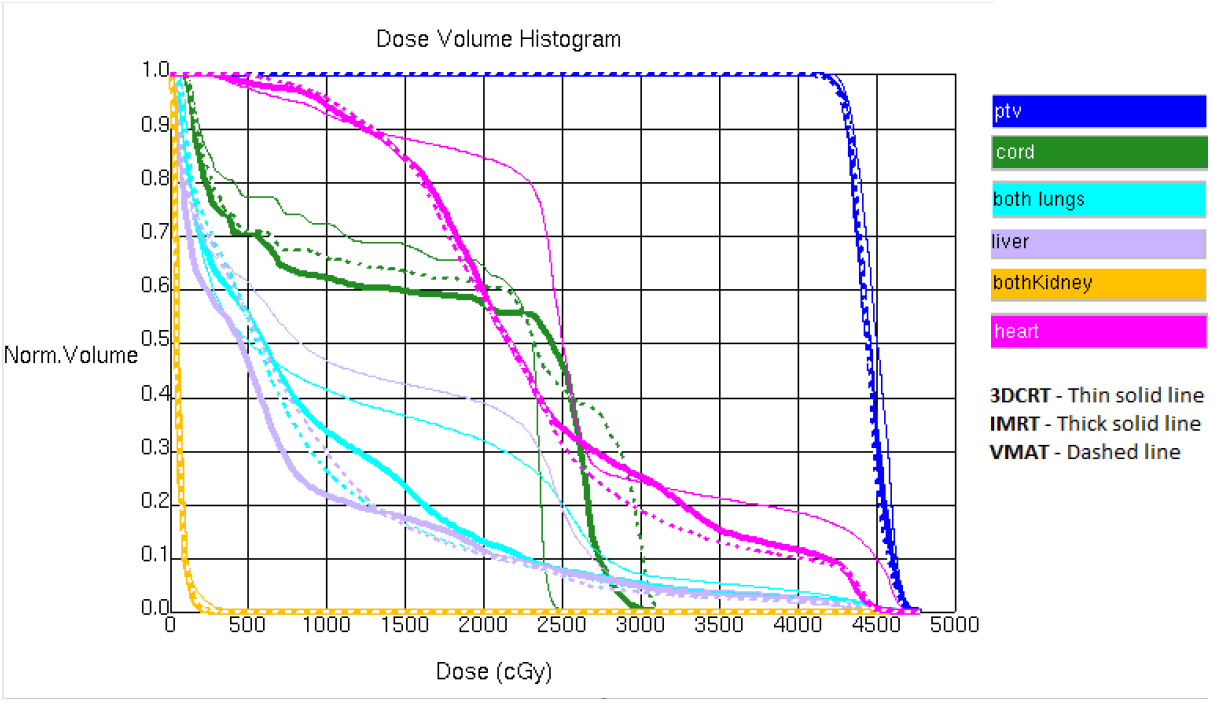


**Figure 3.4** – Dose-volume histogram of example case for studied OAR and PTV.

In the case of many OAR, 3D-CRT appears to have increased dose for many structures at multiple levels of dose. In the range of 1000 cGy to 2000 cGy, there is a significant increase in lung and liver dose as well as a slight increase in heart dose. IMRT and VMAT yield more similar results,

though there is some variability depending on dose level and OAR. In all cases, target PTV appears to be adequately covered.

A summary of target volumes delineated by the physician along with the PTV is represented in Table 3.1.

**Table 3.1** – Volumetric statistics for target volumes.

| | GTV (n=35) | CTV (n=4) | PTV (n=40) |
|---|---|---|---|
| **Median ($cm^3$)** | 241.9 | 252.1 | 838.2 |
| **Interquartile Range** | 153.9 | 290.9 | 477.5 |

Inter-rater reliability was analyzed by calculating Krippendorff's alpha for mean dose to lungs, heart, kidney, and liver as well as maximum dose to spinal cord. An alpha value > 0.8 indicates a strong agreement and > 0.667 would still indicate acceptable agreement [143]. Table 3.2 summarizes inter-rater reliability between the study investigator and another experienced dosimetrist.

**Table 3.2** – Krippendorff's alpha between study investigator and experience dosimetrist for OAR of all treatment techniques.

| | 3D-CRT | IMRT | VMAT | All Techniques |
|---|---|---|---|---|
| **Lung Mean** | 0.912 | 0.726 | 0.476 | 0.736 |
| **Heart Mean** | 0.872 | 0.762 | 0.629 | 0.801 |
| **Spinal Cord Max** | 0.229 | 0.196 | 0.299 | 0.218 |
| **Kidney Mean** | 0.937 | 0.814 | 0.472 | 0.875 |
| **Liver Mean** | 0.849 | 0.828 | 0.908 | 0.865 |

Krippendorff's alpha across all measurements was **0.931**. These results show a strong agreement between plans completed by the study investigator and a separate experienced dosimetrist for all metrics except spinal cord maximum. Spinal cord maximum is a point measurement that can

be highly variable compared to the other measures which are more broad indications of plan quality.

Figures 3.5 and 3.6 represent Box and Whisker plots of Conformity Index and Integral Dose. In this study, Box and Whisker plots will have a middle horizontal line representing the median. The "x" in the box represents the mean of the dataset. The top line of the box represents the third quartile, and the bottom line of the box represents the first quartile. The whiskers from the box then extend to the minimum and maximum values of the dataset. Any outliers (exceeding 1.5 times the interquartile range below and above the first and third quartile) will be displayed as a dot outside the dataset. Table 3.3 displays the median Conformity Index and Integral dose as well as average pairwise difference with respect to the comparison of the 3 treatment techniques in addition to p-value significance.

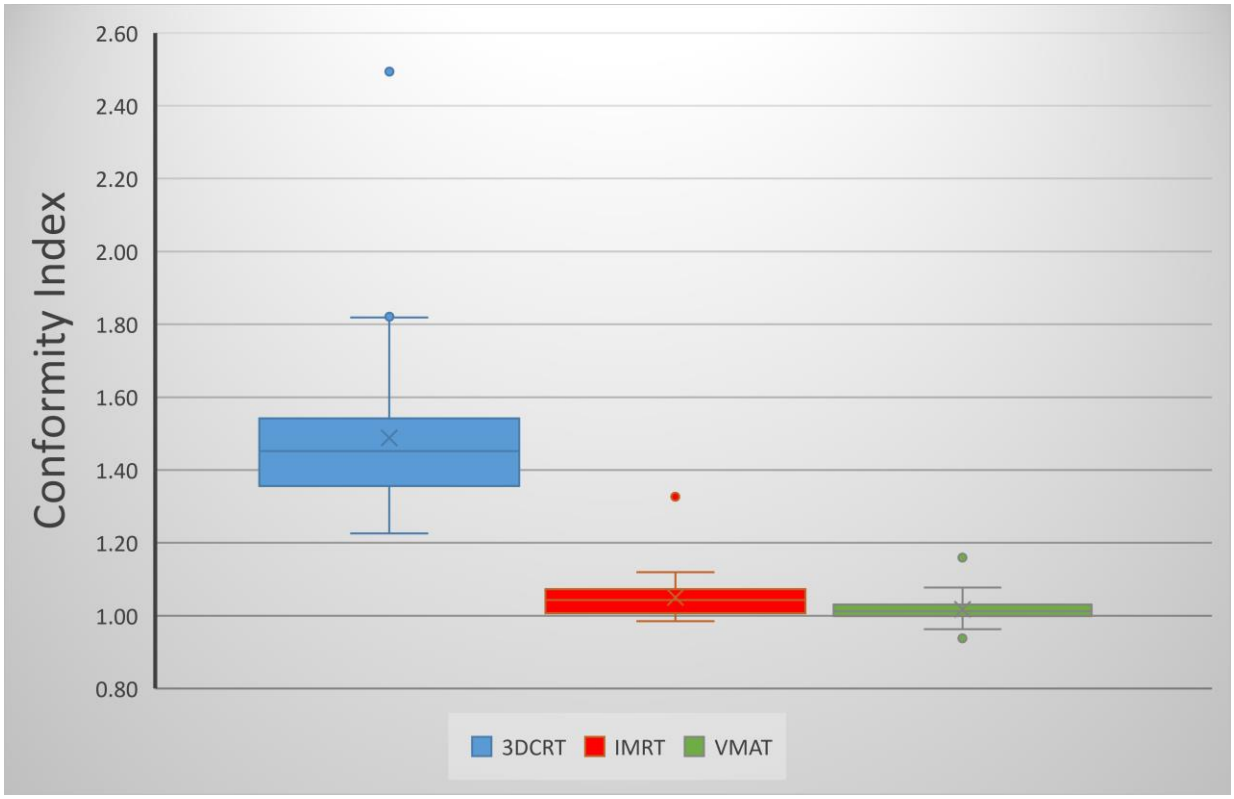


**Figure 3.5** – Box and Whisker plot for Conformity Index of all treatment techniques.

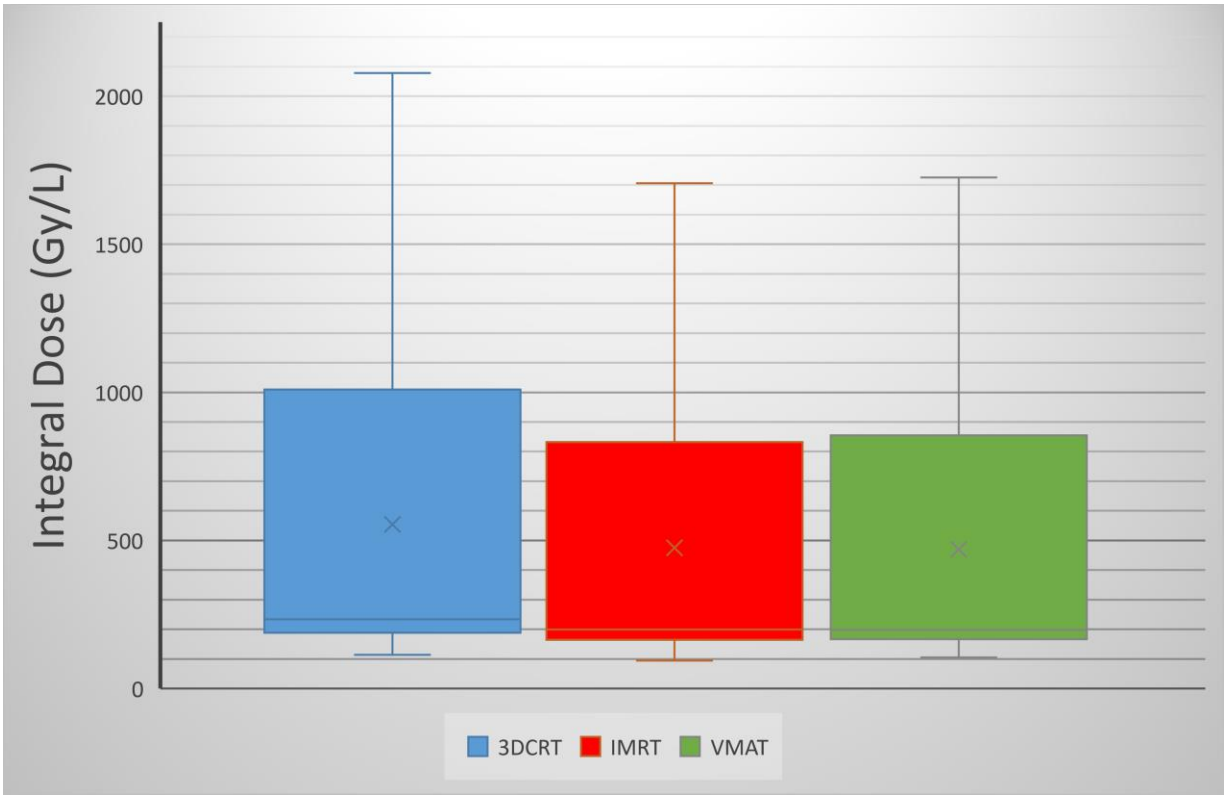


**Figure 3.6** – Box and Whisker plot for Integral Dose of all treatment techniques.

**Table 3.3** – Median Conformity Index and Integral dose. Mean difference was also analyzed between treatment techniques.

| | **Median (Interquartile range)** | | | **Average Pairwise Difference (*P*-value)** | | |
|---|---|---|---|---|---|---|
| | 3D-CRT | IMRT | VMAT | IMRT vs 3D-CRT | VMAT vs 3D-CRT | VMAT vs IMRT |
| **Conformity Index** | 1.45 (1.36 – 1.54) | 1.04 (1.01 – 1.07) | 1.01 (1.00 – 1.03) | -28.51% (<.001) | -30.70% (<.001) | -2.98% (<.001) |
| **Integral Dose (Gy/L)** | 233.2 (188.1 – 1009.3) | 199.6 (164.6 – 832.0) | 197.7 (166.7 – 854.1) | -14.0% (<.001) | -14.8% (<.001) | -0.8% **(0.14)** |

There is a significant difference in conformity index when comparing 3D-CRT with IMRT and VMAT respectively. There is also a significant different between IMRT and VMAT with VMAT providing the most conformal plans of all techniques. Integral dose is also greatly reduced when utilizing IMRT or VMAT as opposed to 3D-CRT. There was negligible difference in integral dose when comparing IMRT and VMAT.

Monitor units were analyzed for all plans. Monitor units refer the measurement of machine output during beam delivery. Linear accelerators are calibrated by departmental policies but typically a single monitor unit is calibrated as the delivery of 1 cGy at a depth of Dmax (maximum point dose) for an open field size of 10cm x 10cm at a source-to-axis distance of 100cm. Higher monitor units correspond to higher machine output and beam-on time. Table 3.4 summarizes monitor unit findings for all cases at each respective treatment method.

**Table 3.4** – Monitor unit comparison for all cases.

| | **Median (Interquartile range)** | | | **Average Pairwise Difference (*P*-value)** | | |
|---|---|---|---|---|---|---|
| | 3D-CRT | IMRT | VMAT | IMRT vs 3D-CRT | VMAT vs 3D-CRT | VMAT vs IMRT |
| **Monitor Units** | 207.0 (202.3 – 213.8) | 400.1 (323.3 – 546.0) | 369.0 (311.8 – 425.3) | 107.2% (<.001) | 80.4% (<.001) | -9.9% (<.001) |

There is a large reduction in monitor units when comparing 3D-CRT to IMRT and VMAT. In the case of 3D-CRT and IMRT, median monitor units are doubled. This would correspond to the fact that 3D-CRT delivers radiation with a predominantly open field requiring less beam on time to achieve the required deposited dose. VMAT does have a significantly relevant decrease in monitor units when compared to IMRT which could indicate an increased efficiency.

*Lung Results*

Figures 3.7, 3.8, 3.9 and 3.10 display box and whisker plots of lung $V_{5Gy}$, $V_{20Gy}$, mean and maximum point dose respectively. Table 3.5 summarizes lung dose statistics.

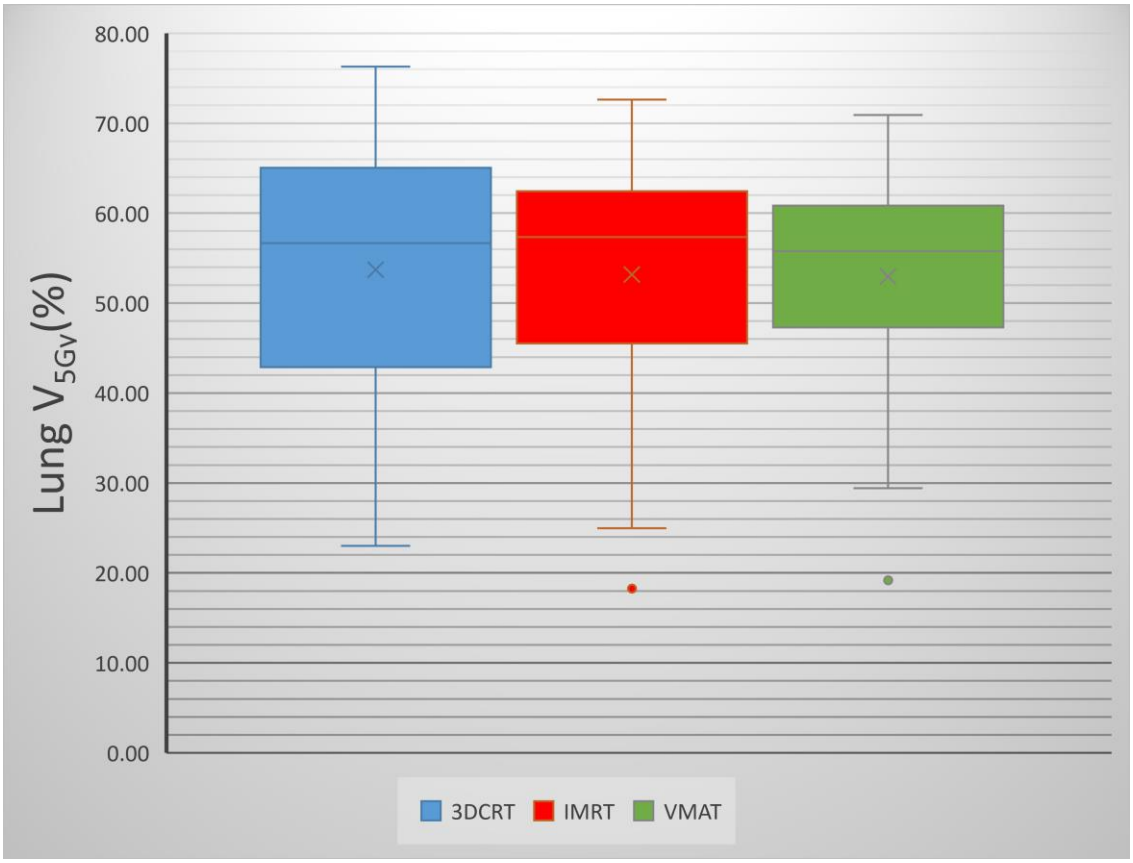


**Figure 3.7** – Box and Whisker plot for lung $V_{5Gy}$ of all treatment techniques.

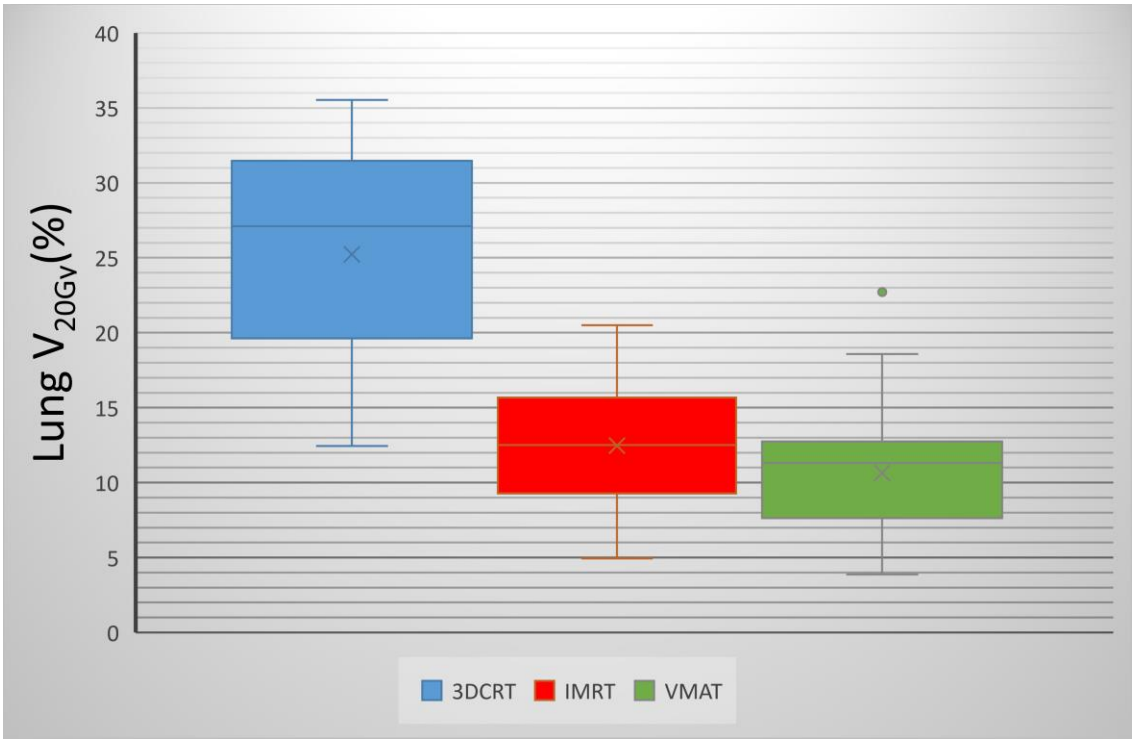


**Figure 3.8** – Box and Whisker plot for lung $V_{20Gy}$ of all treatment techniques.

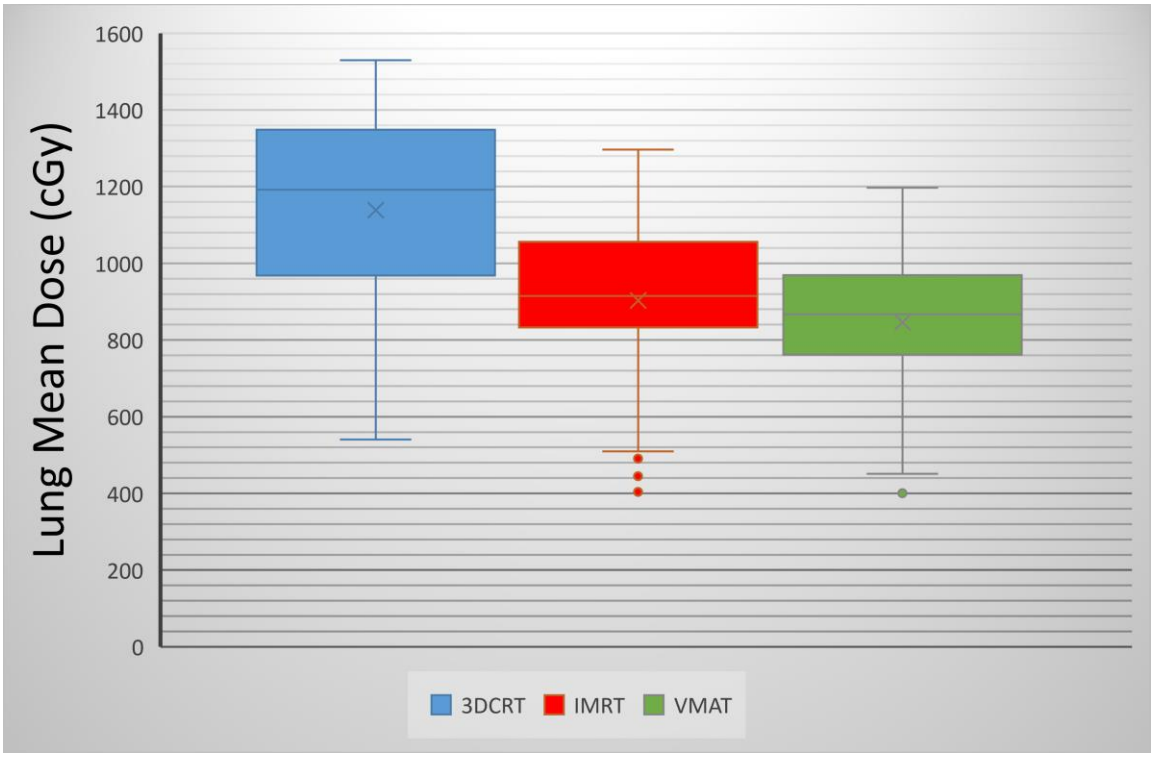


**Figure 3.9** – Box and Whisker plot for lung mean dose of all treatment techniques.

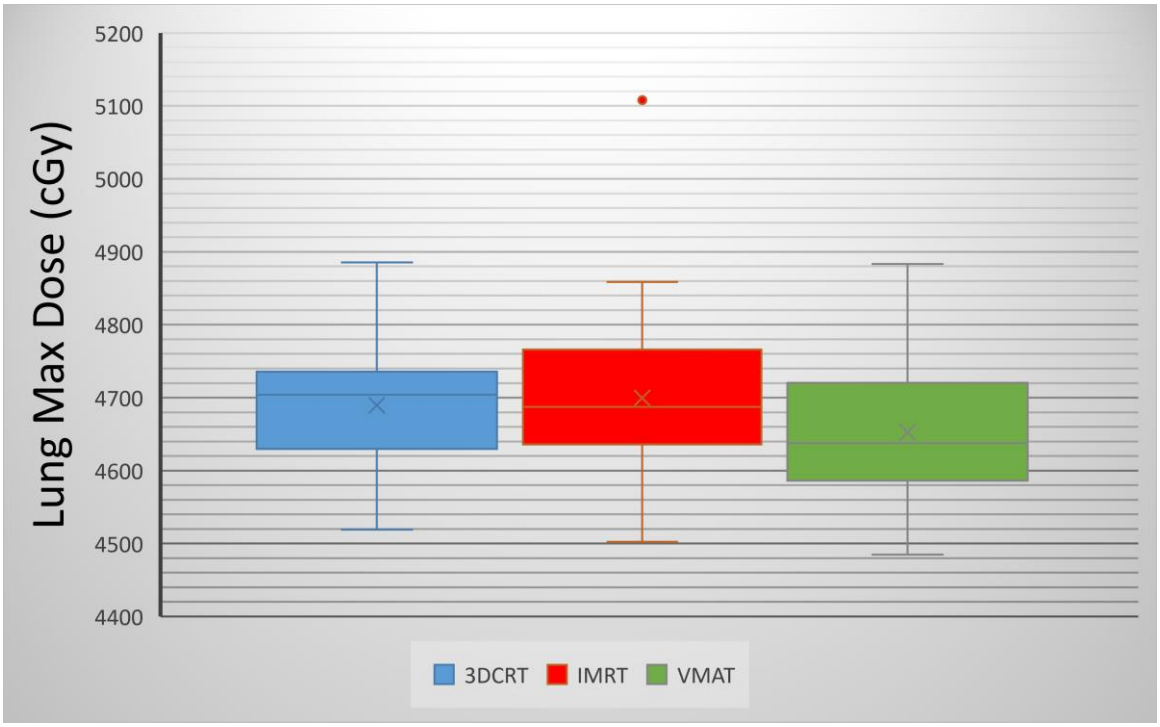


**Figure 3.10** – Box and Whisker plot for lung maximum dose of all treatment techniques.

**Table 3.5** – Lung dose statistics for all treatment techniques.

| | **Median (Interquartile range)** | | | **Average Pairwise Difference (*P*-value)** | | |
|---|---|---|---|---|---|---|
| | 3D-CRT | IMRT | VMAT | IMRT vs 3D-CRT | VMAT vs 3D-CRT | VMAT vs IMRT |
| **Lung $V_{5Gy}$ (%)** | 56.7 (42.9 – 65.0) | 57.4 (45.5 – 62.4) | 55.8 (47.3 – 60.8) | -0.6% **(.50)** | 0.1% **(0.66)** | 0.7% **(.97)** |
| **Lung $V_{20Gy}$ (%)** | 27.1 (19.6 – 31.5) | 12.5 (9.3 – 15.7) | 11.3 (7.6 – 12.8) | -49.7% (<.001) | -57.4% (<.001) | -14.7% (<.001) |
| **Lung Mean Dose (cGy)** | 1192.4 (968.0 - 1348.2) | 914.5 (832.6 – 1055.5) | 866.9 (761.4 – 969.0) | -20.3% (<.001) | -24.9% (<.001) | -5.6% (<.001) |
| **Lung Max Dose (cGy)** | 4704.0 (4629.6 – 4735.4) | 4687.1 (4636.1 – 4765.8) | 4637.8 (4586.4 – 4720.2) | 0.2% **(.78)** | -0.8% (.04) | -1.0% (<.001) |

Lung results differ with respect to the parameter being assessed. With respect to lung $V_{5Gy}$, there is negligible difference among the three treatment techniques with statistical analysis indicating a strong conclusion of their difference can not be made. With respect to lung $V_{20Gy}$ and mean dose, there is significant decrease between 3D-CRT and both IMRT and VMAT. There is also a significant decrease in dose when comparing VMAT to IMRT. There is minimal clinically significant difference in maximum lung dose and as mentioned earlier this parameter is susceptible to high variability due to point dose assessment.

*Heart Results*

Figures 3.11, 3.12, 3.13 display box and whisker plots of heart $V_{30Gy}$, mean and maximum point dose respectively.

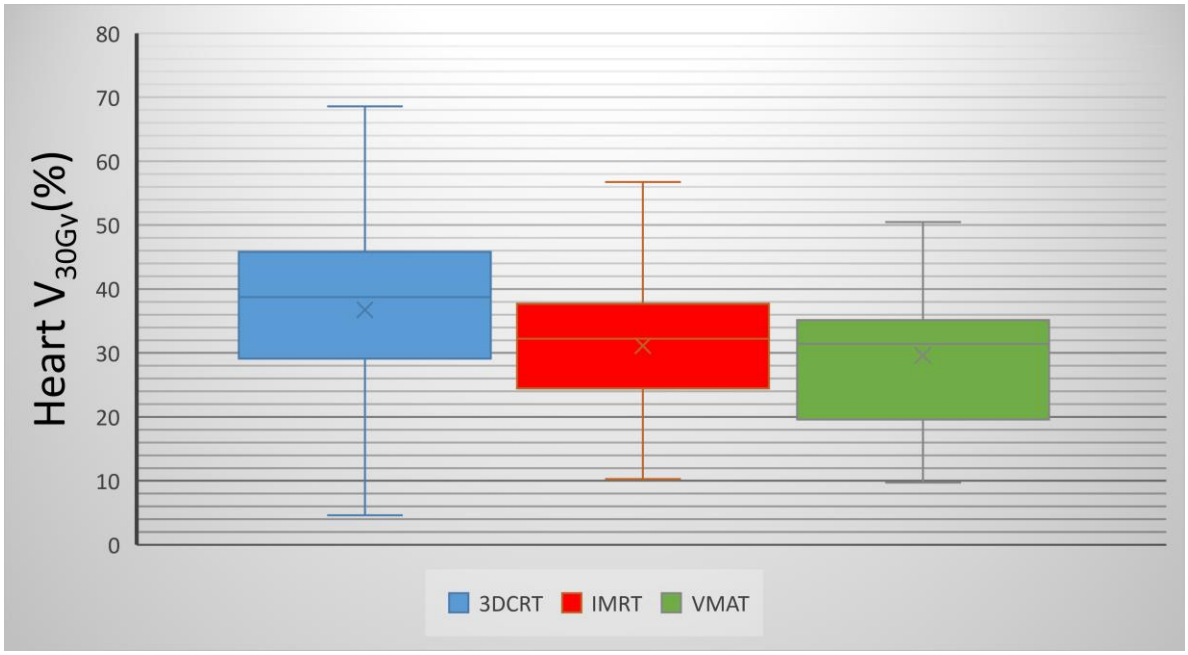


**Figure 3.11** – Box and Whisker plot for heart $V_{30Gy}$ of all treatment techniques.

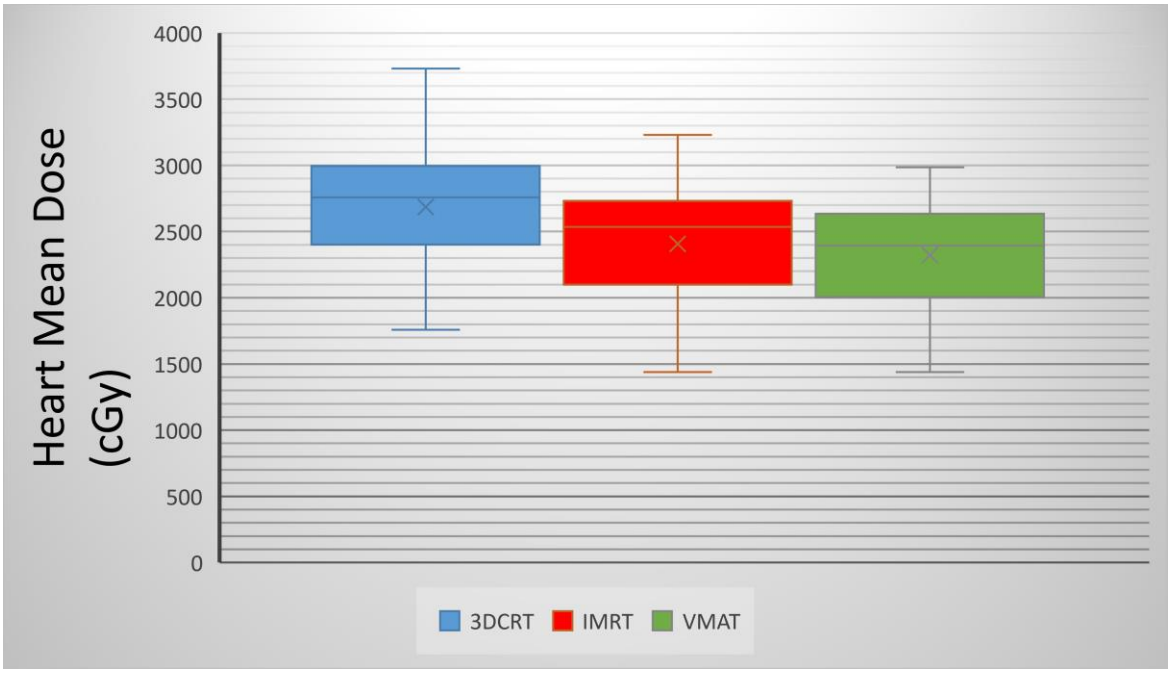


**Figure 3.12** – Box and Whisker plot for heart mean dose of all treatment techniques.

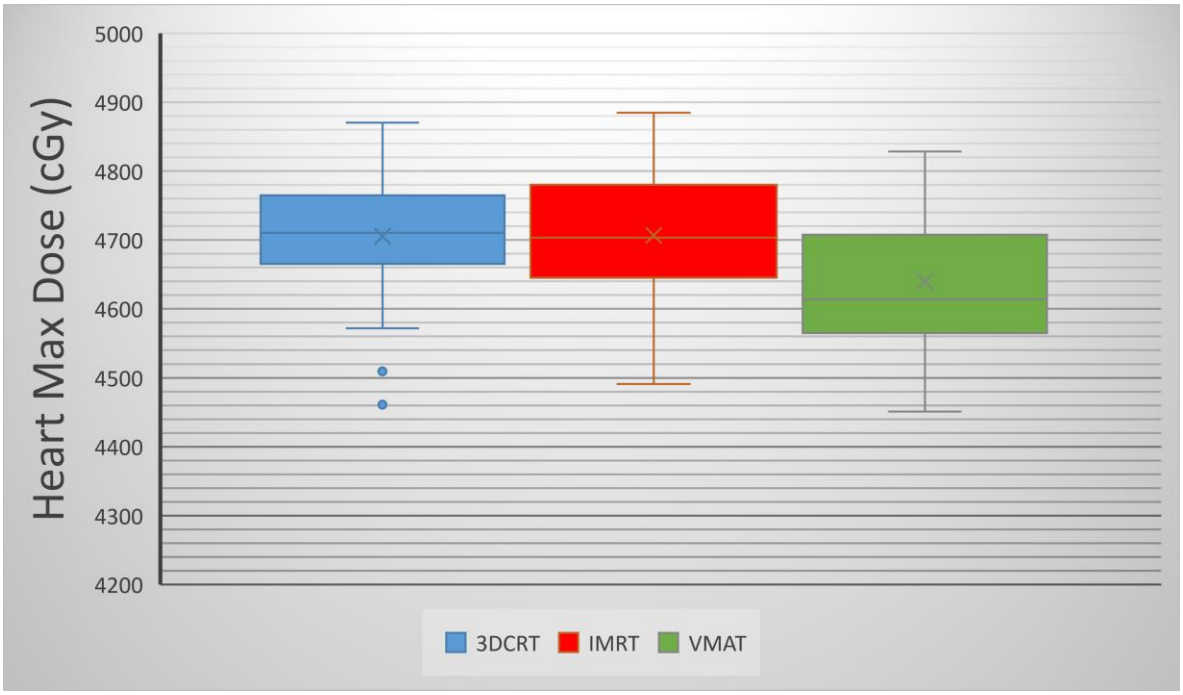


**Figure 3.13** – Box and Whisker plot for heart max dose of all treatment techniques.

Table 3.6 summarizes dose statistics for all treatment techniques in relation to studied heart dose.

**Table 3.6** – Heart dose statistics for all treatment techniques.

| | **Median (Interquartile range)** | | | **Average Pairwise Difference (*P*-value)** | | |
|---|---|---|---|---|---|---|
| | 3D-CRT | IMRT | VMAT | IMRT vs 3D-CRT | VMAT vs 3D-CRT | VMAT vs IMRT |
| **Heart $V_{30Gy}$ (%)** | 38.7 (29.1 – 45.8) | 32.2 (24.4 – 37.7) | 31.4 (19.6 – 35.2) | -10.1% (<.001) | -14.3% (<.001) | -4.0% (.01) |
| **Heart Mean Dose (cGy)** | 2758.8 (2401.4 – 2995.4) | 2533.9 (2100.2 – 2731.6) | 2395.2 (2005.6 – 2633.7) | -10.4% (<.001) | -13.4% (<.001) | -3.2% (<.001) |
| **Heart Max Dose (cGy)** | 4710.6 (4665.1 – 4764.8) | 4703.5 (4645.3 – 4780.2) | 4613.8 (4564.9 – 4707.8) | 0.1% **(0.73)** | -1.4% (.001) | -1.4% (<.001) |

There is a significant difference in heart dose with respect to treatment technique. Heart $V_{30Gy}$ is significantly reduced with IMRT and VMAT by 10.1% and 14.3% respectively when compared to 3D-CRT. Notably there is a small but statistically relevant decrease in heart $V_{30Gy}$ when comparing VMAT to IMRT. Similar results were noted for heart mean dose. IMRT and VMAT resulted in a decrease in pairwise average of 10.4% and 13.4% when compared to 3D-CRT. Similar to heart $V_{30Gy}$, there is a notable decrease in mean dose using VMAT when compared to IMRT. There is minimal clinically significant difference in heart maximum dose.

*Other studied OAR*

Figures 3.14, 3.15, 3.16 and 3.17 display box and whisker plots for spinal cord max dose, kidney $V_{20Gy}$, kidney mean dose and liver mean dose.

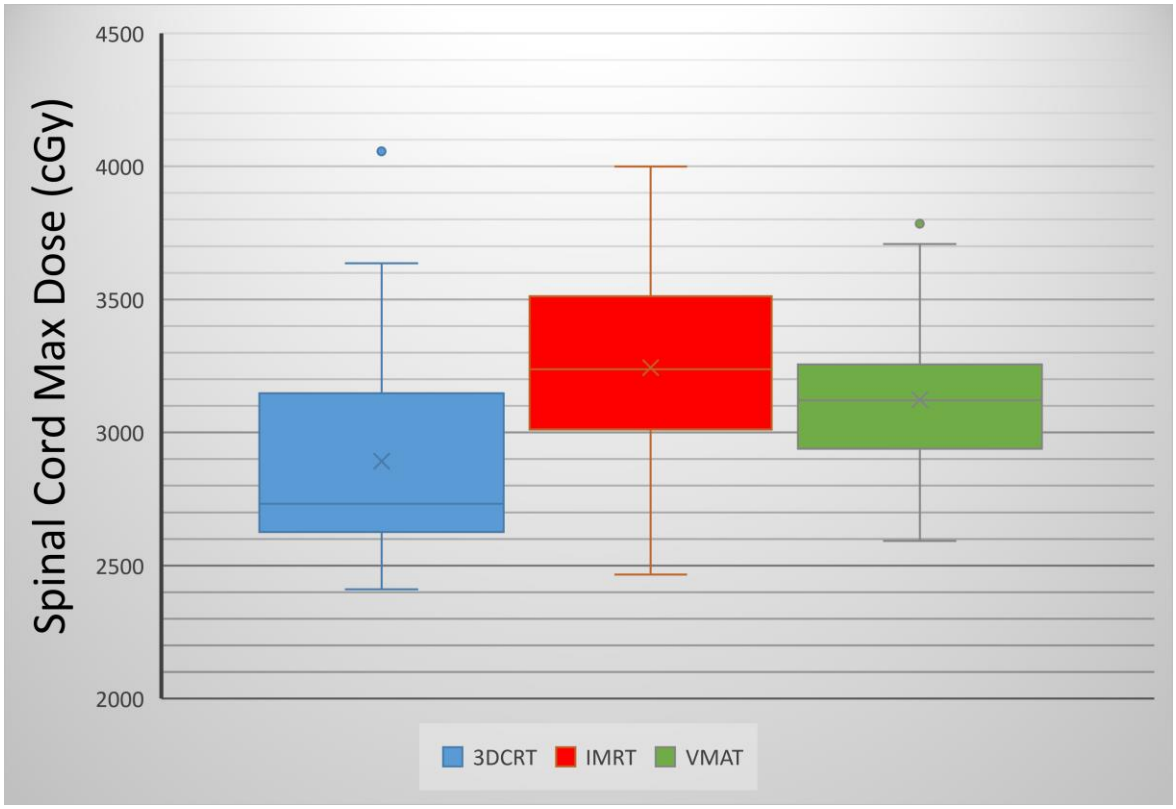


**Figure 3.14** – Box and Whisker plot for Spinal Cord Max dose of all treatment techniques.

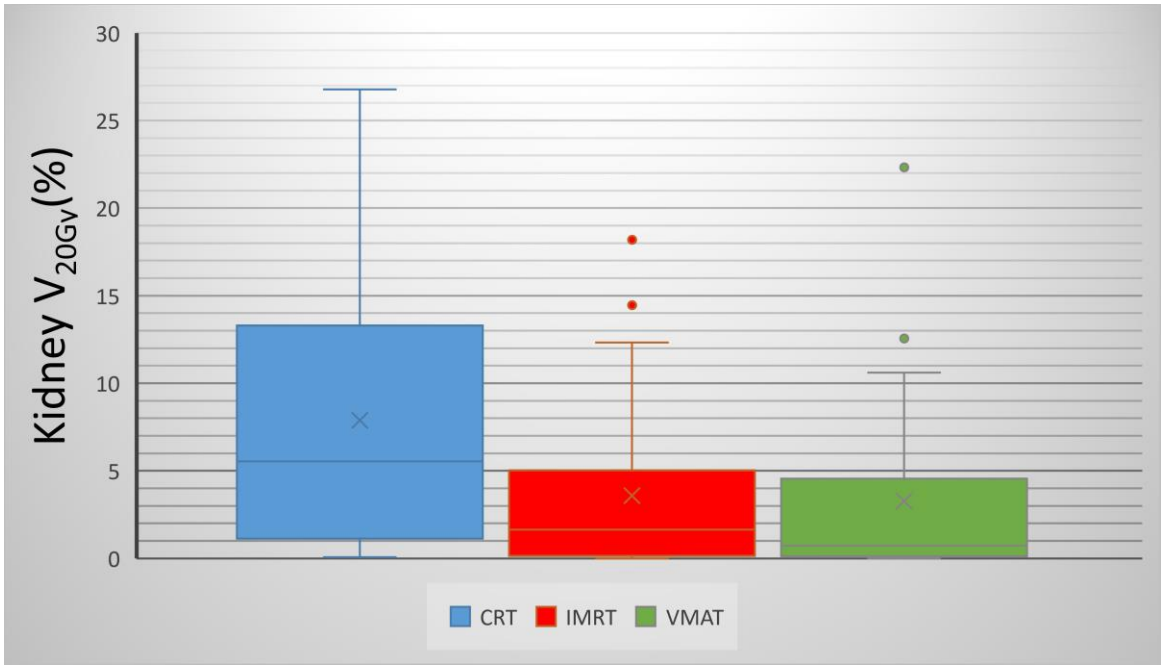


**Figure 3.15** – Box and Whisker plot for kidney $V_{20Gy}$ of all treatment techniques.

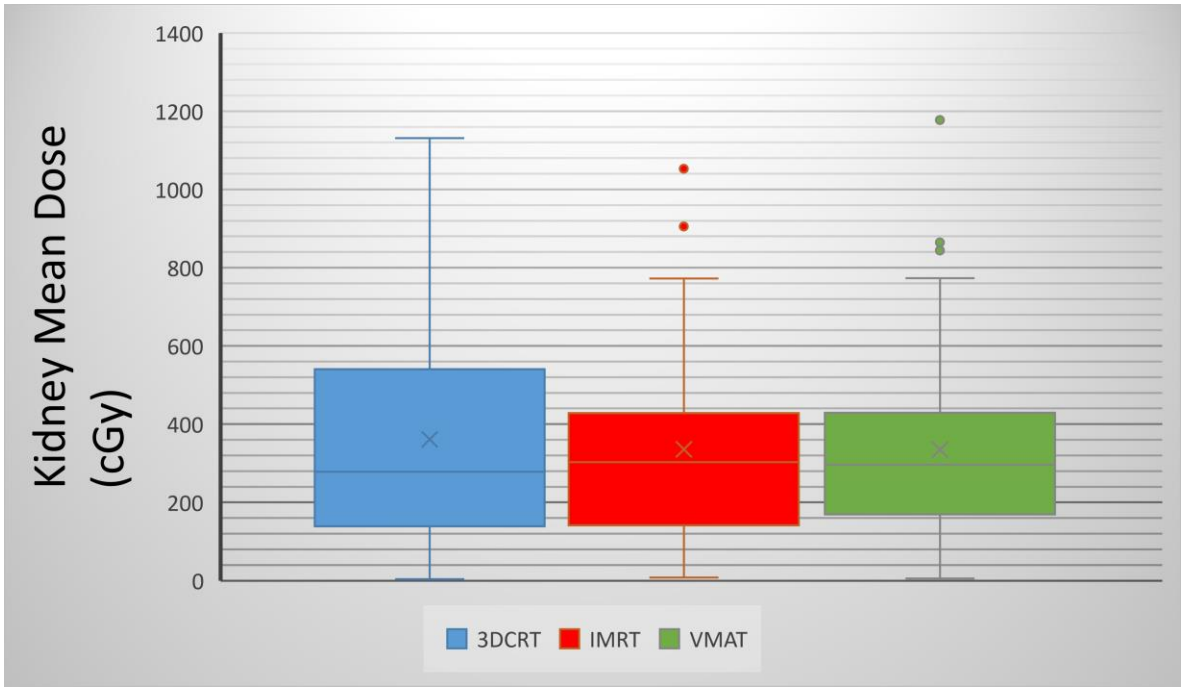


**Figure 3.16** – Box and Whisker plot for kidney mean dose of all treatment techniques.

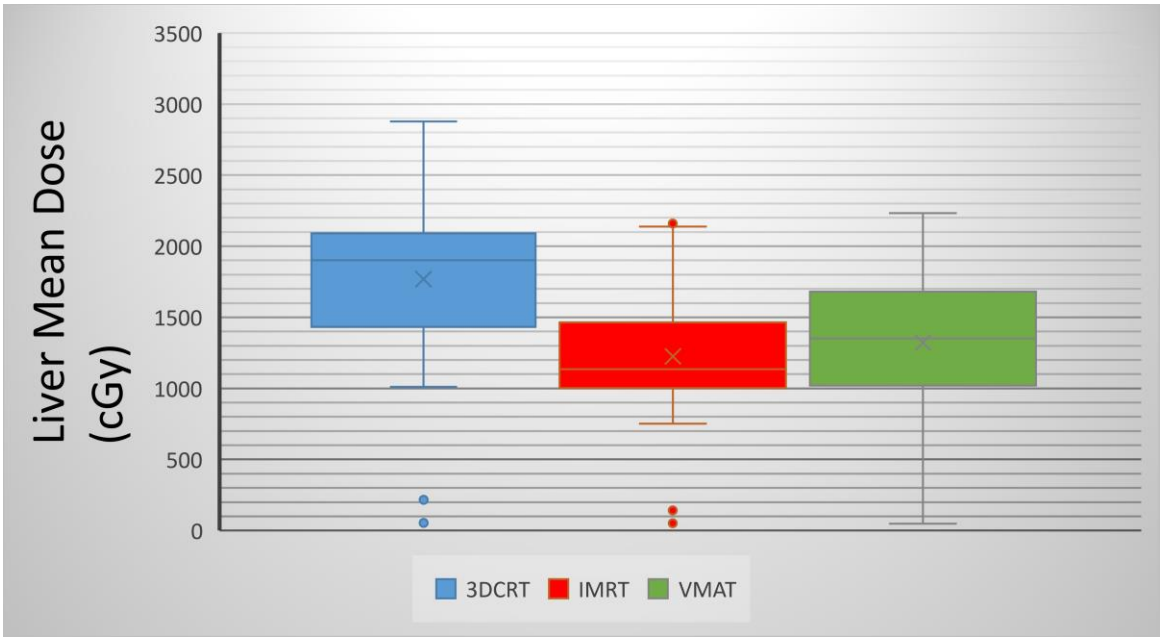


**Figure 3.17** – Box and Whisker plot for liver mean dose of all treatment techniques.

Table 3.7 summarizes dose statistics for Spinal Cord Max, kidney $V_{20Gy}$, kidney mean and liver mean doses for all techniques.

**Table 3.7** – Spinal cord, kidney and liver statistics for all treatment techniques.

| | **Median (Interquartile range)** | | | **Average Pairwise Difference (*P*-value)** | | |
|---|---|---|---|---|---|---|
| | 3D-CRT | IMRT | VMAT | IMRT vs 3D-CRT | VMAT vs 3D-CRT | VMAT vs IMRT |
| **Spinal Cord Max (cGy)** | 2731.4 (2625.5 – 3146.7) | 3237.1 (3010.6 – 3511.8) | 3120.6 (2939.0 – 3255.4) | 13.3% (<.001) | 9.5% (<.001) | -3.0% (<.001) |
| **Kidney $V_{20Gy}$ (%)** | 5.5 (1.1 – 13.3) | 1.7 (0.2 – 5.0) | 0.7 (0.1 – 4.6) | -60.7% (<.001) | -53.6% (<.001) | -17.4% **(.45)** |
| **Kidney Mean Dose (cGy)** | 278.0 (138.9 – 540.3) | 302.6 (141.6 – 428.1) | 296.3 (168.9 – 428-8) | 8.0% **(.40)** | 7.1% **(.32)** | 1.7% **(.90)** |
| **Liver Mean Dose (cGy)** | 1901.8 (1431.2 – 2090.9) | 1134.0 (1001.0 – 1463.2) | 1351.7 (1020.7 – 1680.6) | -29.9% (<.001) | -24.3% (<.001) | 10.3% (.02) |

3D-CRT provided the lowest spinal cord maximum among the three planning techniques. When compared to IMRT, there was an average pairwise reduction of 13.3% and when compared to VMAT that reduction was 9.5%. There was a slight reduction when utilizing VMAT when compared to IMRT. There was negligible dose to kidney $V_{20Gy}$ especially at a clinically relevant level. Similarly for kidney mean dose, values did not reach a clinically significant level and no conclusions could be made with respect to superior treatment technique. Both IMRT and VMAT provided significantly reduced liver mean dose when compared to 3D-CRT. Average pairwise reduction of 29.9% and 24.3% was noted when comparing IMRT and VMAT to 3D-CRT

respectively. There was a statistically significant increase observed for liver mean dose when VMAT and IMRT were compared.

## 4.0 Discussion

With relatively poor overall survival rates for esophageal cancer, studies investigating improvement to treatment techniques are important for this subset of patients. The aim of this paper is to investigate radiation planning dose to OAR and target areas for preoperative esophageal cancer. Specifically, investigation was made to a large dataset comparing 3D-CRT, IMRT and VMAT planning techniques. This study was intending to demonstrate critical organ dose reduction while maintaining target coverage. At the same time, this study was also conducted to demonstrate that the more conformal radiation planning techniques of IMRT and VMAT had comparable low dose to the critical organ of lungs and healthy body tissues with that of 3D-CRT.

The data of this study suggests that conformal radiation planning techniques of IMRT and VMAT both provide superior organ sparing while maintaining target coverage compared to 3D-CRT. Furthermore, the data supports the idea of comparable low dose to lungs and healthy body tissue. VMAT provided lower lung mean, $V_{20Gy}$ and lung max dose compared to IMRT. In addition, VMAT also proved to reduce dose to heart $V_{30Gy}$, mean dose, maximum dose as well as spinal cord maximum and kidney $V_{20Gy}$.

Inter-observer reliability was first assessed before plans were generated for all cases by the study investigator. Fifteen cases were planned by another expert planner and results were compared with the study investigator. Krippendorff's alpha was calculated for lung mean, heart mean, liver mean, kidney mean and spinal cord maximum doses. Krippendorff's alpha was developed for use in assessing agreement between observers wherever two or more methods of generating data is applied to the same objects [144]. An alpha value > 0.8 indicates a strong agreement between observers and > 0.667 would still indicate acceptable agreement. Table 3.2 displays inter-rater reliability between the study investigator and the experienced dosimetrist. Overall, there is strong agreement between planners with an alpha value across all measurements of 0.931. There was minimal agreement in spinal cord maximum dose. Spinal cord maximum dose assessed a single point dose received to the spinal cord. As such, there is

large variability between samples and between treatment techniques. One way to mitigate that in the future is to possibly assess dose to a small volume such as 1cc of spinal cord. This would allow for a less variable representation of clinically relevant maximum dose. 3D-CRT provided the most agreement between planners and outside of spinal cord maximum, all other organs assesses calculated an alpha value > 0.667 indicating acceptable agreement. With this confirmed agreement between an expert planner and the study investigator, confidence was established to proceed with the study investigator planning all remaining cases.

*Conformity Index*

The conformity index was developed by the Radiation Therapy Oncology Group (RTOG) to help evaluate the quality of radiation plans. In 1993, the group established a need and recommendation for evaluation of stereotactic radiation therapy plans [142]. Specific to the conformity index, it can be defined as the ratio of a reference isodose volume to target volume. It is commonly used to evaluate the coverage of the target PTV with the respective target dose. In this study, the conformity index was evaluated as the volume of 42.75 Gy (95%) as a ratio of PTV volume.

There is significant difference between both 3D-CRT compared to IMRT and 3D-CRT compared to VMAT. Figure 3.5 visually displays the results of conformity index. There is a significant range in data for 3D-CRT with one outlier reaching a conformity index of 2.5 meaning the volume of 95% dose coverage was 2.5 times greater than the volume of the PTV. Overall, there is a large degree of over-irradiation of the 95% dose level to normal structures using 3D-CRT. The median data value for this data set was 1.45, or volume of the 95% being 45% greater than the volume of PTV. Due to limitations of field entry and therefore modulation, it is difficult to achieve a highly conformal plan using 3D-CRT. It is especially difficult to push dose around a target when the maximal shape of the target area forces the field size to increase to allow coverage. Figure 3.1 represents a section of a 3D-CRT plan; specific focus can be made on the axial slice where there is a significant gap between the 95% isodose level (yellow) and target area. Having a highly non-conformal plan pushes high dose to normal tissues and sensitive structures around the target

area. This will increase acute toxicity and potentially increase late toxicity in this subset of patients. This is of particular concern to organs such as lung and heart where compromised function may exist due to chemotherapy.

Table 3.3 summarizes conformity index statistics for this study. Median values for IMRT and VMAT were 1.04 and 1.01 respectively. Both IMRT and VMAT were far superior to 3D-CRT with a 28.51% difference between 3D-CRT and IMRT and 30.70% difference between 3D-CRT and VMAT. With the limited capability of 3D-CRT to sculpt dose around a target area, these results were expected and corroborated with other studies when compared to IMRT [121,147]. There was also a significant difference when comparing IMRT to VMAT. While both plans provided excellent conformality, VMAT allowed for a slightly more conformal plan with an average decrease of 2.98%. This was somewhat expected as VMAT allows for more options of entry and modulation therefore allowing dose to shape around a complex target. The benefit for patients is a reduction in high dose delivery outside the tumour area and a reduction of potential side effects. While having a highly conformal treatment is important to reduce dose to normal tissues, the issue of immobilization becomes more important. To have such a highly conformal treatment, there needs to be certainty in patient setup as well as target delineation.

*Integral Dose*

Integral dose was calculated using the formula present by Aoyama *et al* in which the integral dose is defined as the volume integral of the dose deposited in a patient and is equal to the mean dose times the volume irradiated to any dose [80]. For the purposes of this study, integral dose was calculated to the normal body tissues as whole defined as the body minus PTV, going one slice above and below the PTV. This methodology was chosen as the PTV is consistently covered with high dose across the treatment techniques. Regardless of planning technique, all PTV would receive approximately the same dose. The normal tissues were also limited to one slice above and below to better represent the area of treatment.

Statistically significant results were noted when comparing IMRT and 3D-CRT as well as VMAT and 3D-CRT with respect to integral dose. Statistical analysis revealed no significant difference in integral dose between IMRT and VMAT with results summarized in Table 3.3. There are limited studies comparing integral dose for 3D-CRT and IMRT or VMAT. In one study conducted by Fenkell *et al*, dosimetric comparison was made between IMRT and 3D-CRT for cervical esophagus patients [121]. Integral dose was mentioned as a studied parameter in this study however there was no mention of the method of calculation. Nonetheless, the authors concluded that IMRT resulted in higher integral dose to the body when compared to 3D-CRT. In another study of 3D-CRT compared to IMRT for endometrial cancer, Lian *et al* concluded that IMRT had a significant increase in integral dose compared to 3D-CRT. Normal tissue was calculated as whole patient volume minus CTV [145]. This contrasts to our study which demonstrated a statistically significant median reduction of integral dose of 14.0% with IMRT compared to 3D-CRT. There may be variation in calculation methods which could help explain the difference. Similar results were noted for VMAT when comparted to 3D-CRT with a median reduction of 14.8%.

There is more literature available when comparing integral dose for IMRT and VMAT. With respect to esophageal patients, Van Benthuysen *et al* studied the differences of IMRT and VMAT for a limited set of patients. With respect to normal tissue, this study evaluated Body $V_{5Gy}$ which is the amount of body receiving 5Gy. It was concluded that VMAT equated to an additional 15% of low dose spread [137]. In a limited study by Vivekanandan *et al*, 3D-CRT was compared to 4-field IMRT and VMAT for a limited subset of esophageal patients. This study concluded that integral dose to healthy tissue was equal amongst all studied treatment techniques [146]. In another study of prostate patients, Slosarek compared CyberKnife, VMAT, IMRT and TomoTherapy for planning prostate patients. Specific to integral dose, it was concluded that VMAT was significantly lower compared to IMRT for integral dose of the body structure [129]. These results all differ with the results of this study. In this study, there is no significant difference in integral dose between IMRT and VMAT.

There is no accepted standard of determining integral dose to normal tissues. Some studies investigate integral dose to specific organs while other study the body itself. Furthermore, there

is variation on how the body would be defined for these purposes. One study mentioned taking the normal tissue and subtracting CTV while in this study the PTV was subtracted from the body. Since there is no consistency, it would be difficult to interpret results among studies. However, in this study it was quite clear that both IMRT and VMAT provided better integral dose to normal body tissues compared to 3D-CRT. One of the possible explanations for this could be related to the fact that IMRT and VMAT provided very conformal treatment. In other words, there was high dose spill outside of the PTV which influenced the mean dose to the healthy tissues for 3D-CRT. In many studies, integral dose assesses mean dose to the studied structure. There is no differentiation between multiple entries of low dose compared to minimal entries of higher dose. It is difficult to assess the impact of extremely low dose spread using this statistic. In future studies, it may be prudent to assess specific low dose volume at a clinically significant dose level. As mentioned earlier, the risk of secondary malignancy is low in this subset of patients due to overall survival and age of onset however it is important to minimize risk where possible. Both IMRT and VMAT provide significant reduction in integral dose to normal tissues.

*Monitor Units*

Monitor units is a measure of machine output and could be correlated to treatment time with the patient in treatment position. There are other limiting factors such as gantry speed however it is commonly accepted that a reduction in monitor units leads to a reduction in treatment time. This is beneficial to the patient as this will minimize the time the patient is in the treatment position which could be difficult to maintain. This is also beneficial to the facility as it could allow for more patients to be treated in the same amount of time. Monitor unit reduction also allows for a reduction in scatter dose throughout the body as well as a reduction in leakage dose through the MLC shielding. This could also be beneficial with respect to machine longevity as there would be less wear and tear to vital components of the linear accelerator.

Table 3.4 summarizes monitor unit findings for this study. 3D-CRT results in significantly fewer monitor units to deliver treatment. This was expected as there is limited modulation in the 3D-CRT plans and therefore more open fields treated to achieve the target dose quickly. IMRT and

VMAT both resulted in a 107.2% and 80.4% increase in monitor units when comparted to 3D-CRT respectively. While it is beneficial to have a reduction in monitor units for the reasons listed above, this study has proved there is far more benefit to have a more conformal type of treatment. There is a reduction of normal tissues receiving high dose as well as a significant reduction in integral dose.

There was a statistically significant reduction in monitor units for VMAT plans compared to IMRT. VMAT plans on average had a 9.9% reduction. Despite higher degrees of entry in the patient, VMAT plans can provide a little more efficient delivery of radiation. The results of this study correspond to other studies of esophagus planning [137] as well as prostate planning [147]. The reduction of monitor units can be significant when delivering treatment to many patients site wide. This also a consideration for facilities with limited resources and a need for the most efficient treatment possible. Along with practical benefits, there is also the reduction of whole-body scatter dose and leakage dose from the machine. VMAT can deliver more conformal treatment with a reduction in machine output when compared to IMRT.

*Lung Dose*

One of the primary concerns when treating esophagus patients with external beam radiation is total lung dose. As the esophagus is a central lying organ, access to the tumour area requires radiation passing through the lungs. There has been some concern with increasing lung dose when introducing multiple beams of entry. Specifically, there is concern that low dose to lung would be increased despite the high dose conformality offered by IMRT and VMAT compared to 3D-CRT. This study hoped to prove that low dose to lung is equivalent across treatment techniques, but higher dose levels and mean dose is decreased with IMRT and VMAT.

Table 3.5 summarizes lung dose statistics for this study. Lung $V_{5Gy}$ was compared across treatment techniques with minimal difference. When comparing all three techniques with each other, all results concluded with a p-value much greater than 0.05. Based on this we cannot

conclude that any significant difference exists. Figure 3.7 displays the data set for lung $V_{5Gy}$ of all patients. Although the median and average results were the same, there is a larger variance in the 3D-CRT compared to IMRT and VMAT. A major factor of influencing lung dose in 3D-CRT is the volume of treatment and field arrangements. There is not much control in terms of modulation of the open beam as the beams are set to cover the disease. A larger target area will increase lung dose. Despite the increased beams of entry, IMRT and VMAT both provided comparable lung $V_{5Gy}$ to that of 3D-CRT. One of the main focuses of the study was to evaluate lung and heart dose with the subset of patients. When planning IMRT and VMAT, the planner can specify dose objectives which the optimizer will attempt to achieve while respecting other constraints. Going into this study, care was taken to try to reduce lung dose while achieving optimal target coverage. There was marginal difference across all treatment techniques with respect to volume of lung receiving 5 Gy.

Large differences were noted when studying lung $V_{20Gy}$ and mean dose. With respect to lung $V_{20Gy}$, IMRT was able to reduce dose by an average of 49.7% when compared to 3D-CRT. Further improvement was noted with VMAT with an average reduction of 57.4%. These results were statistically significant and result in a large improvement in absorbed lung dose when compared to 3D-CRT. With the ability to control modulation, lung dose can be greatly reduced at the medium and high dose levels. IMRT and VMAT both provide increased conformality and this translates to the reduction of higher doses in lung. Interestingly, there was large and statistically significant difference in lung $V_{20Gy}$ between IMRT and VMAT. VMAT was able to reduce lung $V_{20Gy}$ by an average of 14.7% when compared to IMRT. This could be in part to the increased beamlet options provided by VMAT. High modulation and sculpting are achievable to spare lung tissues as much as reasonably possible. VMAT provided the best reduction in lung $V_{20Gy}$ among all treatment techniques. Figure 4.1 displays an axial slice of a patient planned with 3D-CRT, IMRT and VMAT. The 20 Gy isodose line was displayed to visually assess the dose and how it avoids the lung tissues.

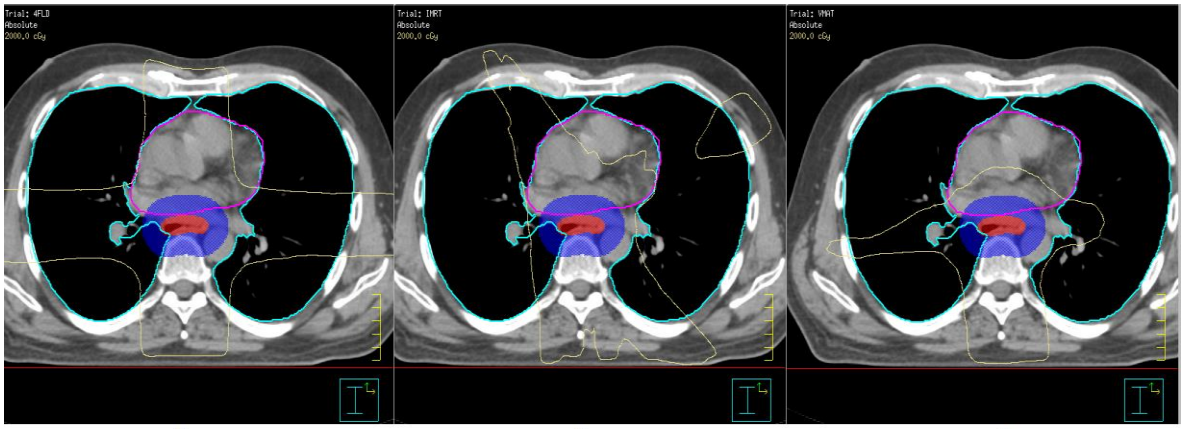


**Figure 4.1** – Axial slice of 20Gy isodose line for 3D-CRT(1), IMRT(2) and VMAT(3).

A similar result was yielded for lung mean dose. IMRT and VMAT were able to reduce lung mean dose by an average of 20.3% and 24.9% respectively. These results are significant and clearly show that both IMRT and VMAT can greatly reduce lung dose. A statistically significant reduction of 5.6% was also noted when comparing VMAT to IMRT. While the results are not as large as the difference in lung $V_{20Gy}$, there is data here to conclude that lung mean dose is best spared with VMAT. When comparing lung maximum dose, there is similarity across treatment techniques. There was no statistically significant difference between IMRT and 3D-CRT; however, there was a slight reduction in maximum point dose when utilizing VMAT compared to 3D-CRT and IMRT. While maximum dose is an important metric, it is expected that maximum dose remains above 45Gy considering the volume of PTV that overlaps lungs. The esophagus lies right beside the lungs so any expansion on the volume to PTV will include lung. Maximum dose also assesses maximum point dose to any pixel of that structure and may not be a clinically relevant metric in the human body. Overall, maximum dose was similar across treatment techniques with not large differences noted.

A major publication in 2010 sought to standardize dose limitations to important organs throughout the body. QUANTEC was developed with dose limits to organs including lung. Specific to lung tissue, the parameters assessed were $V_{20Gy}$ and mean dose. Both these parameters were deemed to be clinically significant parameters in a review published by Marks *et al* [77]. Reduction of these end points reduces lung pneumonitis for patients undergoing

radiation in the thoracic area. This study was able to provide clarity in lung dose for external beam planning of esophagus radiation. There is a significant reduction in lung $V_{20Gy}$ and mean dose with VMAT planning which should correlate to reduced lung pneumonitis in patients undergoing radiation treatment. With comparable low dose volume among all treatment techniques, VMAT is preferable for distal esophageal patients if lung dose is of particular concern.

*Heart Dose*

Another major concern for this subset of patients is heart dose. Distal esophagus patients undergoing pre-operative radiation therapy often also have concurrent chemotherapy. Depending on the chemotherapy regimen for the patient, this could have cytotoxic effects on the heart. Therefore, it is important to maintain low dose to heart to mitigate any effect radiation can have on cardiac issues. Before the commencement of this study, the hypothesis was made that heart dose would be reduced with VMAT planning method.

A summary of results for heart dose is presented in table 3.6. As noted earlier, IMRT and VMAT both offer more conformal radiation delivery. This is especially true at high dose levels close to the target area. Heart $V_{30Gy}$ is reduced by 10.1% and 14.3% from 3D-CRT to IMRT and VMAT respectively. These results are in line with the previously discussed findings of a reduction in dose to organs. IMRT and VMAT are again able to minimize dose at the 30Gy level which can effectively spare the heart tissues. In a study by Wei *et al*, $V_{30Gy}$ was significantly associated with pericardial effusion rates if more than 46% of the heart received this dose. While the median dose for all treatment techniques were under this threshold, there was further reduction with respect to IMRT and VMAT. VMAT also provided a statistically significant reduction in $V_{30Gy}$ of 4.0%. This reduction in heart dose is corroborated by other studies as well [139,140].

Similar results were noted for mean dose to heart. It is shown that a slight reduction occurs with analysis of the plot at figure 3.12. Median heart dose for 3D-CRT was 2758.8 cGy while IMRT and VMAT were able to reduce that to 2533.9 cGy and 2395.2 cGy respectively. This results in a

statistically relevant reduction on average of 10.4% for IMRT compared to 3D-CRT and 13.4% for VMAT compared to 3D-CRT. VMAT again offered further reduction with an average decrease of 3.2% when compared to IMRT. These results follow the same trend as lung mean dose. While VMAT offers minimal additional sparing of heart doses, the results are significant. Any reduction in normal tissues while maintaining target doses is of benefit to the patient both acutely and long term. Reduction of heart doses and other organs allows for a potential of dose escalation. VMAT would provide the best heart sparing out of all techniques.

Heart maximum dose comparison returned similar results to lung maximum dose. There was not enough statistical analysis to draw a conclusion when comparing IMRT to 3D-CRT. However, there was slight reduction in maximum dose when comparing VMAT and 3D-CRT as well as VMAT and IMRT. These results were within an average of 2% so they can be deemed negligible. For the purposes of this study, inference is made that heart maximum dose is similar across all treatment techniques. This is also important to note that even with the fact that heart volumetric doses are reduced, there is no hot spots being pushed into heart tissue.

*Spinal Cord, Kidney, and Liver Doses*

Spinal cord maximum doses increased for IMRT and VMAT with respect to 3D-CRT. Spinal cord maximum dose increased by an average of 13.34% comparing IMRT to 3D-CRT and 9.45% when comparing VMAT to 3D-CRT. These results were statistically significant and represented a noticeable difference. In multiple previous studies, spinal cord maximum was in fact reduced with IMRT and VMAT compared to 3D-CRT [119, 137]. Our study contrasts these results as 3D-CRT had the lowest spinal cord maximum. This was interesting to note as all 3D-CRT plans had a posterior beam entering through the spinal cord with an anterior beam exiting there. This disagreed with the initial thoughts of this study where spinal cord maximum dose was thought to be reduced with IMRT and VMAT. Inverse planning methods allow for control of dose to organs and modulation of the dose distribution. With the results of comparable low dose to lung and reduced lung mean and heart mean dose, it appears that more dose was deposited in the spinal cord area. Since the lung and heart represent most of the anatomy laterally and anterior

to our target area, the only place to deposit dose to the esophagus is through the spinal cord. Care must be taken when planning these cases and priorities assigned to certain organs. Other organs not in priority must still be analyzed. In the case of this study, the median maximum spinal cord dose was 2731.5 cGy for 3D-CRT, 3237.1 cGy for IMRT and 3120.6 cGy. All treatment techniques kept spinal cord maximum dose well within tolerance and away from the level of concern. QUANTEC quantified a maximum dose of 5000 cGy to spinal cord that would indicate a 0.2% chance of myelopathy. While the doses achieved in this study would not be cause for clinical concern, high spinal cord maximum dose at the expense of sparing lungs and heart maybe a consideration for any future dose escalation projects.

Kidney dose was evaluated for this study for all patients. However, it should be noted that target volumes rarely extended inferiorly to the level of the kidneys. The results of this study mainly represent scatter dose and therefore conclusions are difficulty to ascertain. Nonetheless, there are certain situations where kidneys could be an organ for concern and care must be taken when planning for this type of patient. Many of these patients are on chemotherapy so maintaining adequate kidney function is imperative for successful treatment with minimal side effects. Kidneys are a radiosensitive organ with low dose tolerance. Extrapolating from our lung data, organs on the periphery of a centrally located target volume can be spared well using IMRT or VMAT. In this study, there can be no statistically significant conclusions to identify one technique over another. There was a statistically significant difference in $V_{20Gy}$; however, this represented scatter dose with median doses of 5.5 cGy, 1.7 cGy and 0.7 cGy for 3D-CRT, IMRT and VMAT respectively.

The liver is an organ vital for metabolism of important nutrients as well as bile production and excretion. In previous studies, it has been shown that the liver has a large relation to volume effects and mean dose could be useful to set limits. While the esophagus does not travel far inferiorly into the abdomen, there is a fair amount of liver that reach up to the diaphragm. The liver is a large organ and depending on patient anatomy a large portion could be at the level of the target area. In this study, there was a reduction in mean lung dose by an average of 29.86%, 24.29% when comparing 3D-CRT to IMRT and VMAT respectively. This represented a large,

significant reduction in dose. Interestingly, IMRT resulted in an average decrease of 10.3% when compared to VMAT. 3D-CRT resulted in the highest mean dose and could be related to the fact that the liver falls laterally and in the path of one of beams. IMRT was able to spare the liver more than VMAT due to beams avoiding entry and exit through the liver. Anatomically, the liver lies to the right side while the distal esophagus typically enters angling to the left side of the body. Most IMRT would be offset to the left side of the patient and therefore avoided the liver. A liver mean dose under 3000 cGy should be maintained to decrease the risk of radiation induced liver disease. All treatment techniques were well below this level with doses of 1901.80 cGy, 1134.00 cGy and 1351.65 cGy for 3D-CRT, IMRT and VMAT.

## 5.0 Conclusion and Future Direction

The intention of this research was to evaluate radiation dose delivered to OAR and target volumes for 3D-CRT, IMRT and VMAT planning techniques for distal esophageal cancer treatment. The data was analyzed with intention to provide evidence that more conformal radiation treatment planning techniques of IMRT and VMAT can provide decreased normal organ dose while satisfying target dose criteria.

In contrast to other studies, this study provided a large and robust amount of data to draw strong conclusions. There are also extremely limited studies comparing 3D-CRT, IMRT and VMAT with each other for distal esophagus radiation planning. With a cohort of 40 patients, statistically significant conclusions could be used to influence an institutions decision on treatment technique. VMAT provided superior dose conformality as well as a reduction in normal tissue doses. VMAT also provided superior monitor unit reduction which is beneficial for treating facilities. In the event VMAT is not supported at a treating facility, IMRT also provided similar benefits over 3D-CRT. Overall, VMAT accounted for increased organ sparing when compared to 3D-CRT and IMRT while maintaining excellent target coverage. These results were in line with the hypothesis of this study and provide statistically significant conclusions with a large sample size.

One of the limitations of this study is in possible bias of this retrospective review. While retrospective reviews may be inherent to bias, there is possible bias in this study with the planning of VMAT plans. VMAT is used at this facility for a multitude of other disease sites so there may be unintended bias to influence VMAT planning as being the ideal choice. Also, there is no data on the overall survival or toxicity of any of these patients. It is unclear if 3D-CRT had significant toxicities that could be improved upon with a change in treatment techniques.

This also ties into future studies that would be available to pursue. Toxicity and patient outcomes should be studied and compared to evaluate if there is any clinical benefit to these reduction in normal tissue doses. While VMAT does provide a theoretical benefit, it would be

prudent to evaluate any clinical benefits. Studies could also be done to investigate dose escalation in this subset of patients. If VMAT can provide adequate organ sparing, there may be a window to boost doses to tumour areas with the hope to control disease and improve overall survival.

For this subset of patients being treated with external beam radiation, VMAT planning and delivery can effectively spare organs at risk while maintaining target coverage. Low dose to lung was shown to be equivalent to 3D-CRT while VMAT was able to reduce overall integral dose as well as decrease monitor units and treatment times. For this treatment facility, VMAT should be recommended as the treatment planning and delivery method of choice. IMRT also provides superior reduction in organ dose when compared to 3D-CRT and can be utilized in facilities without VMAT capabilities.

## 6.0 Reference List

[1] Chaudhry SR, Bordoni B. Anatomy, Thorax, Esophagus. [Updated 2019 Apr 8]. In: StatPearls [Internet]. Treasure Island (FL): StatPearls Publishing; 2020 Jan-. Available from: https://www.ncbi.nlm.nih.gov/books/NBK482513/

[2] Oezcelik, A., & DeMeester, S. R. (2011). General Anatomy of the Esophagus. *Thoracic Surgery Clinics*, *21*(2), 289–297. https://doi.org/10.1016/j.thorsurg.2011.01.003

[3] Patti, M. G., Gantert, W., & Way, L. W. (1997). Surgery of the esophagus: anatomy and physiology. *Surgical Clinics*, *77*(5), 959-970.

[4] Reiner, M. A. (2002). Anatomy and physiology. *Laparoscopic Hernia Surgery: An Operative Guide*, *77*(5), 179–185. https://doi.org/10.5005/jp/books/13093_3

[5] Ji, X., Cai, J., Chen, Y., & Chen, L. Q. (2016). Lymphatic spreading and lymphadenectomy for esophageal carcinoma. *World journal of gastrointestinal surgery*, *8*(1), 90.

[6] Canadian-Cancer-Statistics-2019-EN (PDF)

[7] Surveillance, Epidemiology, and End Results Program. (n.d.). *Cancer Stat Facts: Esophageal Cancer.* https://seer.cancer.gov/statfacts/html/esoph.html

[8] Zhang, Y. (2013). Epidemiology of esophageal cancer. *World Journal of Gastroenterology*, *19*(34), 5598–5606. https://doi.org/10.3748/wjg.v19.i34.5598

[9] Liang, H., Fan, J. H., & Qiao, Y. L. (2017). Epidemiology, etiology, and prevention of esophageal squamous cell carcinoma in China. *Cancer Biology and Medicine*, *14*(1), 33–41. https://doi.org/10.20892/j.issn.2095-3941.2016.0093

[10] Otterstatter, M. C., Brierley, J. D., De, P., Ellison, L. F., MacIntyre, M., Marrett, L. D., … Weir, H. K. (2012). Esophageal cancer in Canada: Trends according to morphology and anatomical location. *Canadian Journal of Gastroenterology*, *26*(10), 723–727. https://doi.org/10.1155/2012/649108

[11] Bray, F., Ferlay, J., Soerjomataram, I., Siegel, R. L., Torre, L. A., & Jemal, A. (2018). Global cancer statistics 2018: GLOBOCAN estimates of incidence and mortality worldwide for 36 cancers in 185 countries. *CA: a cancer journal for clinicians*, *68*(6), 394-424.

[12] Miyamoto A, Kuriyama S, Nishino Y, et al. Lower risk of death from gastric cancer among participants of gastric cancer screening in Japan: a population-based cohort study. *Prev Med*. 2007;44(1):12-19. doi:10.1016/j.ypmed.2006.07.016

[13] Choi, K. S., Jun, J. K., Suh, M., Park, B., Noh, D. K., Song, S. H., ... & Park, E. C. (2015). Effect of endoscopy screening on stage at gastric cancer diagnosis: results of the National Cancer Screening Programme in Korea. *British journal of cancer*, *112*(3), 608-612.

[14] Enzinger, P. C., & Mayer, R. J. (2003). Esophageal cancer. *New England Journal of Medicine*, *349*(23), 2241-2252.

[15] Hashibe, M., Morgenstern, H., Cui, Y., Tashkin, D. P., Zhang, Z. F., Cozen, W., ... & Greenland, S. (2006). Marijuana use and the risk of lung and upper aerodigestive tract cancers: results of a population-based case-control study. *Cancer Epidemiology and Prevention Biomarkers*, *15*(10), 1829-1834.

[16] Huang, Y. H. J., Zhang, Z. F., Tashkin, D. P., Feng, B., Straif, K., & Hashibe, M. (2015). An epidemiologic review of marijuana and cancer: an update. *Cancer Epidemiology and Prevention Biomarkers*, *24*(1), 15-31.

[17] Holmes, R. S., & Vaughan, T. L. (2007, January). Epidemiology and pathogenesis of esophageal cancer. In *Seminars in radiation oncology* (Vol. 17, No. 1, pp. 2-9). WB Saunders.

[18] Gammon, M. D., Ahsan, H., Schoenberg, J. B., West, A. B., Rotterdam, H., Niwa, S., ... & Fraumeni Jr, J. F. (1997). Tobacco, alcohol, and socioeconomic status and adenocarcinomas of the esophagus and gastric cardia. *Journal of the National Cancer Institute*, *89*(17), 1277-1284.

[19] Garavello, W., Negri, E., Talamini, R., Levi, F., Zambon, P., Dal Maso, L., ... & La Vecchia, C. (2005). Family history of cancer, its combination with smoking and drinking, and risk of squamous cell carcinoma of the esophagus. *Cancer Epidemiology and Prevention Biomarkers*, *14*(6), 1390-1393.

[20] Lagergren, J. (2005). Adenocarcinoma of oesophagus: what exactly is the size of the problem and who is at risk?. *Gut*, *54*(suppl 1), i1-i5.

[21] Lindblad, M., Rodríguez, L. A. G., & Lagergren, J. (2005). Body mass, tobacco and alcohol and risk of esophageal, gastric cardia, and gastric non-cardia adenocarcinoma among men and women in a nested case-control study. *Cancer Causes & Control*, *16*(3), 285-294.

[22] Abbas, G., & Krasna, M. (2017). Overview of esophageal cancer. *Annals of cardiothoracic surgery*, *6*(2), 131.

[23] Lagergren, J., Bergström, R., Lindgren, A., & Nyrén, O. (1999). Symptomatic gastroesophageal reflux as a risk factor for esophageal adenocarcinoma. *New England journal of medicine*, *340*(11), 825-831.

[24] Huang, F. L., & Yu, S. J. (2018). Esophageal cancer: risk factors, genetic association, and treatment. *Asian journal of surgery*, *41*(3), 210-215.

[25] Sun, L., Zhang, Z., Xu, J., Xu, G., & Liu, X. (2017). Dietary fiber intake reduces risk for Barrett's esophagus and esophageal cancer. *Critical reviews in food science and nutrition*, *57*(13), 2749-2757.

[26] Hoyo, C., Cook, M. B., Kamangar, F., Freedman, N. D., Whiteman, D. C., Bernstein, L., ... & Gammon, M. D. (2012). Body mass index in relation to oesophageal and oesophagogastric junction adenocarcinomas: a pooled analysis from the International BEACON Consortium. *International journal of epidemiology*, *41*(6), 1706-1718.

[27] Smith, M., Zhou, M., Whitlock, G., Yang, G., Offer, A., Hui, G., ... & Chen, Z. (2008). Esophageal cancer and body mass index: results from a prospective study of 220,000 men in China and a meta-analysis of published studies. *International journal of cancer*, *122*(7), 1604-1610.

[28] Lindkvist, B., Johansen, D., Stocks, T., Concin, H., Bjørge, T., Almquist, M., ... & Manjer, J. (2014). Metabolic risk factors for esophageal squamous cell carcinoma and adenocarcinoma: a prospective study of 580 000 subjects within the Me-Can project. *BMC cancer*, *14*(1), 1-12.

[29] Jansson, C., Johansson, A. L. V., Nyrén, O., & Lagergren, J. (2005). Socioeconomic factors and risk of esophageal adenocarcinoma: A nationwide Swedish case-control study. *Cancer Epidemiology Biomarkers and Prevention*, *14*(7), 1754–1761. https://doi.org/10.1158/1055-9965.EPI-05-0140

[30] Ye, W., Held, M., Lagergren, J., Engstrand, L., Blot, W. J., McLaughlin, J. K., & Nyrén, O. (2004). Helicobacter pylori infection and gastric atrophy: risk of adenocarcinoma and squamous-cell carcinoma of the esophagus and adenocarcinoma of the gastric cardia. *Journal of the National Cancer Institute*, *96*(5), 388-396.

[31] Mudan S, Kang J. Epidemiology and clinical presentationin esophageal cancer. In: Rankin S (ed.).Carcinoma of the Esophagus. Cambridge University Press, New York 2008;1–10.

[32] Gibbs, J. F., Rajput, A., Chadha, K. S., Douglas, W. G., Hill, H., Nwogu, C., ... & Sabel, M. S. (2007). The changing profile of esophageal cancer presentation and its implication for diagnosis. *Journal of the National Medical Association*, *99*(6), 620.

[33] Koshy, M., Esiashvilli, N., Landry, J. C., Thomas Jr, C. R., & Matthews, R. H. (2004). Multiple management modalities in esophageal cancer: epidemiology, presentation and progression, work-up, and surgical approaches. *The oncologist*, *9*(2), 137-146.

[34] Canadian Cancer Society. (n.d.). *Esophageal Cancer.* https://www.cancer.ca/en/cancer-information/cancer-type/esophageal/diagnosis/?region=on

[35] Puli, S. R., Reddy, J. B., Bechtold, M. L., Antillon, D., Ibdah, J. A., & Antillon, M. R. (2008). Staging accuracy of esophageal cancer by endoscopic ultrasound: a meta-analysis and systematic review. *World journal of gastroenterology: WJG*, *14*(10), 1479.

[36] Heeren, P. A., Jager, P. L., Bongaerts, F., van Dullemen, H., Sluiter, W., & Plukker, J. T. M. (2004). Detection of distant metastases in esophageal cancer with 18F-FDG PET. *Journal of nuclear medicine*, *45*(6), 980-987.

[37] Jain, S., & Dhingra, S. (2017). Pathology of esophageal cancer and Barrett's esophagus. *Annals of cardiothoracic surgery*, *6*(2), 99.

[38] Rice, T. W., Patil, D. T., & Blackstone, E. H. (2017). AJCC/UICC staging of cancers of the esophagus and esophagogastric junction: application to clinical practice. *Annals of cardiothoracic surgery*, *6*(2), 119.

[39] Sohda, M., & Kuwano, H. (2017). Current status and future prospects for esophageal cancer treatment. *Annals of Thoracic and Cardiovascular Surgery*, *23*(1), 1-11.

[40] Mawhinney, M. R., & Glasgow, R. E. (2012). Current treatment options for the management of esophageal cancer. *Cancer management and research*, *4*, 367.

[41] Ilson, D. H. (2008). Esophageal cancer chemotherapy: recent advances. *Gastrointestinal cancer research: GCR*, *2*(2), 85.

[42] Sabra, M. J., Alwatari, Y. A., Wolfe, L. G., Xu, A., Kaplan, B. J., Cassano, A. D., & Shah, R. D. (2020). Ivor Lewis vs Mckeown esophagectomy: analysis of operative outcomes from the ACS NSQIP database. *General thoracic and cardiovascular surgery*, 1-10.

[43] Cooper, J. S., Guo, M. D., Herskovic, A., Macdonald, J. S., Martenson Jr, J. A., Al-Sarraf, M., ... & Leichman, L. L. (1999). Chemoradiotherapy of locally advanced esophageal cancer: long-term follow-up of a prospective randomized trial (RTOG 85-01). *Jama*, *281*(17), 1623-1627.

[44] Shridhar, R., Almhanna, K., Meredith, K. L., Biagioli, M. C., Chuong, M. D., Cruz, A., & Hoffe, S. E. (2013). Radiation therapy and esophageal cancer. *Cancer Control*, *20*(2), 97-110.

[45] Macdonald, J. S., Smalley, S. R., Benedetti, J., Hundahl, S. A., Estes, N. C., Stemmermann, G. N., ... & Martenson, J. A. (2001). Chemoradiotherapy after surgery compared with surgery alone for adenocarcinoma of the stomach or gastroesophageal junction. *New England Journal of Medicine*, *345*(10), 725-730.

[46] Van Hagen, P., Hulshof, M. C. C. M., Van Lanschot, J. J. B., Steyerberg, E. W., Henegouwen, M. V. B., Wijnhoven, B. P. L., ... & van der Gaast, A. (2012). Preoperative chemoradiotherapy for esophageal or junctional cancer. *New England Journal of Medicine*, *366*(22), 2074-2084.

[47] Shapiro, J., Van Lanschot, J. J. B., Hulshof, M. C., van Hagen, P., van Berge Henegouwen, M. I., Wijnhoven, B. P., ... & CROSS Study Group. (2015). Neoadjuvant chemoradiotherapy plus surgery versus surgery alone for oesophageal or junctional cancer (CROSS): long-term results of a randomised controlled trial. *The lancet oncology*, *16*(9), 1090-1098.

[48] Linz, U. (Ed.). (2012). *Ion Beam Therapy*. Springer Berlin Heidelberg.

[49] Coutard, H. (1937). The results and methods of treatment of cancer by radiation. *Annals of surgery*, *106*(4), 584.

[50] Gianfaldoni, S., Gianfaldoni, R., Wollina, U., Lotti, J., Tchernev, G., & Lotti, T. (2017). An overview on radiotherapy: From its history to its current applications in dermatology. *Open Access Macedonian Journal of Medical Sciences*, *5*(4 Special Issue GlobalDermatology), 521–525. https://doi.org/10.3889/oamjms.2017.122

[51] Lawrence, E. (1951). *The evolution of the cyclotron*. Nobel Lecture.

[52] Kerst, D.W. (1943). The Betatron. *Radiology*, *40*(2), 115-119.

[53] Clarke, R., & Valentin, J. (2005). A History of the International commission on Radiological Protection. *Health Physics*, *88*(5), 407-422.

[54] Johns, H.E., Bates, L.M., Epp, E.R., Cormack, D.V., Fedoruk, S.O. (1951). 1000-Curie Cobalt-60 Units for Radiation Therapy. *Nature, 168,* 1035-1036.

[55] Weissbluth, M., Karzmark, C. J., Steele, R. E., & Selby, A. H. (1959). The Stanford Medical Linear Accelerator. *Radiology, 77*(2), 242-253.

[56] Huh, H. Do, & Kim, S. (2020). History of Radiation Therapy Technology. *Progress in Medical Physics*, *31*(3), 124–134. https://doi.org/10.14316/pmp.2020.31.3.124.

[57] Webb, S., & Evans, P. M. (2006). Innovative Techniques in Radiation Therapy: Editorial, Overview, and Crystal Ball Gaze to the Future. *Seminars in Radiation Oncology*, *16*(4), 193–198. https://doi.org/10.1016/j.semradonc.2006.04.001

[58] Hall, Eric J. (2006). *Radiobiology for the radiologist*. Lippincott Williams & Wilkins.

[59] Withers, H. R. (1975). The four R's of radiotherapy. In *Advances in radiation biology* (Vol. 5, pp. 241-271). Elsevier.

[60] Webb, S., & Evans, P. M. (2006). Innovative Techniques in Radiation Therapy: Editorial, Overview, and Crystal Ball Gaze to the Future. *Seminars in Radiation Oncology*, *16*(4), 193–198. https://doi.org/10.1016/j.semradonc.2006.04.001

[61] Rockwell, S., Dobrucki, I. T., Kim, E. Y., Marrison, S. T., & Vu, V. T. (2009). Hypoxia and radiation therapy: past history, ongoing research, and future promise. *Current molecular medicine*, *9*(4), 442-458.

[62] University of Leicester. (n.d.). *The cellcycle, mitosis and meiosis*. Virtual Genetics Education Centre. https://le.ac.uk/vgec/topics/cell-cycle

[63] Vogin, G., & Foray, N. (2013). The law of Bergonié and Tribondeau: a nice formula for a first approximation. *International journal of radiation biology*, *89*(1), 2-8. [64] Combined Chemotherapy and Radiotherapy Compared with Radiotherapy Alone in Patients with Cancer of the Esophagus

[65] Minsky, B. D., Pajak, T. F., Ginsberg, R. J., Pisansky, T. M., Martenson, J., Komaki, R., ... & Kelsen, D. P. (2002). INT 0123 (Radiation Therapy Oncology Group 94-05) phase III trial of combined-modality therapy for esophageal cancer: high-dose versus standard-dose radiation therapy. *Journal of clinical oncology*, *20*(5), 1167-1174.

[66] Werner-Wasik, M., Yorke, E., Deasy, J., Nam, J., & Marks, L. B. (2010). Radiation dose-volume effects in the esophagus. *International Journal of Radiation Oncology* Biology* Physics*, *76*(3), S86-S93.

[67] Emami, B., Lyman, J., Brown, A., Cola, L., Goitein, M., Munzenrider, J. E., ... & Wesson, M. (1991). Tolerance of normal tissue to therapeutic irradiation. *International Journal of Radiation Oncology* Biology* Physics*, *21*(1), 109-122.

[68] Bentzen, S. M., Constine, L. S., Deasy, J. O., Eisbruch, A., Jackson, A., Marks, L. B., ... & Yorke, E. D. (2010). Quantitative Analyses of Normal Tissue Effects in the Clinic (QUANTEC): an introduction to the scientific issues. *International Journal of Radiation Oncology* Biology* Physics*, *76*(3), S3-S9.

[69] Marks, L. B., Yorke, E. D., Jackson, A., Ten Haken, R. K., Constine, L. S., Eisbruch, A., ... & Deasy, J. O. (2010). Use of normal tissue complication probability models in the clinic. *International Journal of Radiation Oncology* Biology* Physics*, *76*(3), S10-S19.

[70] Borger, J. H., Hooning, M. J., Boersma, L. J., Snijders-Keilholz, A., Aleman, B. M., Lintzen, E., ... & Van Leeuwen, F. E. (2007). Cardiotoxic effects of tangential breast irradiation in early breast cancer patients: the role of irradiated heart volume. *International Journal of Radiation Oncology* Biology* Physics*, *69*(4), 1131-1138.

[71] Harris, E. E., Correa, C., Hwang, W. T., Liao, J., Litt, H. I., Ferrari, V. A., & Solin, L. J. (2006). Late cardiac mortality and morbidity in early-stage breast cancer patients after breast-conservation treatment. *Journal of clinical oncology*, *24*(25), 4100-4106.

[72] Hooning, M. J., Botma, A., Aleman, B. M., Baaijens, M. H., Bartelink, H., Klijn, J. G., ... & Van Leeuwen, F. E. (2007). Long-term risk of cardiovascular disease in 10-year survivors of breast cancer. *Journal of the National Cancer Institute*, *99*(5), 365-375.

[73] Darby, S. C., Cutter, D. J., Boerma, M., Constine, L. S., Fajardo, L. F., Kodama, K., ... & Shore, R. E. (2010). Radiation-related heart disease: current knowledge and future prospects. *International journal of radiation oncology, biology, physics*, *76*(3), 656-665.

[74] Gagliardi, G., Constine, L. S., Moiseenko, V., Correa, C., Pierce, L. J., Allen, A. M., & Marks, L. B. (2010). Radiation dose–volume effects in the heart. *International Journal of Radiation Oncology* Biology* Physics*, *76*(3), S77-S85.

[75] Wei, X., Liu, H. H., Tucker, S. L., Wang, S., Mohan, R., Cox, J. D., ... & Liao, Z. (2008). Risk factors for pericardial effusion in inoperable esophageal cancer patients treated with definitive chemoradiation therapy. *International Journal of Radiation Oncology* Biology* Physics*, *70*(3), 707-714.

[76] Dawson, L. A., Kavanagh, B. D., Paulino, A. C., Das, S. K., Miften, M., Li, X. A., ... & Schultheiss, T. E. (2010). Radiation-associated kidney injury. *International Journal of Radiation Oncology* Biology* Physics*, *76*(3), S108-S115.

[77] Marks, L. B., Bentzen, S. M., Deasy, J. O., Bradley, J. D., Vogelius, I. S., El Naqa, I., ... & Jackson, A. (2010). Radiation dose–volume effects in the lung. *International Journal of Radiation Oncology* Biology* Physics*, *76*(3), S70-S76.

[78] Dawson, L. A., Normolle, D., Balter, J. M., McGinn, C. J., Lawrence, T. S., & Ten Haken, R. K. (2002). Analysis of radiation-induced liver disease using the Lyman NTCP model. *International Journal of Radiation Oncology* Biology* Physics*, *53*(4), 810-821.

[79] Kirkpatrick, J. P., Van Der Kogel, A. J., & Schultheiss, T. E. (2010). Radiation dose–volume effects in the spinal cord. *International Journal of Radiation Oncology* Biology* Physics*, *76*(3), S42-S49.

[80] Aoyama, H., Westerly, D. C., Mackie, T. R., Olivera, G. H., Bentzen, S. M., Patel, R. R., ... & Mehta, M. P. (2006). Integral radiation dose to normal structures with conformal external beam radiation. *International Journal of Radiation Oncology* Biology* Physics*, *64*(3), 962-967.

[81] D'Souza, W. D., & Rosen, I. I. (2003). Nontumor integral dose variation in conventional radiotherapy treatment planning. *Medical physics*, *30*(8), 2065-2071.

[82] Patel, S., Drodge, S., Jacques, A., Warkentin, H., Powell, K., & Chafe, S. (2015). A comparative planning analysis and integral dose of volumetric modulated arc therapy, helical tomotherapy, and three-dimensional conformal craniospinal irradiation for pediatric medulloblastoma. *Journal of Medical Imaging and Radiation Sciences*, *46*(2), 134-140.

[83] Saw, C. B., Yakoob, R., Enke, C. A., Lau, T. P., & Ayyangar, K. M. (2001). Immobilization devices for intensity-modulated radiation therapy (IMRT). *Medical Dosimetry*, *26*(1), 71-77.

[84] Li, W., Moseley, D. J., Bissonnette, J. P., Purdie, T. G., Bezjak, A., & Jaffray, D. A. (2010). Setup reproducibility for thoracic and upper gastrointestinal radiation therapy: Influence of immobilization method and on-line cone-beam CT guidance. *Medical Dosimetry*, *35*(4), 287-296.

[85] Balter, J. M., Ten Haken, R. K., Lawrence, T. S., Lam, K. L., & Robertson, J. M. (1996). Uncertainties in CT-based radiation therapy treatment planning associated with patient breathing. *International Journal of Radiation Oncology* Biology* Physics*, *36*(1), 167-174.

[86] Pan, T., Lee, T. Y., Rietzel, E., & Chen, G. T. (2004). 4D-CT imaging of a volume influenced by respiratory motion on multi-slice CT. *Medical physics*, *31*(2), 333-340.

[87] Yaremko, B. P., Guerrero, T. M., McAleer, M. F., Bucci, M. K., Noyola-Martinez, J., Nguyen, L. T., ... & Liao, Z. (2008). Determination of respiratory motion for distal esophagus cancer using four-dimensional computed tomography. *International Journal of Radiation Oncology* Biology* Physics*, *70*(1), 145-153.

[88] Brandner, E. D., Wu, A., Chen, H., Heron, D., Kalnicki, S., Komanduri, K., ... & Shou, Z. (2006). Abdominal organ motion measured using 4D CT. *International Journal of Radiation Oncology* Biology* Physics*, *65*(2), 554-560.

[89] Mori, S., Ko, S., Ishii, T., & Nishizawa, K. (2009). Effective doses in four-dimensional computed tomography for lung radiotherapy planning. *Medical Dosimetry*, *34*(1), 87-90.

[90] Conti, P. S., Lilien, D. L., Hawley, K., Keppler, J., Grafton, S. T., & Bading, J. R. (1996). PET and [18F]-FDG in oncology: a clinical update. *Nuclear medicine and biology*, *23*(6), 717-735.

[91] Canadian Cancer Society. (n.d.). *Positron emission tomography (PET) scan*. https://cancer.ca/en/treatments/tests-and-procedures/positron-emission-tomography-pet-scan

[92] MacManus, M., Nestle, U., Rosenzweig, K. E., Carrio, I., Messa, C., Belohlavek, O., ... & Jeremic, B. (2009). Use of PET and PET/CT for radiation therapy planning: IAEA expert report 2006–2007. *Radiotherapy and oncology*, *91*(1), 85-94.

[93] Duong, C. P., Demitriou, H., Weih, L., Thompson, A., Williams, D., Thomas, R. J., & Hicks, R. J. (2006). Significant clinical impact and prognostic stratification provided by FDG-PET in the staging of oesophageal cancer. *European journal of nuclear medicine and molecular imaging*, *33*(7), 759-769.

[94] Moureau-Zabotto, L., Touboul, E., Lerouge, D., Deniaud-Alexandre, E., Grahek, D., Foulquier, J. N., ... & Talbot, J. N. (2005). Impact of CT and 18F-deoxyglucose positron emission tomography image fusion for conformal radiotherapy in esophageal carcinoma. *International Journal of Radiation Oncology* Biology* Physics*, *63*(2), 340-345.

[95] van Rossum, P. S., van Hillegersberg, R., Lever, F. M., Lips, I. M., van Lier, A. L., Meijer, G. J., ... & Ruurda, J. P. (2013). Imaging strategies in the management of oesophageal cancer: what's the role of MRI?. *European radiology*, *23*(7), 1753-1765.

[96] Vollenbrock, S. E., Nowee, M. E., Voncken, F. E., Kotte, A. N., Goense, L., van Rossum, P. S., ... & Nijkamp, J. (2019). Gross tumor delineation in esophageal cancer on MRI compared with 18F-FDG-PET/CT. *Advances in Radiation Oncology*, *4*(4), 596-604.

[97] Mohan, R., Barest, G., Brewster, L. J., Chui, C. S., Kutcher, G. J., Laughlin, J. S., & Fuks, Z. (1988). A comprehensive three-dimensional radiation treatment planning system. *International Journal of Radiation Oncology* Biology* Physics*, *15*(2), 481-495.

[98] Ahnesjö, A. (1989). Collapsed cone convolution of radiant energy for photon dose calculation in heterogeneous media. *Medical physics*, *16*(4), 577-592.

[99] Fogliata, A., Vanetti, E., Albers, D., Brink, C., Clivio, A., Knöös, T., ... & Cozzi, L. (2007). On the dosimetric behaviour of photon dose calculation algorithms in the presence of simple geometric heterogeneities: comparison with Monte Carlo calculations. *Physics in Medicine & Biology*, *52*(5), 1363.

[100] Kitabatake, T., & Takahashi, S. (1968). Conformation radiotherapy by means of 6 MeV linear accelerator. *The Tohoku Journal of Experimental Medicine*, *94*(1), 37-43.

[101] Fraass, B. A. (1995). The development of conformal radiation therapy. *Medical physics*, *22*(11), 1911-1921.

[102] Zelefsky, M., Leibel, S., Gaudin, P., Kutcher, G., Fleshner, N., Venkatramen, E. S., ... & Fuks, Z. (1998). Dose escalation with three-dimensional conformal radiation therapy affects the outcome in prostate cancer. *International Journal of Radiation Oncology* Biology* Physics*, *41*(3), 491-500.

[103] Fiveash, J. B., Hanks, G., Roach III, M., Wang, S., Vigneault, E., McLaughlin, P. W., & Sandler, H. M. (2000). 3D conformal radiation therapy (3D-CRT) for high grade prostate cancer: a multi-institutional review. *International Journal of Radiation Oncology* Biology* Physics*, *47*(2), 335-342.

[104] Emami, B., Graham, M. V., & Purdy, J. A. (1994). Three-dimensional conformal radiotherapy in bronchogenic carcinoma: considerations for implementation. *Lung Cancer*, *11*, S117-S128.

[105] McGibney, C., Holmberg, O., McClean, B., Williams, C., McCrea, P., Sutton, P., & Armstrong, J. (1999). Dose escalation of chart in non-small cell lung cancer: is three-dimensional conformal radiation therapy really necessary?. *International Journal of Radiation Oncology* Biology* Physics*, *45*(2), 339-350.

[106] Guzel, Z., Bedford, J. L., Childs, P. J., Nahum, A. E., Webb, S., Oldham, M., & Tait, D. (1998). A comparison of conventional and conformal radiotherapy of the oesophagus: work in progress. *The British Journal of Radiology*, *71*(850), 1076-1082.

[107] Tai, P., Van Dyk, J., Yu, E., Battista, J., Schmid, M., Stitt, L., ... & Coad, T. (2000). Radiation treatment for cervical esophagus: patterns of practice study in Canada, 1996. *International Journal of Radiation Oncology* Biology* Physics*, *47*(3), 703-712.

[108] Shapiro, J., Van Lanschot, J. J. B., Hulshof, M. C., van Hagen, P., van Berge Henegouwen, M. I., Wijnhoven, B. P., ... & CROSS Study Group. (2015). Neoadjuvant chemoradiotherapy plus surgery versus surgery alone for oesophageal or junctional cancer (CROSS): long-term results of a randomised controlled trial. *The lancet oncology*, *16*(9), 1090-1098.

[109] Brahme, A., Roos, J. E., & Lax, I. (1982). Solution of an integral equation encountered in rotation therapy. *Physics in Medicine & Biology*, *27*(10), 1221.

[110] Bortfeld, T. (2006). IMRT: a review and preview. *Physics in Medicine & Biology*, *51*(13), R363.

[111] Hamacher, H. W., & Küfer, K. H. (1999). Inverse radiation therapy planning: A multiple objective optimisation approach. In *Monitoring, Evaluating, Planning Health Services* (pp. 177-189).

[112] Ling, C. C., Burman, C., Chui, C. S., Kutcher, G. J., Leibel, S. A., LoSasso, T., ... & Fuks, Z. (1996). Conformal radiation treatment of prostate cancer using inversely-planned intensity-modulated photon beams produced with dynamic multileaf collimation. *International Journal of Radiation Oncology* Biology* Physics*, *35*(4), 721-730.

[113] Zelefsky, M. J., Fuks, Z., Happersett, L., Lee, H. J., Ling, C. C., Burman, C. M., ... & Leibel, S. A. (2000). Clinical experience with intensity modulated radiation therapy (IMRT) in prostate cancer. *Radiotherapy and Oncology*, *55*(3), 241-249.

[114] Portelance, L., Chao, K. C., Grigsby, P. W., Bennet, H., & Low, D. (2001). Intensity-modulated radiation therapy (IMRT) reduces small bowel, rectum, and bladder doses in patients with cervical cancer receiving pelvic and para-aortic irradiation. *International Journal of Radiation Oncology* Biology* Physics*, *51*(1), 261-266.

[115] Bezjak, A., Rumble, R. B., Rodrigues, G., Hope, A., Warde, P., & IMRT Indications Expert Panel. (2012). Intensity-modulated radiotherapy in the treatment of lung cancer. *Clinical oncology*, *24*(7), 508-520.

[116] Gupta, T., Agarwal, J., Jain, S., Phurailatpam, R., Kannan, S., Ghosh-Laskar, S., ... & D'Cruz, A. (2012). Three-dimensional conformal radiotherapy (3D-CRT) versus intensity modulated radiation therapy (IMRT) in squamous cell carcinoma of the head and neck: a randomized controlled trial. *Radiotherapy and Oncology*, *104*(3), 343-348.

[117] Milano, M. T., Jani, A. B., Farrey, K. J., Rash, C., Heimann, R., & Chmura, S. J. (2005). Intensity-modulated radiation therapy (IMRT) in the treatment of anal cancer: toxicity and clinical outcome. *International Journal of Radiation Oncology* Biology* Physics*, *63*(2), 354-361.

[118] Nutting, C. M., Bedford, J. L., Cosgrove, V. P., Tait, D. M., Dearnaley, D. P., & Webb, S. (2001). A comparison of conformal and intensity-modulated techniques for oesophageal radiotherapy. *Radiotherapy and Oncology*, *61*(2), 157-163.

[119] Wu, V. W. C., Sham, J. S. T., & Kwong, D. L. W. (2004). Inverse planning in three-dimensional conformal and intensity-modulated radiotherapy of mid-thoracic oesophageal cancer. *The British journal of radiology*, *77*(919), 568-572.

[120] Chandra, A., Guerrero, T. M., Liu, H. H., Tucker, S. L., Liao, Z., Wang, X., ... & Komaki, R. (2005). Feasibility of using intensity-modulated radiotherapy to improve lung sparing in treatment planning for distal esophageal cancer. *Radiotherapy and Oncology*, *77*(3), 247-253.

[121] Fenkell, L., Kaminsky, I., Breen, S., Huang, S., Van Prooijen, M., & Ringash, J. (2008). Dosimetric comparison of IMRT vs. 3D conformal radiotherapy in the treatment of cancer of the cervical esophagus. *Radiotherapy and Oncology*, *89*(3), 287-291.

[122] Xu, D., Li, G., Li, H., & Jia, F. (2017). Comparison of IMRT versus 3D-CRT in the treatment of esophagus cancer: a systematic review and meta-analysis. *Medicine*, *96*(31).

[123] Yu, C. X. (1995). Intensity-modulated arc therapy with dynamic multileaf collimation: an alternative to tomotherapy. *Physics in Medicine & Biology*, *40*(9), 1435.

[124] Otto, K. (2008). Volumetric modulated arc therapy: IMRT in a single gantry arc. *Medical physics*, *35*(1), 310-317.

[125] Palma, D., Vollans, E., James, K., Nakano, S., Moiseenko, V., Shaffer, R., ... & Otto, K. (2008). Volumetric modulated arc therapy for delivery of prostate radiotherapy: comparison with intensity-modulated radiotherapy and three-dimensional conformal radiotherapy. *International Journal of Radiation Oncology* Biology* Physics*, *72*(4), 996-1001.

[126] Zhang, P., Happersett, L., Hunt, M., Jackson, A., Zelefsky, M., & Mageras, G. (2010). Volumetric modulated arc therapy: planning and evaluation for prostate cancer cases. *International Journal of Radiation Oncology* Biology* Physics*, *76*(5), 1456-1462.

[127] Verbakel, W. F., Cuijpers, J. P., Hoffmans, D., Bieker, M., Slotman, B. J., & Senan, S. (2009). Volumetric intensity-modulated arc therapy vs. conventional IMRT in head-and-neck cancer: a comparative planning and dosimetric study. *International Journal of Radiation Oncology* Biology* Physics*, *74*(1), 252-259.

[128] Vanetti, E., Clivio, A., Nicolini, G., Fogliata, A., Ghosh-Laskar, S., Agarwal, J. P., ... & Cozzi, L. (2009). Volumetric modulated arc radiotherapy for carcinomas of the oro-pharynx, hypo-pharynx and larynx: a treatment planning comparison with fixed field IMRT. *Radiotherapy and Oncology*, *92*(1), 111-117.

[129] Ślosarek, K., Osewski, W., Grządziel, A., Radwan, M., Dolla, Ł., Szlag, M., & Stąpór-Fudzińska, M. (2015). Integral dose: Comparison between four techniques for prostate radiotherapy. *Reports of Practical Oncology and Radiotherapy*, *20*(2), 99-103.

[130] Cozzi, L., Dinshaw, K. A., Shrivastava, S. K., Mahantshetty, U., Engineer, R., Deshpande, D. D., ... & Fogliata, A. (2008). A treatment planning study comparing volumetric arc modulation with RapidArc and fixed field IMRT for cervix uteri radiotherapy. *Radiotherapy and oncology*, *89*(2), 180-191.

[131] Lee, Y. K., Brooks, C. J., Bedford, J. L., Warrington, A. P., & Saran, F. H. (2012). Development and evaluation of multiple isocentric volumetric modulated arc therapy technique for craniospinal axis radiotherapy planning. *International Journal of Radiation Oncology* Biology* Physics*, *82*(2), 1006-1012.

[132] Wang, Y., Zhu, L., Xia, W., & Wang, F. (2018). Anatomy of lymphatic drainage of the esophagus and lymph node metastasis of thoracic esophageal cancer. *Cancer Management and Research*, *10*, 6295.

[133] Ruben, J. D., Davis, S., Evans, C., Jones, P., Gagliardi, F., Haynes, M., & Hunter, A. (2008). The effect of intensity-modulated radiotherapy on radiation-induced second malignancies. *International Journal of Radiation Oncology* Biology* Physics*, *70*(5), 1530-1536.

[134] Abo-Madyan, Y., Aziz, M. H., Aly, M. M., Schneider, F., Sperk, E., Clausen, S., ... & Glatting, G. (2014). Second cancer risk after 3D-CRT, IMRT and VMAT for breast cancer. *Radiotherapy and Oncology*, *110*(3), 471-476.

[135] Lin, S. H., Wang, L., Myles, B., Thall, P. F., Hofstetter, W. L., Swisher, S. G., ... & Liao, Z. (2012). Propensity score-based comparison of long-term outcomes with 3-dimensional conformal radiotherapy vs

intensity-modulated radiotherapy for esophageal cancer. *International Journal of Radiation Oncology* Biology* Physics*, *84*(5), 1078-1085.

[136] Haefner, M. F., Lang, K., Verma, V., Koerber, S. A., Uhlmann, L., Debus, J., & Sterzing, F. (2017). Intensity-modulated versus 3-dimensional conformal radiotherapy in the definitive treatment of esophageal cancer: comparison of outcomes and acute toxicity. *Radiation Oncology*, *12*(1), 1-7.

[137] Van Benthuysen, L., Hales, L., & Podgorsak, M. B. (2011). Volumetric modulated arc therapy vs. IMRT for the treatment of distal esophageal cancer. *Medical Dosimetry*, *36*(4), 404-409.

[138] Yin, L., Wu, H., Gong, J., Geng, J. H., Jiang, F., Shi, A. H., ... & Zhu, G. Y. (2012). Volumetric-modulated arc therapy vs c-IMRT in esophageal cancer: A treatment planning comparison. *World journal of gastroenterology: WJG*, *18*(37), 5266.

[139] Wu, Z., Xie, C., Hu, M., Han, C., Yi, J., Zhou, Y., ... & Jin, X. (2014). Dosimetric benefits of IMRT and VMAT in the treatment of middle thoracic esophageal cancer: is the conformal radiotherapy still an alternative option?. *Journal of applied clinical medical physics*, *15*(3), 93-101.

[140] Münch, S., Aichmeier, S., Hapfelmeier, A., Duma, M. N., Oechsner, M., Feith, M., ... & Habermehl, D. (2016). Comparison of dosimetric parameters and toxicity in esophageal cancer patients undergoing 3D conformal radiotherapy or VMAT. *Strahlentherapie und Onkologie*, *192*(10), 722-729.

[141] Hardemark, B., Liander, A., Rehbinder, H. & Lof, J. (2004). *P3IMRT Direct machine parameter optimization.* Stanford. https://web.stanford.edu/class/cme304/docs/DMPO_whitePaper.pdf

[142] Feuvret, L., Noël, G., Mazeron, J. J., & Bey, P. (2006). Conformity index: a review. *International Journal of Radiation Oncology* Biology* Physics*, *64*(2), 333-342.

[143] Krippendorff, K. (2004). *Content Analysis: An Introduction to Its Methodology (2nd ed.).* Thousand Oaks, CA: Sage Publications.

[144] Krippendorff, K. (2011). Computing Krippendorff's alpha-reliability.

[145] Lian, J., Mackenzie, M., Joseph, K., Pervez, N., Dundas, G., Urtasun, R., & Pearcey, R. (2008). Assessment of extended-field radiotherapy for stage IIIC endometrial cancer using three-dimensional conformal radiotherapy, intensity-modulated radiotherapy, and helical tomotherapy. *International Journal of Radiation Oncology* Biology* Physics*, *70*(3), 935-943.

[146] Vivekanandan, N., Sriram, P., Kumar, S. S., Bhuvaneswari, N., & Saranya, K. (2012). Volumetric modulated arc radiotherapy for esophageal cancer. *Medical Dosimetry*, *37*(1), 108-113.

[147] Kole, T. P., Aghayere, O., Kwah, J., Yorke, E. D., & Goodman, K. A. (2012). Comparison of heart and coronary artery doses associated with intensity-modulated radiotherapy versus three-dimensional conformal radiotherapy for distal esophageal cancer. *International Journal of Radiation Oncology* Biology* Physics*, *83*(5), 1580-1586.

[148] Palma, D., Vollans, E., James, K., Nakano, S., Moiseenko, V., Shaffer, R., ... & Otto, K. (2008). Volumetric modulated arc therapy (VMAT) for delivery of prostate radiotherapy: Reduction in treatment time and monitor unit requirements compared to intensity modulated radiotherapy. *International journal of radiation oncology, biology, physics*, *72*(1), S312.